ESTABLISHING SPATIAL AND TEMPORAL PATTERNS IN *MICROCYSTIS* SEDIMENT SEED STOCK VIABILITY AND THEIR RELATIONSHIP TO SUBSEQUENT BLOOM DEVELOPMENT IN WESTERN LAKE ERIE

by

Christine Marie Knight

A thesis submitted
in partial fulfillment of the requirements
for the degree of Master of Science
(Natural Resources and Environment)
at the University of Michigan
April 2017

Faculty advisor(s):

Dr. Thomas H. Johengen, Chair

Dr. Timothy W. Davis, NOAA Great Lakes Environmental Research Lab

Acknowledgements

Many people were involved in generating this thesis. I want to express my gratitude to both Tom Johengen, who guided me through this whole process and suffered through the occasional break downs I had in his office. You're the real MVP, Tom. I also want to thank Tim Davis for co-advising me on this project, walking me through all the genetic techniques, giving me a deep appreciation for the mad pipetting skills a person needs to perform any kind of molecular level research. I also want to thank Dack Stuart for helping me collect core samples and both Danna Palladino and Ashley Burtner for guiding me through the many lab analyses needed for this project.

This project was completed using resources at the NOAA Great Lakes Environmental Research Laboratory and was funded through the Great Lakes Restoration Initiative.

Table of Contents

Abstract

This study assesses variation in the abundance and viability of sediment *Microcystis* vegetative seed stocks in Western Lake Erie across both seasons and years. Previous research suggests that lake sediment seed stocks can serve as inocula for reoccurring harmful algal blooms (HABs). However, there are few studies aimed at understanding the distribution, abundance, and viability of sediment seed stocks in Western Lake Erie and specifically how these variables are potentially related to past and subsequent bloom formation.

We conducted a two-year study of vegetative seed stocks in the Western Lake Erie basin, the region where annual algal blooms generally develop. Sediment was collected from 16 sites within Western Lake Erie covering an area of 375 km^2 with water column depths ranging from 3-9 meters. Sample collection occurred in November 2014, April 2015, November 2015, and April 2016. The total and potentially-toxic portions of *Microcystis* were determined using quantitative polymerase chain reaction. A series of laboratory experiments using lake sediment samples were conducted to assess the viability of *Microcystis* vegetative seed stocks.

The abundance and viability of *Microcystis* vegetative seed stocks varied both spatially and temporally. Across all sampling periods, the abundance of total *Microcystis* in the sediment ranged from 6.6×10^4 to 1.7×10^9 cell equivalents g^{-1}, and potentially-toxic Microcystis ranged from 1.4×10^3 to 4.7×10^6 cell equivalents g^{-1}. The abundance of total *Microcystis* diminished significantly across winter with densities in the spring nearly 10 times less than the previous fall. No correlation was found between abundance at specific sites and sediment composition, depth, or distance offshore. Further, total sediment *Microcystis* abundance was not relatively larger in November 2015, even though 2015 yielded one of the largest blooms on record. However, a higher percentage of the sediment population in November 2015 was potentially-toxic across all sites, which may have been the result of the large nutrient loads and higher than normal in-lake nutrient concentrations.

Culture experiments using sediment inocula and WC-Si growth media were used to examine potential viability of the sedimented cells. The sites with the greatest abundance of total and potentially-toxic *Microcystis* cells did not necessarily yield the most recruitment and growth over time, suggesting that abundance alone does not explain potential viability of sediment seed stocks. However, on average, the total abundance of cells in the grow-out flasks was more than twice the estimated amount present in the inocula, indicating that substantial growth occurred following recruitment from the sediment into the overlying water. Additional research will be needed to understand what specific factors influences the total contribution of *Microcystis* sediment seed stocks to recurrent annual blooms. However, numerical analysis suggests that sediment recruitment may have a significant impact on subsequent blooms, particularly when recruitment is paired with subsequent continual growth.

1. Introduction

Approximately 12 million people live in the Lake Erie watershed, with the lake providing drinking water to 11 million of these residents (United States EPA, 2016). Due to this high population density, intensive land-use activity, and shallow morphology, Lake Erie is plagued by a long history of harmful algal blooms (HABs) that are detrimental to human health and aesthetic values. In addition, the rapid death of HABs and subsequent bacterial respiration depletes water oxygen concentrations, which may lead to increased stress and mortality of aquatic fauna (Scavia et al, 2014; Schindler, 2006, 2012; Smith & Schindler, 2009). Certain genera of cyanobacteria, e.g. *Microcystis*, form HABs that produce metabolites that can be harmful to humans and other terrestrial mammals (i.e. microcystin). In the 1960s and 1970s, research showed that anthropogenic activities added excess phosphorus to Lake Erie and the resulting eutrophication of the lake promoted dense algal blooms (Bertram, 1993; Makarewicz & Bertram, 1991; Rosa & Burns, 1987). The research findings, combined with growing public concern, galvanized the government into developing policies to reduce phosphorus inputs into the Lake. Subsequent management actions during the 70's and 80's successfully reduced phosphorus inputs to targeted levels with a corresponding decrease in the extent of HAB development (DePinto et al., 1986; Scavia et al, 2014). However, in the past two decades, problems associated with HABs have returned. The worst recorded HABs occurred in 2011 and 2015. The 2011 algal mat extended more than 5,000 km^2, or three times larger than the previous record (Michalak et al, 2013). In August, 2014, nearly 500,000 residents of Toledo and surrounding areas lost access to clean water for two days as the result of a *Microcystis* bloom that accumulated near the intake pipe of the drinking water treatment plant.

While the recent algal blooms are similar to those that occurred in the 1960s and 1970s, the consequences of toxic cyanobacterial HABs are different, and the response of the ecosystem to targeted total phosphorus inputs no longer meets desired water quality from either aesthetics or as a source of drinking water. There is need for new studies that will reassess the mechanisms that regulate the development of HABs and control the production of toxic compounds within these cyanobacterial populations. One such mechanism contributing to the development of *Microcystis* blooms is the inoculation of the water column via sediment seed stocks. Prior studies show seed stocks in lake sediments are a likely source of inoculation for annual *Microcystis* blooms. However, given the specificity of this process across various ecosystems, it is necessary to evaluate the specific patterns of seed stocks and bloom response in Lake Erie.

1.1 Basics of Microcystis

Microcystis is a genus of cyanobacteria within the Order Chroococcales. In the environment, *Microcystis* cells form colonies held together by a mucilaginous matrix. Blooms of planktonic *Microcystis* develop globally in standing and torpid freshwaters. (Bridgeman et al., 2013; Fahnenstiel et al., 2008; Joehnk et al. 2008; Michalak et al., 2013; Oliver and Grant, 2000; Otten & Paerl, 2011; Qin et al.; Vanderploeg et al., 2001; Zohary & Robarts, 1990). A key feature of *Microcystis* is the presence of gas vesicles, which allows for buoyancy control and reinvasion into the water column. This buoyancy control is related to the carbohydrate content of

a cell, which operates as a form of ballast (Sejnohova & Marsalek, 2012). The typical annual cycle of *Microcystis* in temperate regions includes overwintering in the upper layers of sediment, reinvasion into the water column in the spring, summer bloom formation, and autumn sinking into the sediments (Reynolds et al, 1981).

Further, some strains of *Microcystis* also produce the hepatotoxin known as microcystin (Oliver and Grant, 2000; Davis et al., 2009, 2014; Harke et al., 2016, and references therein). Evidence suggests that both the occurrence and toxicity of *Microcystis* blooms is highly influenced by N availability (Gobler et al., 2016, and references therein). Microcystin is an N-rich compound and therefore *Microcystis* needs sufficient amounts of inorganic nitrogen to synthesize the toxin. However, unlike many other major bloom-forming cyanobacteria genera, *Microcystis* is incapable of fixing N_2 and relies on exogenous sources of nitrogen for growth and toxin synthesis (Carr & Whitton, 1982; Potts & Whitton, 2000; Davis et al., 2010). In Western Lake Erie, the Maumee River, which is a major source of nutrient loading to the lake, has an annual TN:TP minimum during the summer bloom months (Chaffin et al., 2013, 2014b). As concentrations of nitrate decrease in the summer months, diazotrophic cyanobacteria alleviate low N conditions by releasing ammonia and amino acids into the water column during N_2 fixation. Additionally, ammonia and ammonium are released from the sediments during the summer months due to increased decomposition occurring in the sediments (Wetzel, 2001, and references therein). *Microcystis* has demonstrated a high affinity for ammonium and therefore has a competitive advantage over other phytoplankton during these times, promoting late summer cyanobacteria blooms (Chaffin, 2011; Harke et al., 2016, and references therein; Gobler et al., 2016, and references therein). Toxic strains of *Microcystis* have a higher N requirement than non-toxic strains and tend to outcompete non-toxic strains at levels of high inorganic nitrogen. However, as inorganic nitrogen levels decrease, non-toxic strains tend to dominate over the toxic strains (Davis et al., 2010; Gobler et al., 2016 and references therein).

Prior studies demonstrate that vegetative colonies of *Microcystis* are capable of surviving extended time periods in the sediments (Reynolds et al. 1981; Boström et al. 1989). While *Microcystis* colonies experience losses during the overwintering period, significant fractions of colonies survive and can reinoculate the water column in the following spring (Brunberg 2002; Brunberg & Blomqvist 2003). Latour et al. (2007) demonstrated that *Microcystis* cells are capable of remaining morphologically intact and retaining microcystin producing capabilities in sediments as deep as 35 cm for more than a year. Rinta-Kanto (2009) found that genetic signatures for cyanobacteria, including microcystin producing and non-microcystin producing *Microcystis* spp. exist as deep as 12 cm in collected sediment samples from Lake Erie in 2004.

Further, several studies indicate that not only are sediment populations of *Microcystis* spp. capable of surviving for extended periods of time, but they are also capable of re-inoculating the water column and initiating both toxic and non-toxic blooms. For example, Lake Biwa (Japan), Lake Limmaren (central Sweden), Lake Volkerak (the Netherlands), and the Grangent reservoir (France) experience seasonal *Microcystis* blooms in a similar manner to Western Lake Erie (Tsujimura et al., 2000; Brunberg and Blomqvist, 2002; Brunberg and Blomqvist, 2003; Verspagen et al., 2005; Rinta-Kanto et al., 2009; Latour et al., 2007). Analyses and culturing of

sediment samples from the aforementioned water bodies demonstrate the viability of sediment populations of *Microcystis* spp. and therefore their potential to act as inocula for seasonal blooms.

1.2 Fluvial Versus Lake Sediment Sources of Seed Populations

While findings from the previously noted studies clearly highlight the importance of *Microcystis* sediment recruitment to seasonal bloom formation, uncertainty exists regarding the importance of this process in Western Lake Erie. Prior studies conducted within and around Lake Erie have indicated two potential sources of seed populations for annual blooms: fluvial sources and lake sediments. While both sources could be contributing seed populations to annual blooms, it is undetermined whether one of these sources offers a more significant contribution than the other. Some studies conclude that sediment sources are insignificant compared to fluvial sources (Bridgeman et al., 2011; Rinta-Kanto et al., 2005) while others come to opposite conclusions (Kutovaya et al., 2012; Chaffin et al. 2014a).

A study by Bridgeman et al. provides evidence suggesting that the Maumee River serves as a significant source of seed colonies for blooms in Western Lake Erie (2011). The study was designed to quantify the phytoplankton community composition of the river-lake coupled ecosystem of the Maumee River and Western Lake Erie. Coordinated sampling of both the river and the lake occurred in June, August, and September. The sampling months were intended to correspond to pre-bloom, mid-bloom, and late-bloom periods, respectively. *Microcystis* was quantified in the lake using a vertical plankton tow that extended from 1 m from the lake bottom to the surface (samples preserved with 4% formalin until analysis for biovolume); *Microcystis* was quantified in the stream using integrated water column samples collected with a tube sampler. Analysis of samples in June indicated that significant *Microcystis* populations only existed in the river assemblage (17% of total chlorophyll α). Subsequent analysis of August samples showed *Microcystis* populations had decreased to 3% of total chlorophyll α in the Maumee River, but had increased significantly in the lake (32% of total chlorophyll α). The initial lack of *Microcystis* in the lake followed by a simultaneous increase in lake populations and decrease in river populations suggests that the Maumee River serves as a seed population for Western Lake Erie blooms.

A second study conducted by Conroy et al. suggests that both the Maumee and Sandusky River serve as significant sources of *Microcystis* inocula (2014). In order to identify the initiation of *Microcystis* blooms both spatially and temporally along both rivers, investigators collected samples from early to mid-March along both rivers and performed a number of analyses, including phytoplankton enumeration, chlorophyll α determination, and phycocyanin determination. Upstream river samples from both the Maumee and Sandusky Rivers comprised of more than 60% *Microcystis* at bloom biomasses (>17 mg/L). Conroy et al further hypothesized that dams along the Maumee River could cause the river to function more like a lacustrine environment, therefore promoting bloom growth along the river. The blooms developed within the river would then go on to seed the annual Western Lake Erie blooms.

Conroy (2007) examined the hypothesis that tributaries contain phytoplankton that are light limited due to high nutrient concentrations and light attenuation; additionally, offshore phytoplankton are nutrient limited and subject to low light attenuation. The study analyzed field samples from the Sandusky River, Sandusky Bay, and Lake Erie in 2005 and 2006 and found high phytoplankton biomasses in the Sandusky River and Bay and concluded that, as tributary phytoplankton move offshore, productivity increased with increasing light availability and blooms develop (Conroy, 2007; Conroy et al., 2008).

Rinta-Kanto et al. (2005) also provided evidence in favor of the fluvial seeding of *Microcystis* blooms by analyzing the spatial variation in both chlorophyll α (as a proxy for phytoplankton biomass) and toxicity concentrations. Samples were collected from a 1 m depth using a surface water pump or Niskin bottles and were collected by 3 independent groups who were working concurrently in Western Lake Erie in August 2003. Both standard polymerase chain reaction (PCR) and quantitative real-time polymerase chain reaction (qPCR) were utilized to quantify the abundance of toxic *Microcystis* cells in 2003 samples from Western Lake Erie. Results from qPCR analyses of samples revealed that chlorophyll α and toxicity concentrations were highest in samples collected near the mouth of the Maumee River. Therefore, Rinta-Kanto et al. theorize that the Maumee River serves as a potential seed population for the annual *Microcystis* blooms.

However, despite the implications of the 2005 study, another study by Rinta-Kanto et al. in 2009 provided evidence supporting the hypothesis that lake sediments are a significant source of seed populations for summer blooms. Box cores of sediments were obtained from 3 locations in Lake Erie in July 2004 and corresponding surface water samples were collected in the same locations in August 2004 using a submersible pump. *Microcystis* was quantified using qPCR. Not only did the study underscore the viability of sediment seed stock populations culture experiments, it also showed that July sediment populations likely fueled August bloom events. The latter hypothesis was supported by the fact that *mcyA* sequences collected from August 2004 pelagic samples were consistent with *mcyA* sequences from July sediment populations (Rinta-Kanto et al., 2009). The genetic similarity indicates that August blooms may have originated from re-suspended sediment populations. Further, clear genetic differences existed between river and lake forms. Therefore, despite claims from 2004, later studies by Rinta-Kanto et al. indicate that sediment populations act as bloom inocula.

Kutovaya et al. (2012) also found little evidence that the Maumee River is a major source of toxic *Microcystis* spp. in Western Lake Erie. The study analyzed the spatial distribution of toxic cyanobacteria in the Maumee using genetic tools. Water samples were collected from the Maumee River, Maumee Bay, and Western Lake Erie. Phylogenetic analyses of *mcyA* sequences from the Maumee River and Western Lake Erie showed that *Planktothrix* spp. populated the Maumee River points whereas *Microcystis* spp. populated the Western Lake Erie points. Further, DNA from sediment samples in Western Lake Erie are genetically consistent with bloom populations and *Microcystis* could be cultured from Lake Erie sediment samples (Rinta-Kanto et al., 2009). Kutovaya recognized the possibility that river nontoxic *Microcystis* spp. genotypes

could contribute to the blooms upon entering Maumee Bay, but ultimately proposed that toxic blooms primarily arise from endemic lake sediment seed populations.

Another study by Chaffin et al. also generated evidence indicating that *Microcystis* blooms in Western Lake Erie originate from the sediments and not from the Maumee River or any other major tributary (2014a). Both water and sediment samples were collected from 7 lake locations and 1 location each in the Maumee and Sandusky rivers. Water samples were collected using an integrated tube sampler while the top 2 cm of sediment were collected using a ponar. DNA from water and soil samples were extracted using the MoBio Power Water kit and the MoBio Powermax Soil DNA kit, respectively. Denaturing gradient gel electrophoresis analyses of samples determined the genetic similarity between phytoplankton assemblages at each site. The Maumee River sample only possessed a 38% similarity to any of the other sample assemblages. Therefore, the Maumee River was not considered a major contributor to bloom events.

1.3 Conclusion

Numerous studies have indicated that sediment populations of *Microcystis* possess high survivability and can seed seasonal *Microcystis* blooms. However, exactly how much sediment populations contribute to blooms is less clear, especially when considered against fluvial sources. For example, while *Microcystis* comprised a large percentage of algal assemblages in the Maumee and Sandusky Rivers in March 2009 (Conroy et al., 2014), genetic differences have been demonstrated between river and lake forms (Rinta-Kanto et al., 2009) as well as river and lake microcystin producers (Kutovaya et al., 2012; Davis et al., 2014). Therefore, while evidence indicates that both fluvial and benthic sources of *Microcystis* potentially serve as inocula for blooms, currently existing evidence is unable to definitively show which of the sources is the more significant contributor to bloom events.

While previous studies have quantified the benthic *Microcystis* populations, those studies possess both limited spatial and temporal coverage. First, by only sampling sediments from a few sites, studies do not address the potential for a spatial gradient in *Microcystis* population. Second, only sampling during a single summer season does not take into consideration remnant *Microcystis* populations from previous bloom seasons. To thoroughly evaluate the potential for sediments to serve as a source of inoculum, a study must be conducted over multiple years and for several different study sites.

This study seeks to expand upon efforts to quantify the abundance and vitality of *Microcystis* sediments seed stocks in Western Lake Erie by drawing on the methods utilized by both Rinta-Kanto et al. and Chaffin et al. (2009 and 2014a, respectively). However, sampling occurs over a greater spatial and temporal extent and will focus on evaluating overwintering populations as opposed to summer bloom populations. Results will lead to a better understanding of the contribution of remnant overwintering populations to subsequent bloom development.

2. Study Objectives

The overall goal of this research is to quantify the spatial and temporal differences in vegetative seed stocks in Western Lake Erie and to analyze that data for potential relationships between the distribution, abundance, and toxicity of seed stocks to the preceding and subsequent harmful algal bloom development. Our specific objectives are as follows:

First, to quantify whether there are changes in the abundance of the vegetative seed stocks from the initial settling in the fall to potential recruitment in the spring through the analysis of spatial and temporal patterns in the over-wintering vegetative seed stocks.

Second, to assess the viability of cells and their capability of re-inoculating the water column through lab culture experiments.

Third, to determine whether sediment recruitment is relevant to summer bloom development in Western Lake Erie through comparisons of the abundance/vitality of sediment seed stocks versus subsequent bloom size.

3. Methods

3.1 Site description and sampling

Lake Erie is in the southernmost portion of the Laurentian Great Lakes system. Possessing a mean depth of 18.7 m, Lake Erie is the shallowest of the Laurentian Great Lakes. It has a surface area of 25,320 km^2 and a volume of 470 km^3 (Schertzer et al., 2008). Lake Erie can be divided into 3 distinct regions: the western, central, and eastern basins. Depth gradually increases across the 3 regions, ranging from a maximum of 10 m in the western basin to 64 m in the eastern basin. Sixteen sites were selected from the western basin for sampling based on the observed patterns of past blooms (Figure 1; Table 1). Of the total 16 sites, 6 correspond to pre-existing long term monitoring sites at the NOAA Great Lakes Environmental Research Laboratory: Sites 1.1, 3, 4, 8, 10, and 13 correspond to pre-existing monitoring sites WLE8, WLE6, WLE2, WLE12, WLE4, and WLE13, respectively.

Samples were collected in November 2014, April 2015, November 2015, and April 2016. Sampling times are intended to reflect conditions during initial settling (i.e. fall/November) and during recruitment (i.e. spring/April). Most sediment samples were collected using a Pylonex HTH Sediment Corer [http://www.pylonex.com/]. Cores were extruded from the barrel on site, the overlying water siphoned off. The top 2 cm of sediment was removed using a spatula, which was rinsed between sites, and transferred to a sterile Whirl-Pak bag. In situations where sediment samples could not be collected using a corer, a ponar was used instead (Table 2). Observation of core samples showed that freshly settled sediment possessed a distinct texture and color (i.e. less compact and pale brown in color), so in instances where it was difficult to delineate the top 2 cm of ponar samples, surface sediment of the previously noted characteristics was collected. Samples were stored in a refrigerator until processing, typically within a week of sampling. Note that samples were not collected for Sites 9, 10, 13, 14, and 15.1 in the November 2014 sampling due to boat scheduling and weather constraints.

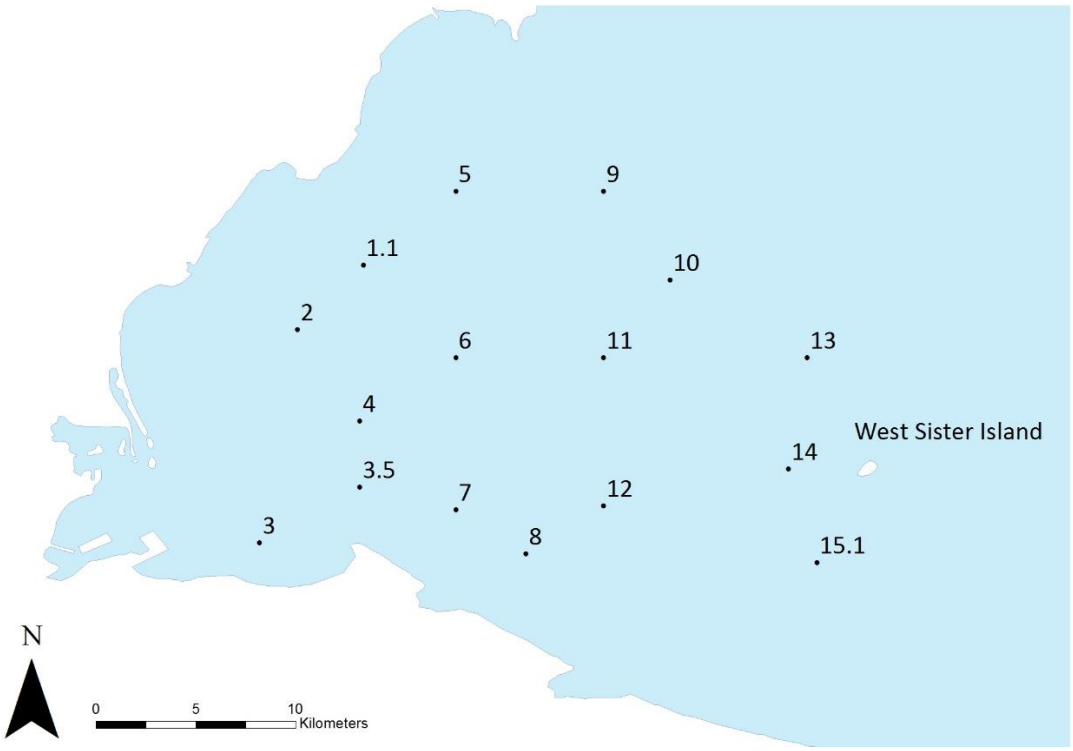

Figure 1- Sixteen sites were selected for sampling over a two-year period.

Table 1- Location of stations as well as water column depth (Z, m) and distance offshore (D, km)

Station ID	Latitude	Longitude	Z (m)	D (km)
1.1	41 50.0	83 20.0	6	5
2	41 48.26	83 21.78	6	5
3	41 42.5	83 22.8	3	2
3.5	41 44.0	83 20.1	4	3
4	41 45.8	83 20.1	5	6
5	41 52.0	83 17.5	6	5
6	41 47.5	83 17.5	7	10
7	41 43.4	83 17.5	6	4
8	41 42.2	83 15.6	6	4
9	41 52.0	83 13.5	7	8
10	41 69.6	83 11.7	8	13
11	41 47.5	83 13.5	8	13
12	41 43.5	83 13.5	7	7
13	41 47.5	83 08.0	9	18
14	41 44.5	83 08.5	9	13
15.1	41 41.972	83 07.725	8	9

Table 2- Samples were collected at each station using either a corer or ponar. While core samples were preferable, technical difficulties or sediment composition called for the use of a ponar at several sites. Sample collections denoted as "core & ponar" indicate instances where a second core collection was attempted due to insufficient material from the first core collection, but attempts continually failed and, therefore, a ponar was used. Samples that were not collected are indicated by "ND" (i.e. "No data").

	Collection Method			
Station ID	Nov 2014	April 2015	Nov 2015	April 2016
1.1	core	core	ponar	ponar
2	core	core	ponar	core
3	ponar	core	core & ponar	ponar
3.5	ponar	ponar	ponar	ponar
4	core	core	ponar	ponar
5	core	ponar	ponar	ponar
6	core	core	core	core
7	core	core	core	core
8	core	core	core	core
9	ND	ponar	ponar	ponar
10	ND	core	core	ponar
11	core	core	ponar	ponar
12	core	core	core	ponar
13	ND	core	core	ponar
14	ND	core	core	core
15.1	ND	core	core & ponar	core

Sediment and overlying water samples were stored at 7° C until processing in the laboratory, which occurred within 24-48 hours of collection. Specific processing and subsequent storage for parameters of interest are described below.

3.2 Culturing cell material from sediments

To confirm the viability of the *Microcystis* sediment seed stocks, a series of culture experiments were performed. After each sampling event, 3-5 grams of wet sediment was removed from each sample and added to a single 1-L flask in addition to 600 mL of WC-Si media. The WC-Si media was intended to mimic mesotrophic/eutrophic freshwater and was prepared according to the recipe described by Vanderploeg et al. (2001). Each flask (hereafter referred to as a "recruitment flasks") was corked with styrofoam and covered with aluminum foil to minimize airborne contamination but allow for gas exchange. Flasks were stored in a Percival Intellus Environmental Control biological incubator for a total incubation time of 6 weeks. Temperatures were kept at 20 °C and under 12/12 day light conditions. Each flask was swirled weekly to represent occasional resuspension events that occur at various time scales (from weeks to months) in the natural system.

Every two weeks and prior to swirling, 250 mL of media was siphoned from the top of each flask without disturbing the sediment by inserting a rubber tube below the water surface and using a syringe to reverse pressure in the tube to generate a flow of water. The siphoned water was filtered through a 3.0 µm Nucleopore Track-Etch Membrane filter and frozen at -80 degrees until DNA extraction. Fresh media was added back to each flask after sub-sampling to maintain a

total volume of 600 mL. This process was repeated for a total of 3 different time points, corresponding to t_1 (week 2), t_2 (week 4), and t_3 (week 6). It was assumed that at t_0, when the cultures were first prepared, there were no *Microcystis* cells in the overlying media. Trial incubations from the November 2014 sampling initially only used lake water as a growth media. However, after several weeks yielded no growth, lake water was spiked with 300 mL of WC-Si media. While some growth occurred after adding the media, culture data for November 2014 was omitted from analysis due to these complications. Subsequent collected samples were incubated using only WC-Si media.

During the November 2015 culture experiments, additional 30 mL subsamples were siphoned from 5 flasks (i.e. Sites 2, 3, 6, 11, 15) during the regular biweekly subsampling at t_2. The subsamples were then added to 150 mL flasks in addition to 70 mL of WC-Si media (hereafter referred to as "growth rate flasks"). At t_4, the entire 100 mL culture was filtered and stored in the same fashion as the recruitment flasks. These samples were used to estimate cell growth rates under similar experimental conditions as the recruitment flasks.

Growth rates (μ, $days^{-1}$) for growth rate flasks were calculated using the following formula:

$$\mu = \frac{ln(x_{t+1}/x_t)}{t}$$

, where x_t is the concentration of cell equivalents at time *t*.

Because population changes in the recruitment flasks were the result of both growth and recruitment processes, changes were described in terms of "accumulation rates" (Δx, cell equivalents mL^{-1} day^{-1}) as opposed to growth rates and were calculated as follows:

$$\Delta x = \frac{x_{t+1} - x_t}{\Delta t}$$

, where x_t is the concentration of cell equivalents at time *t*. Initial concentrations for each time interval were corrected for starting dilution levels.

3.3 Molecular Analysis

Total nucleic acids were extracted from freeze-dried sediment samples using the PowerMax® Soil DNA Isolation Kit [https://mobio.com/] and the user protocol available online at [http://www.mobio.com/images/custom/file/protocol/12988-10.pdf]. Generally, 5 grams of freeze-dried sediment were extracted from except in cases where sediment samples were limited. Filters containing filtered media samples from recruitment flasks and growth rate flasks were cut in half. Total cellular nucleic acids were extracted from filter halves using the DNeasy Blood and Tissue Kit [https://www.qiagen.com/us/] and the user protocol available online at [https://www.qiagen.com/us/shop/sample-technologies/dna/genomic-dna/dneasy-blood-and-tissue-kit/#resources] with two modifications: 1) after the chemical lyses step, a shredder column was used to homogenize the lysate and 2) the final elution step was repeated in order to increase

the elution volume. The quantity and quality of nucleic acids were determined using a Thermo Scientific NanoDrop Lite Spectrophotometer. DNA extract was frozen at -80 °C until analysis.

Table 3- A list of primers (Integrated DNA Technologies, IA, USA) and probes (Applied Biosystems, Foster City, CA, USA) used in the qPCR analysis)

DNA Target	Primer	Sequence (5'-3')	Reference
Microcystis 16s rDNA	184F	GCCGCRAGGTGAAAMCTAA	Neilan et al. (1997)
	431R	AATCCAAARACCTTCCTCCC	Neilan et al. (1997)
	Probe	(Taq) FAM-AAGAGCTTGCGTCTGATTAGCTAGT-BHQ-1[a]	Rinta-Kanto et al (2005)
Microcystis mcyD	F2	GGTTCGCCTGGTCAAAGTAA	Kaebernick et al. (2000)
	R2	CCTCGCTAAAGAAGGGTTGA	Kaebernick et al. (2000)
	Probe	(Taq) FAM-ATGCTCTAATGCAGCAACGGCAAA-BHQ-1[a]	Rinta-Kanto et al (2005)

F: forward primer R: reverse primer.

[a] Black Hole Quencher-1 (quenching range 480-580 nm)

Two *Microcystis*-specific genetic targets were used during this study, the 16S rRNA gene (16S rDNA) and *mcyD* gene. Targeting the 16S rRNA gene allowed for quantification of the abundance of total *Microcystis* population. The *mcyD* gene is found within the microcystin synthetase gene operon which is responsible for the production of microcystin and is only found in toxic strains of *Microcystis* (Tillet et al., 2000). Quantitative polymerase chain reaction (qPCR) was executed using an Applied Biosystems 7500 Fast Instrument using TaqMan® labeled probes (Applied Biosystems) and *Microcystis*-specific mcyD and 16S rDNA primers (Table 2). For amplification of the 16S targets, the cycling conditions were 95 °C for 10 minutes, followed by 45 cycles of 95 °C for 15 seconds and 60 °C for 1 minute. For amplification of the *mcyD* gene, the cycling conditions were 95 °C for 10 minutes, followed by 45 cycles of 95 °C for 15 seconds, 50 °C for 1 minute, and 60 °C for 1 minute. Since some *Microcystis* cells may carry multiple copies of the 16S rDNA gene and mcyD gene, data was generally expressed as "cell equivalents" (Rinta-Kanto et al., 2005; Davis et al., 2009; Davis et al., 2010).

Because the quality of the standard curves varied for initial qPCR runs, the following formula was used to calculate total/potentially-toxic gene copies to guarantee the comparability of data across individual runs:

$$x = 10^{\frac{C_T - 43.808}{-3.445}}$$

, where x is the corrected value for the cell copies in a sample and C_T is the threshold cycle. This equation is derived from the equation that the software uses to determine gene quantities based on a generated standard curve:

$$C_T = m\,(\log_{10} x) + b$$

, where m is the slope of the standard curve, b is the y-intercept of the standard curve, x is the calculated gene quantity, and C_T is the threshold cycle. Therefore, to determine the quantity of

gene copies based on the C_T value and parameters of the standard curve, the previous equation is rearranged as follows:

$$x = 10^{\frac{C_T - b}{m}}$$

Using the rearranged formula and the parameters from a select standard curve, the final formula used is thus:

$$x = 10^{\frac{C_T - 43.808}{-3.445}}$$

The slope and y-intercept values used in the final formula were taken from a run in which the standard curve possessed both a high efficiency and R^2 value.

Total cell equivalents determined by qPCR were converted to cell equivalents per gram of sediment using the following equation:

$$x^* = \frac{x}{5} * 5000 * \frac{1}{y}$$

, where x^* is the concentration of *Microcystis* (cell equivalents g^{-1}), *x* is the total number of *Microcystis* cell copies determined by qPCR, 5 refers to the amount of extract analyzed (µL), 5000 refers to elution volume (µL), and *y* is the amount of freeze-dried sediment that DNA was extracted from.

3.4 Algal Pigment Concentration

Chlorophyll α and phycocyanin were extracted from both overlying water and sediment samples. Dependent on the sample material, phycocyanin was determined by either filtering 10-20 mL of water through a Whatman GF/F filter or weighing 0.5-0.7 g of wet sediment onto the same filter type. Filters were stored in 15 mL Falcon tubes at -80 °C until processing. Subsequent steps were completed in low level light. Each tube received 9 mL of phosphate buffer [Ricca Chemical, pH 6.8]. Tubes with filters and buffer were then placed on a shaker table in a dark incubator at 5 °C for 15 minutes. Tubes were then vortexed at medium speed by hand for 10 seconds. To remove the maximum amount of substrate from each filter, samples were subject to two freeze-thaw cycles. Samples were placed in a standard freezer (-20 °C to -10 °C) for 2 hours and then placed on a shaker table in a dark incubator at 5 °C to thaw for two hours. After the second thaw was complete, samples were sonicated in ice water for 20 minutes using a Fisher FS110 H sonicator. After sonication, samples extracted overnight on a shaker table in a dark incubator at 5 °C. Samples were then vortexed by hand for 10 seconds and centrifuged at 7 °C and 4700 rpm for 20 minutes. Samples were then decanted into a plastic cuvette and measured for phycocyanin using a Turner Aquafluor fluorometer.

Samples preserved for chlorophyll analysis were removed from freezer and 8 mL of N, N-dimethylformamide was added to each tube (Speziale et al., 1984). Samples were placed in a water bath at 65 °C for 15 minutes. Once samples were removed from the bath and cooled to

room temperature, tubes were vortexed by hand for 15-20 seconds. Tubes were then centrifuged at 20 °C and 4700 rpm for 10 minutes. Liquid from each sample was decanted into a cuvette and the fluorescence analyzed using a Turner Designs fluorometer calibrated with chlorophyll α standards.

3.5 Percent Wet Weight and Bulk Density

Samples were weighed in aluminum weigh boats and dried in an oven at 100 °C for 24 hours. Dried samples were then weighed to determine percent wet weight.

3.6 Total Phosphorus Determination

Total phosphorus content of sediments was determined using a combustion and hot HCl extraction procedure (Anderson, 1976). Sediment samples were freeze-dried and homogenized. Roughly 0.5 g of each sample was weighed onto pre-tared glassine weigh paper using a Mettler AT250 balance. Each weighed sample was transferred to a pre-numbered (etched), acid-washed Pyrex test tube. Samples were then combusted at 500°C for two hours. Combusted samples were kept at dry, room temperature conditions until further processing occurred. Twenty-five milliliters of 1.0 N HCl was added to each tube using a Brinkman repeat pipette. Samples were placed in 99°C water bath for 45 minutes. After samples cooled, an additional 25 milliliters of double deionized water was added to each tube, resulting in a total sample volume of 50 milliliters. A half of a milliliter was subsampled from each tube and added to a pre-labeled polypropylene tube. Each polypropylene tube received 10 milliliters of double de-ionized water, resulting in a sample extract dilution factor of 21. Samples were then analyzed using a SEAL AutoAnalyzer 3 HR.

3.7 Percent Carbon and Nitrogen Determination

Particulate carbon and nitrogen were determined by flash combustion method using a Carlos Erba EA1110 configured for CHN. Triplicate samples of freeze-dried samples were weighed into 8x5 mm tin capsules [Costech.com]. Weighed samples were kept in a desiccator until analysis. Standard curves were determined for each run using National Institute of Standards & Technology (NIST) certified Buffalo River sediment, methionine, and NIST Oyster tissue. Samples were combusted under a catalyst of chromium oxide and with O_2 injection (Combustion Tube) followed by elemental copper reduction (Reduction Tube). Combusted gases then entered a 5 m gas chromatograph (GC) column and the gaseous element were sorted and exited the GC column as purified C, H, and N under the instrument configuration used. The purified gases contacted a thermal detector at the end of the GC column and the detector measures the heat of the gas pulse as a voltage, which was converted to elemental mass based on the predetermined calibration curve.

3.8 Graphs and Statistical Analyses

Maps were generated in ArcMap version 10.4.1. All graphs and statistical comparisons were generated using Excel 2016 and SigmaPlot version 12.0. The non-parametric Mann-Whitney Rank Sum test was used for all cell equivalent data sets from sediments and cultures because data sets were not normally distributed and uneven sampling occurred. Results where $p < 0.05$ were considered statistically significant.

4. Results

4.1 Abundance and Distribution of Microcystis *in Lake Sediments*

For the November 2014 sampling event, the abundance of total *Microcystis* ranged from 3.1×10^6 to 1.7×10^9 cell equivalents g^{-1} ($\bar{x} = 2.6 \times 10^8 \pm 5.1 \times 10^8$). The lowest abundance was found at Site 7 and the highest abundance at Site 5 (Figure 2). The abundance of potentially-toxic *Microcystis* ranged from 7.5×10^4 to 2.7×10^6 cell equivalents g^{-1} ($\bar{x} = 6.6 \times 10^5 \pm 9.1 \times 10^5$), with the lowest abundance located at Site 8 and the highest abundance at Site 12 (Figure 3). The percentage of potentially-toxic *Microcystis* ranged from <0-6%, with there being <0% at multiple sites (2, 3.5, 5, and 6) and 6% at Site 7 (Figure 12).

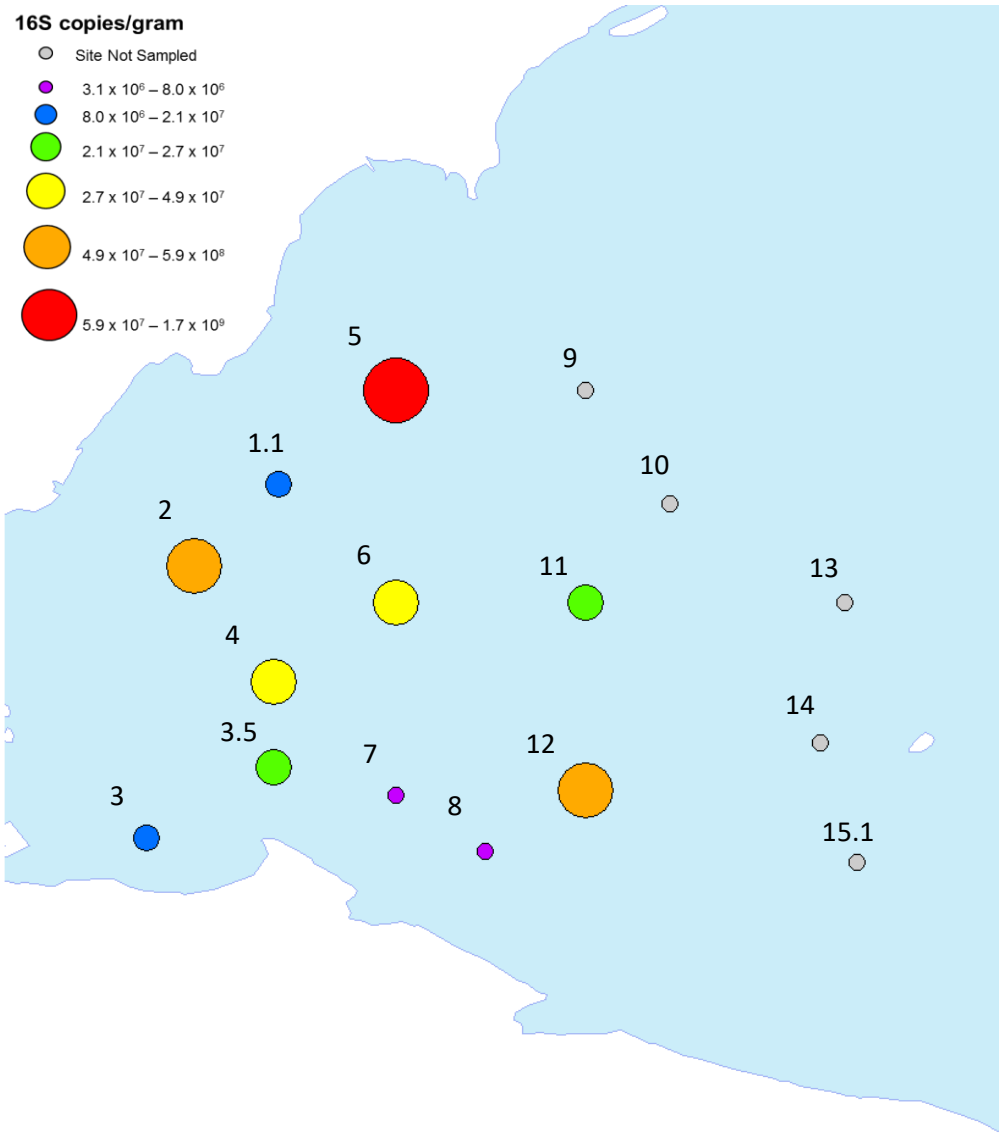

Figure 2- Bubble map of total Microcystis *abundance (cell equivalents g^{-1}, synonymous with 16S copies g^{-1}) at various stations for November 2014. Bubble size and color indicate the relative magnitude of total* Microcystis*. Ranges for different symbols are based on where natural breaks in data occur as determined by ArcMap.*

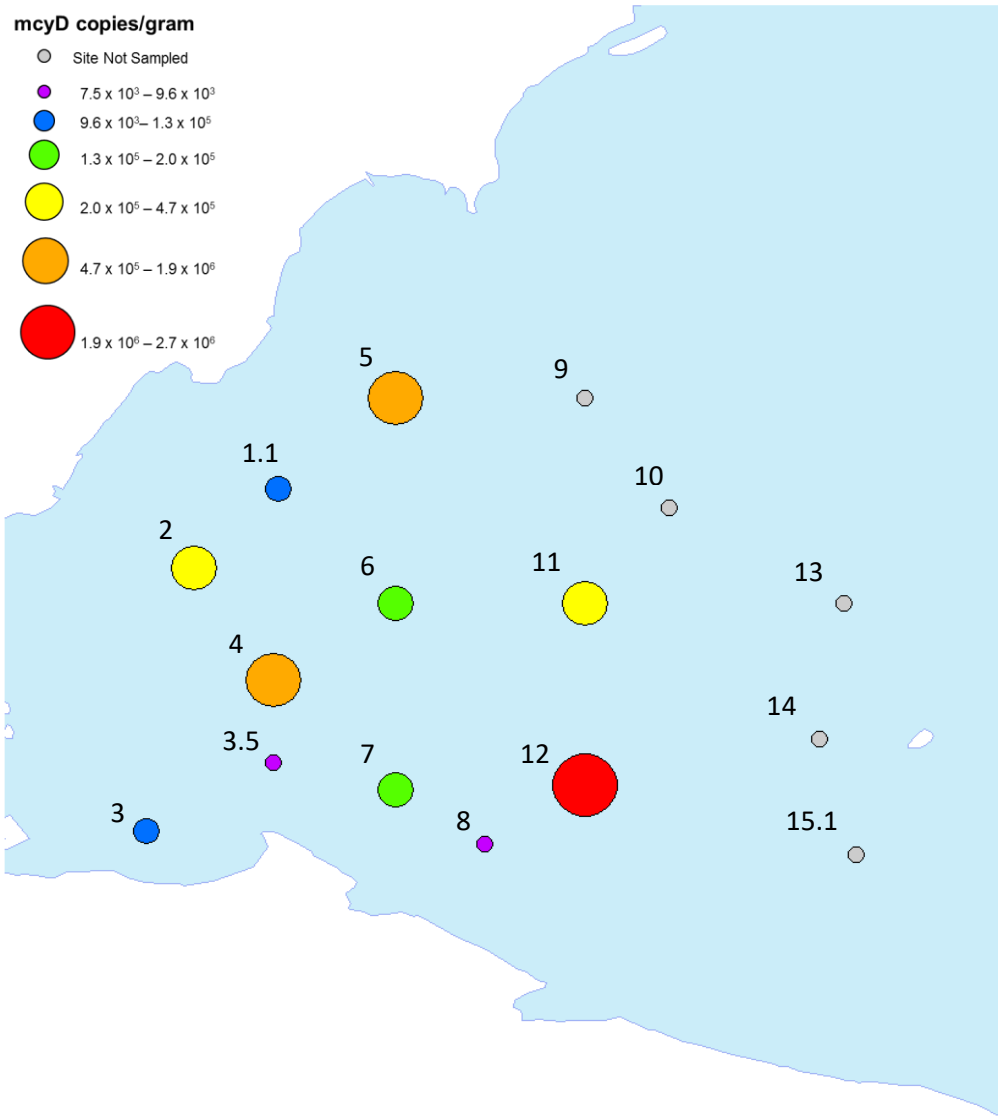

Figure 3- Bubble map of potentially-toxic Microcystis *abundance (cell equivalents g^{-1}, synonymous with mcyD copies g^{-1}) at various stations for November 2014. Bubble size and color indicate the relative magnitude of potentially-toxic* Microcystis*. Ranges for different symbols are based on where natural breaks in data occur as determined by ArcMap.*

For the April 2015 sampling event, the abundance of both total and potentially toxic *Microcystis* were approximately 10-fold lower than the previous fall. Total *Microcystis* abundance ranged from 6.4×10^5 to 2.5×10^8 cell equivalents g^{-1} ($\bar{x} = 2.6 \times 10^7 \pm 6.5 \times 10^7$), with the lowest concentration at Site 15.1 and the highest at Site 5 (Figure 4). The abundance of potentially-toxic *Microcystis* ranged from 9.5×10^3 to 5.1×10^5 cell equivalents g^{-1} ($\bar{x} = 7.8 \times 10^4 \pm 1.3 \times 10^5$), with the lowest concentration at Site 15.1 and the highest at Site 5 (Figure 5). The percentage of potentially-toxic *Microcystis* ranged from 0-4%, with there being <0% at multiple sites (i.e. 3, 4, 5, 7, 12, 13, 14) and 4% at Site 6 (Figure 12).

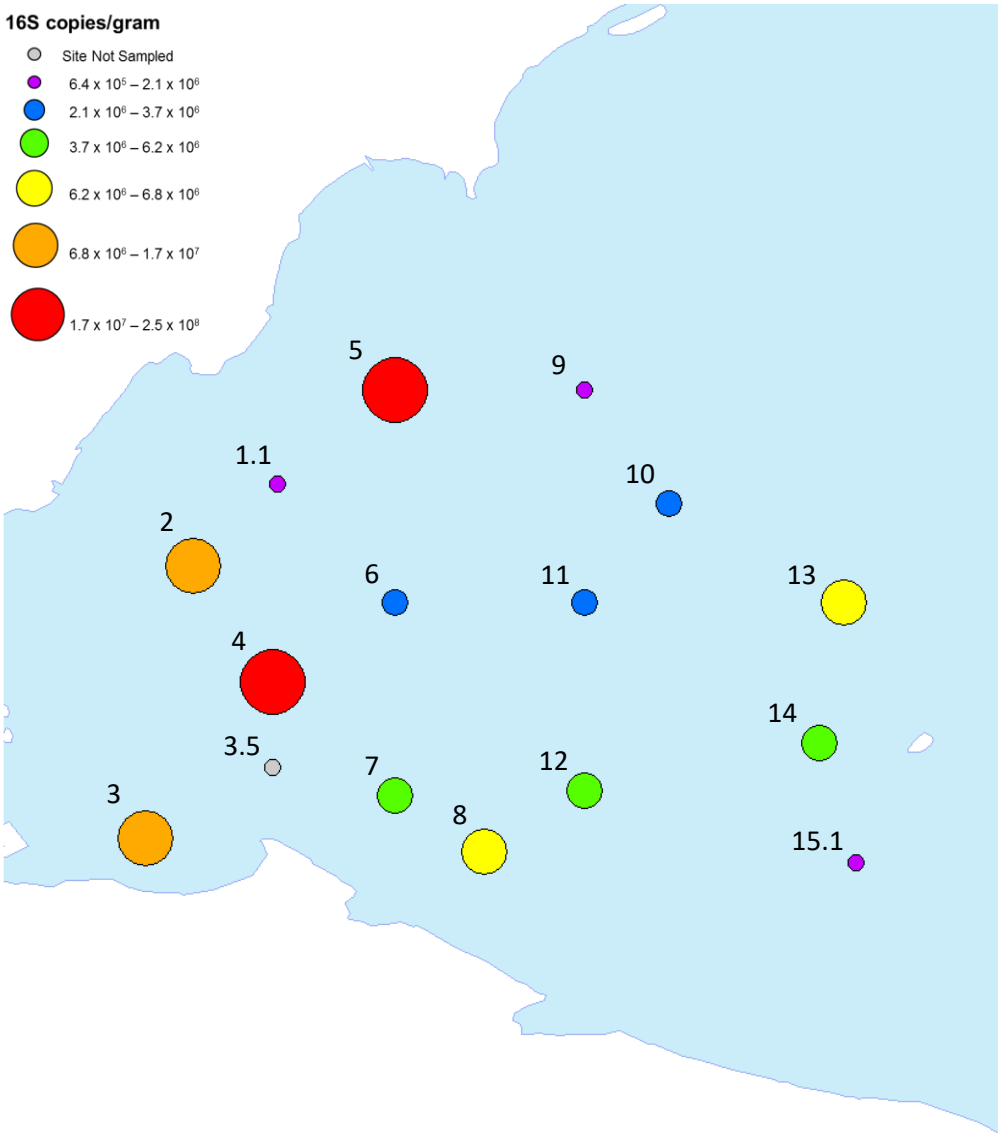

Figure 4- Bubble map of total Microcystis *abundance (cell equivalents g^{-1}, synonymous with 16S copies g^{-1}) at various stations for April 2015. Bubble size and color indicate the relative magnitude of total* Microcystis*. Ranges for different symbols are based on where natural breaks in data occur as determined by ArcMap.*

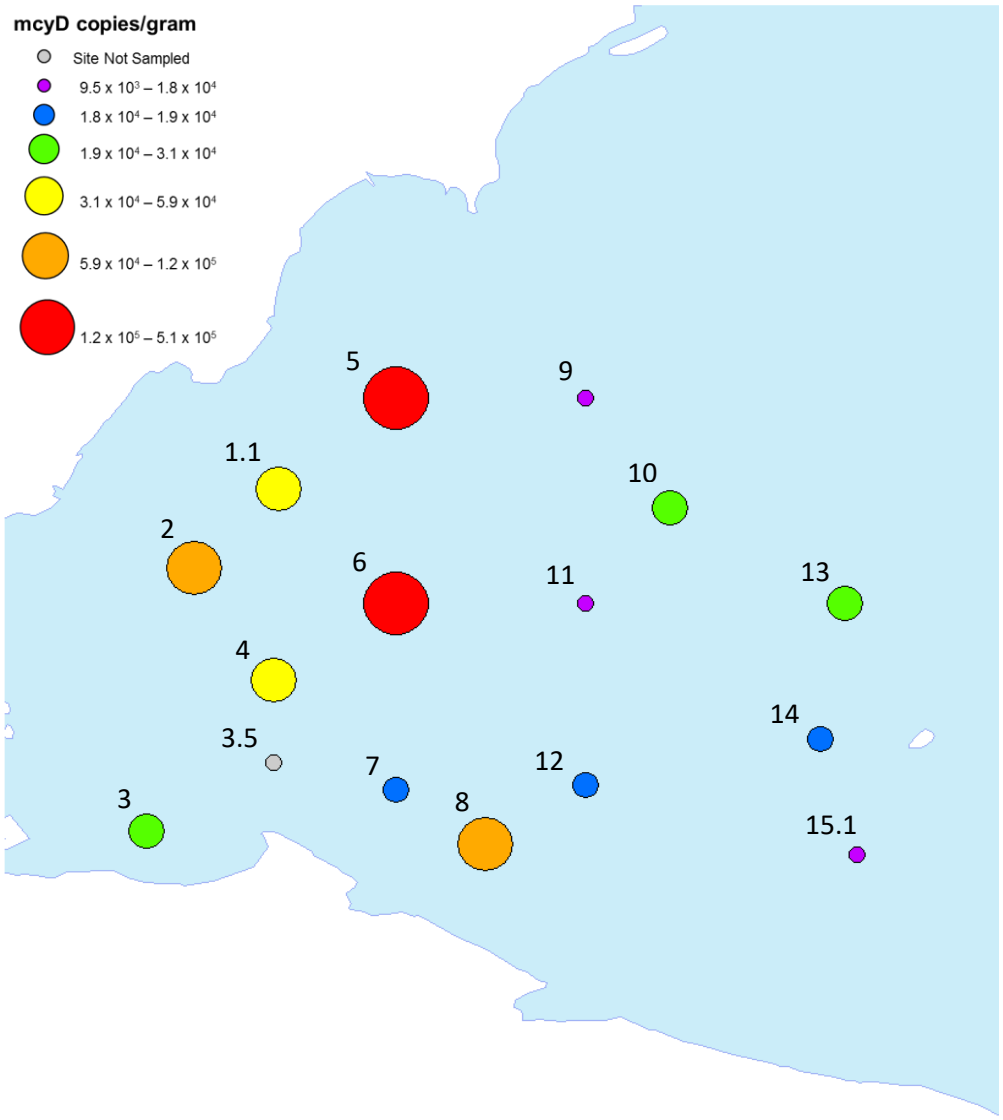

Figure 5- Bubble map of potentially-toxic Microcystis *abundance (cell equivalents g^{-1}, synonymous with mcyD copies g^{-1}) at various stations for April 2015. Bubble size and color indicate the relative magnitude of potentially-toxic* Microcystis*. Ranges for different symbols are based on where natural breaks in data occur as determined by ArcMap.*

For the November 2015 sampling event, cell abundances were nearly 10-fold lower than in November 2014 despite a record setting bloom extent in 2015. The abundance of total *Microcystis* ranged from 5.3×10^5 to 4.6×10^7 cell equivalents g^{-1} ($\bar{x} = 8.1 \times 10^6 \pm 1.2 \times 10^7$), with the lowest abundance at Site 6 and the highest at Site 8 (Figure 6). The abundance of potentially-toxic *Microcystis* ranged from 6.9×10^4 to 4.7×10^6 cell equivalents g^{-1} ($\bar{x} = 8.6 \times 10^5 \pm 1.4 \times 10^6$), with the lowest abundance at Site 6 and the greatest at Site 4 (Figure 7). The percentage of potentially-toxic *Microcystis* ranged from 2-68%, with the lowest percentage at Sites 3 and 15.1 and the highest percentage at Site 11 (Figure 12).

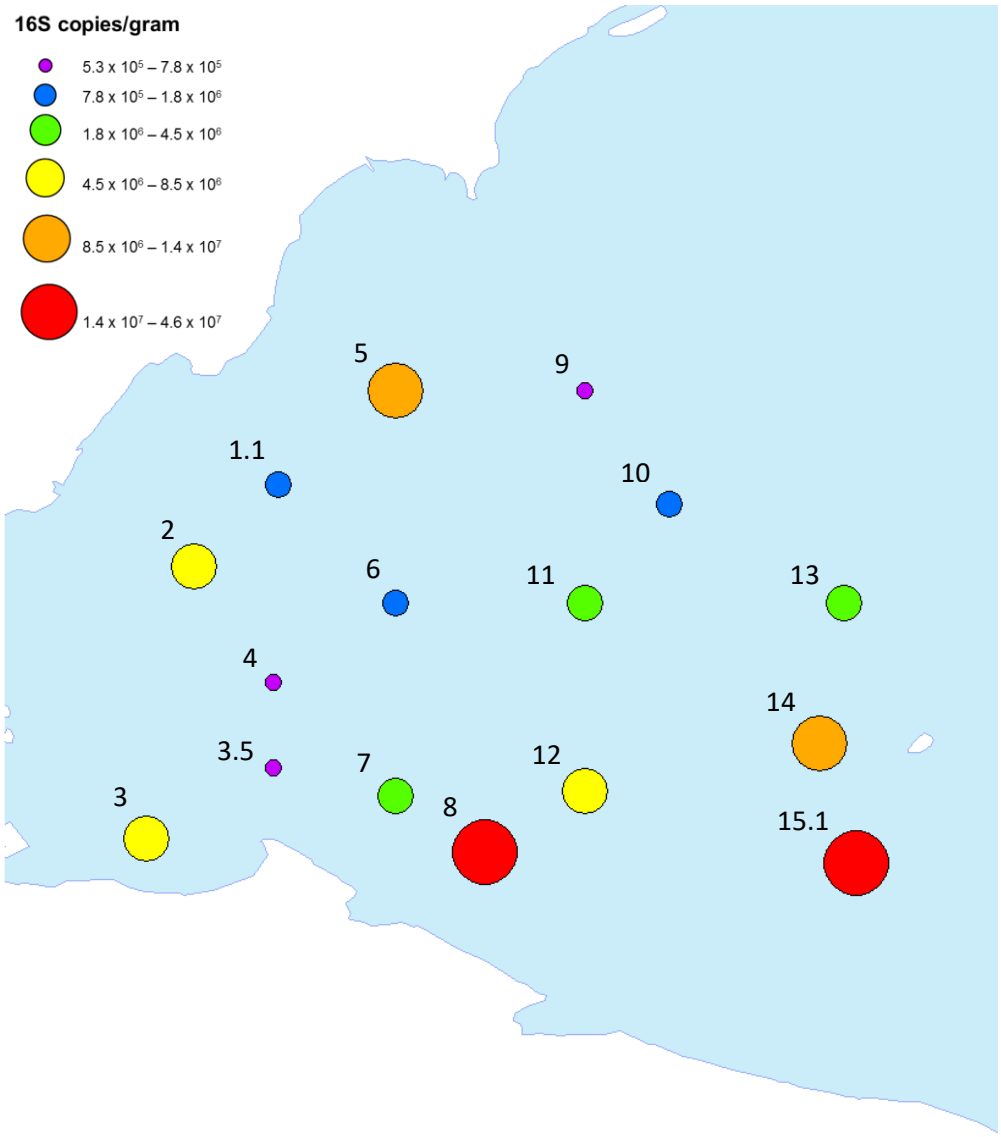

Figure 6- Bubble map of total Microcystis *abundance (cell equivalents g^{-1}, synonymous with 16S copies g^{-1}) at various stations for November 2015. Bubble size and color indicate the relative magnitude of total* Microcystis*. Ranges for different symbols are based on where natural breaks in data occur as determined by ArcMap.*

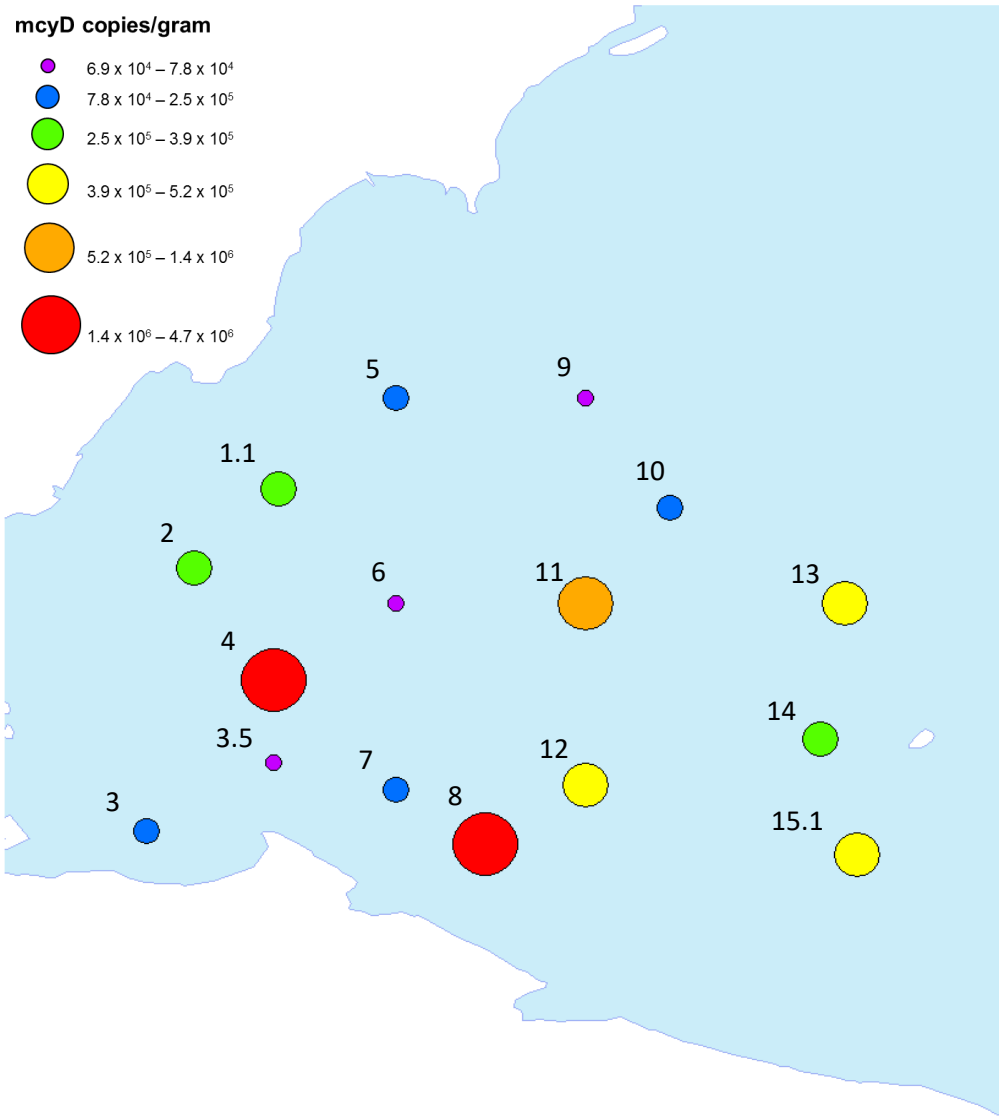

Figure 7- Bubble map of potentially-toxic Microcystis *abundance (cell equivalents g^{-1}, synonymous with mcyD copies g^{-1}) at various stations for November 2015. Bubble size and color indicate the relative magnitude of potentially-toxic* Microcystis*. Ranges for different symbols are based on where natural breaks in data occur as determined by ArcMap.*

For the April 2016 sampling event, the abundance of total *Microcystis* ranged from 6.6 x 10^4 to 8.0 x 10^6 cell equivalents g^{-1} ($\bar{x}$ = 1.9 x 10^6 ± 2.4 x 10^6), with the lowest abundance at Site 3.5 and the highest at Site 6 (Figure 8). The abundance of potentially-toxic *Microcystis* ranged from 1.4 x 10^3 to 5.4 x 10^5 cell equivalents g^{-1} ($\bar{x}$ = 9.0 x 10^4 ± 1.4 x 10^5), with the lowest abundance at Site 3.5 and the greatest at Site 6 (Figure 9). The percentage of potentially-toxic *Microcystis* ranged from 1-14%, with the lowest percentage at Sites 12 and 15.1 and the highest percentage at Site 10 (Figure 12). The over-winter decline in both total (77%) and toxic (90%) cell abundance from the previous fall was similar to that observed in the previous sampling year.

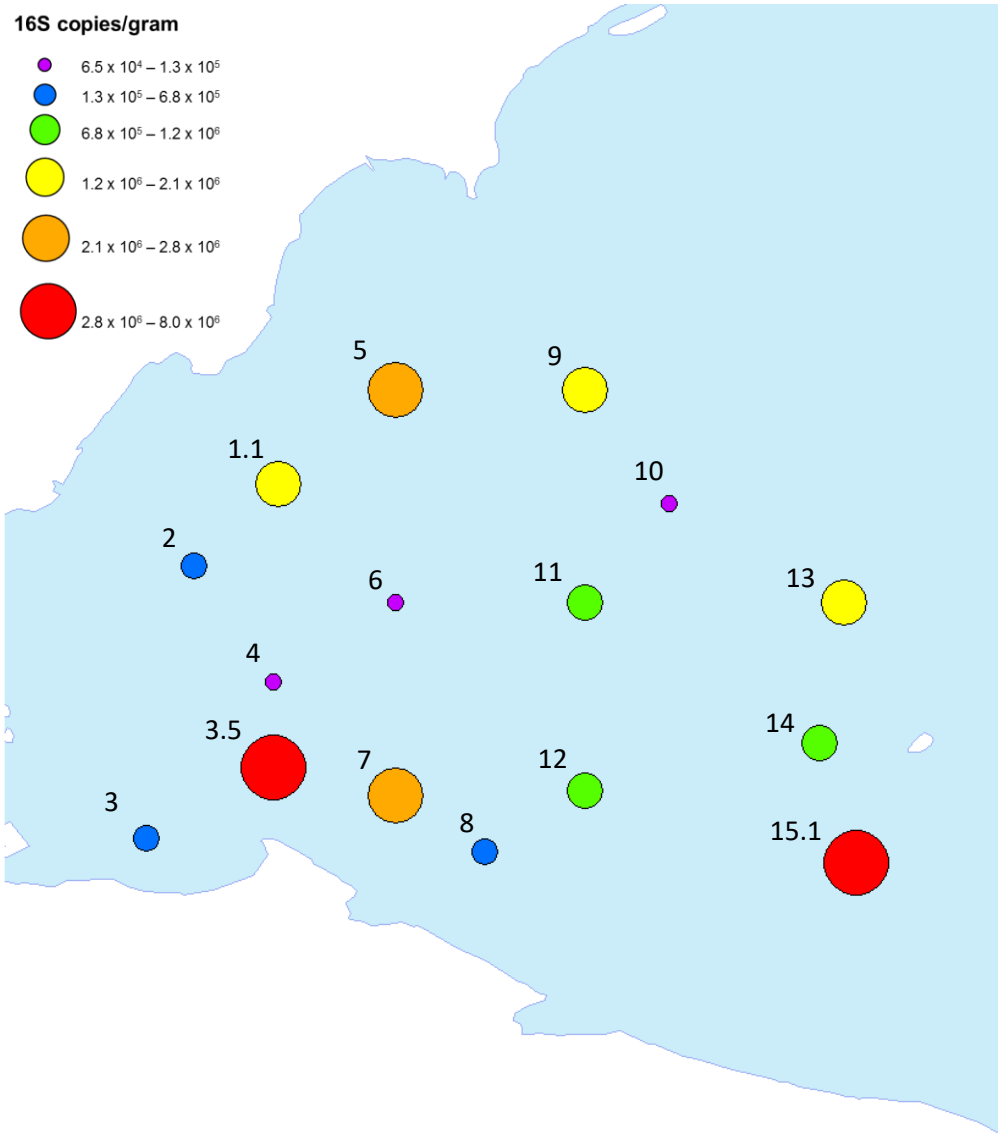

Figure 8- Bubble map of total Microcystis *abundance (cell equivalents g^{-1}, synonymous with 16S copies g^{-1}) at various stations for April 2016. Bubble size and color indicate the relative magnitude of total* Microcystis*. Ranges for different symbols are based on where natural breaks in data occur as determined by ArcMap.*

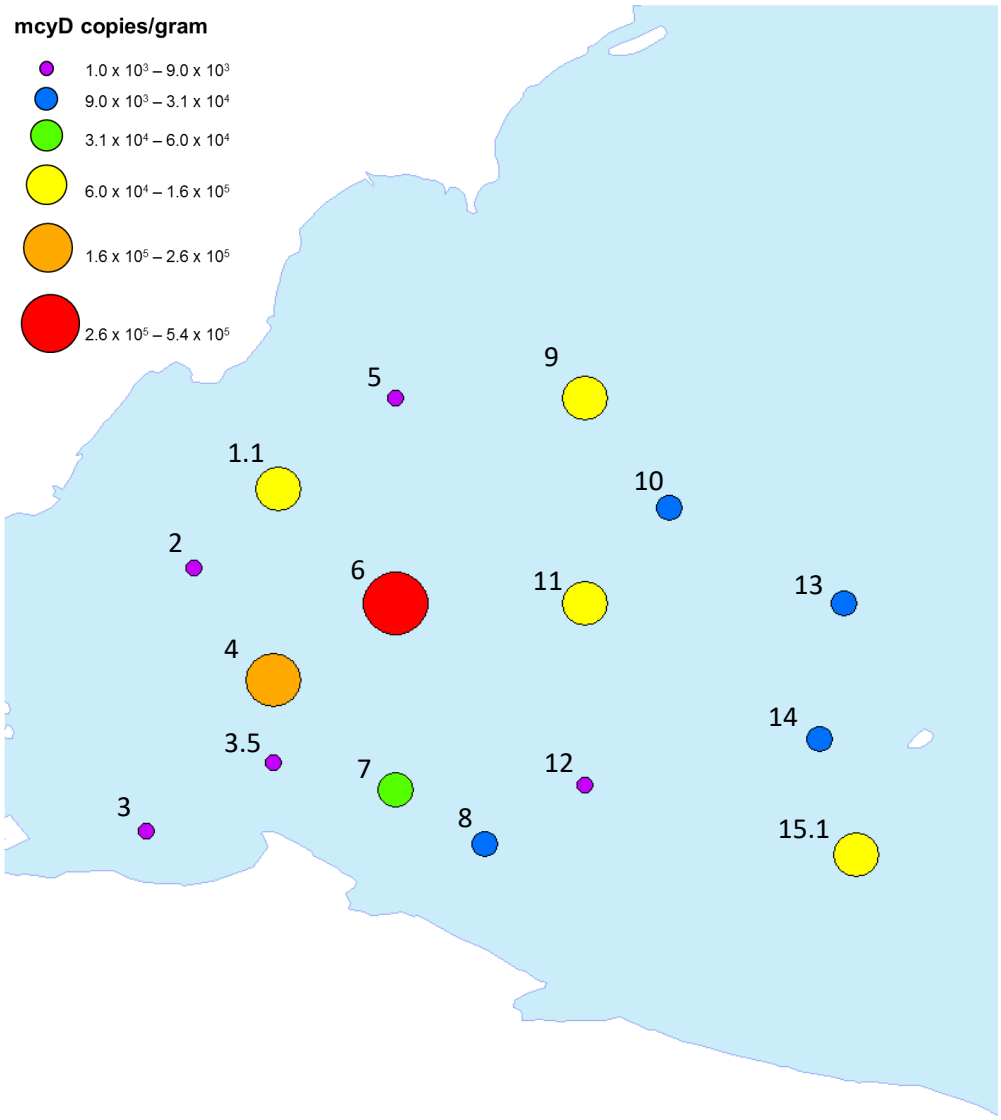

Figure 9- Bubble map of potentially-toxic Microcystis *abundance (cell equivalents g^{-1}, synonymous with mcyD copies g^{-1}) at various stations for April 2016. Bubble size and color indicate the relative magnitude of potentially-toxic* Microcystis*. Ranges for different symbols are based on where natural breaks in data occur as determined by ArcMap.*

The abundance of *Microcystis* for the entire spatial and temporal extent of the study are summarized in Figure 10 and Figure 11 (total and potentially-toxic, respectively). The percentage of the total populations that were potentially toxic are shown in Figure 12. The highest concentrations are not found closest to the river mouth, but are generally closer to shore in relatively shallow water.

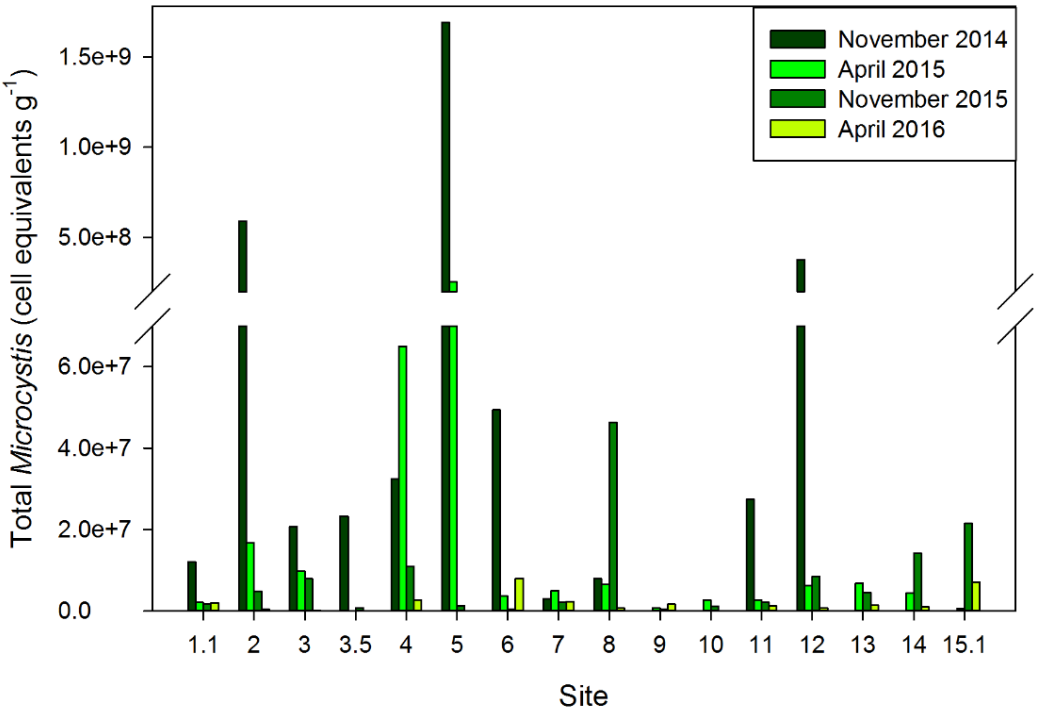

Figure 10- Total Microcystis *abundance in sediments (cell equivalents per gram dry weight of sediment).*

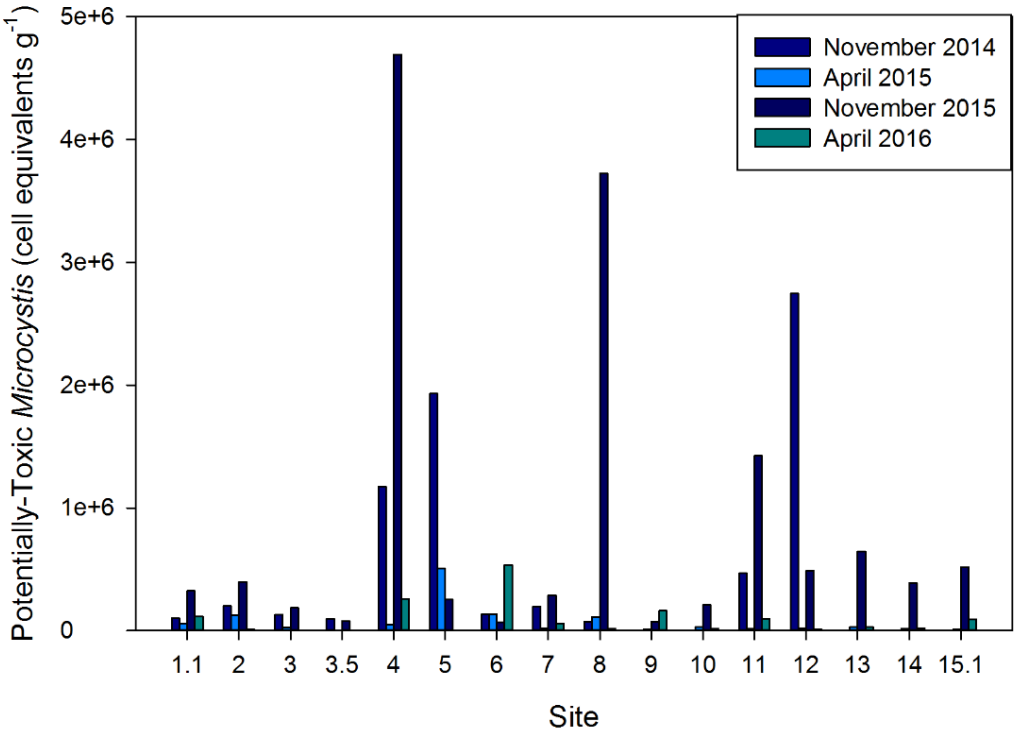

Figure 11- Potentially-toxic Microcystis *abundance in sediments (cell equivalents per gram dry weight of sediment). Note that the abundance of potentially-toxic* Microcystis *tended to be an order of magnitude less than that of total* Microcystis.

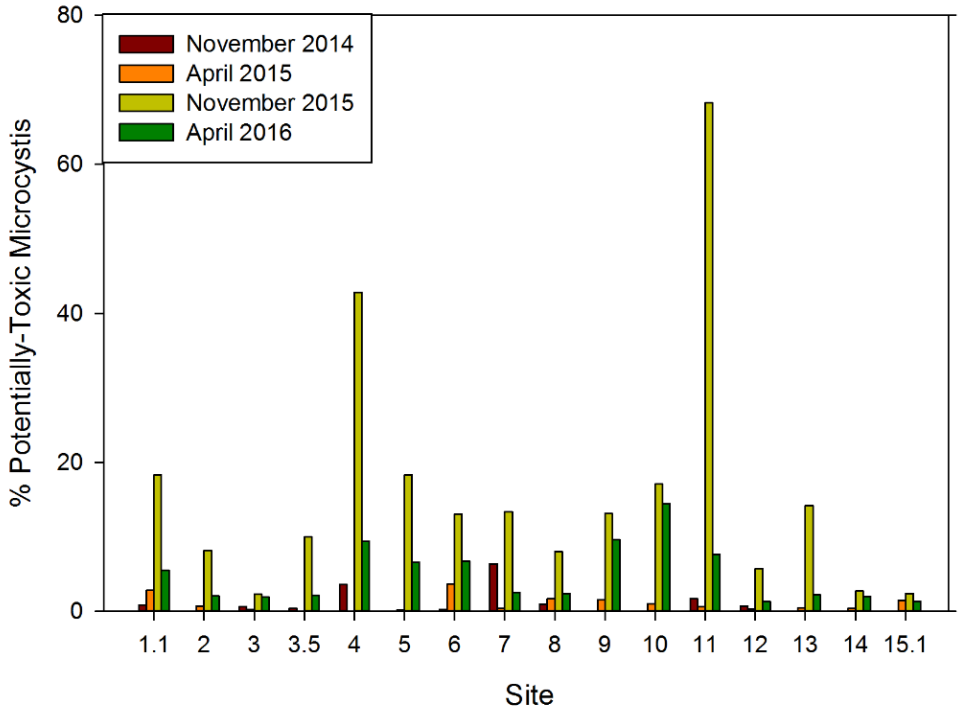

Figure 12- Percentage of potentially-toxic Microcystis *across the spatial and temporal extent of the study.*

The change across years (i.e. April 2015 to April 2016 and November 2014 to November 2015), across seasons (i.e. November 2014 to April 2015 and November 2015 to April 2016), and within the years (i.e. April 2015 to November 2015) are detailed in Table 4 and Table 5 (total and potentially-toxic *Microcystis*, respectively). The greatest change in magnitude of total cell equivalents occurred from November 2014 to November 2015 and from November 2014 to April 2015, reflective of the comparatively higher abundance of total *Microcystis* in November 2014. The greatest change in magnitude of potentially-toxic cells occurred from November 2014 to November 2015, November 2015 to April 2016, and April 2015 to November 2015, reflective of the comparatively higher abundance of potentially-toxic *Microcystis* in November 2015.

The Mann-Whitney Rank Sum test indicated differences in total *Microcystis* between the following pairs: November 2014 and April 2015, November 2014 and November 2015, April 2015 and April 2016, and November 2015 and April 2016. The same test indicated differences in toxic *Microcystis* between the following pairs: November 2014 and April 2015, April 2015 and November 2015, and November 2015 and April 2016.

Table 4- Change in total Microcystis *in sediments across years (i.e. April 2015 to April 2016 and November 2014 to November 2015), across overwintering periods (i.e. November 2014 to April 2015 and November 2015 to April 2016), and within years (i.e. April 2015 to November 2015).*

	Change (cell equivalents g^{-1})				
Site	April 2015 to April 2016	November 2014 to November 2015	November 2014 to April 2015	November 2015 to April 2016	April 2015 to November 2015
1.1	-4.0×10^4	-1.0×10^7	-1.0×10^7	2.9×10^5	-3.3×10^5
2	-1.6×10^7	-5.9×10^8	-5.7×10^8	-4.4×10^6	-1.2×10^7
3	-9.6×10^6	-1.3×10^7	-1.1×10^7	-7.8×10^6	-1.9×10^6
3.5	ND	-2.3×10^7	ND	-7.2×10^5	ND
4	-6.2×10^7	-2.2×10^7	3.3×10^7	-8.2×10^6	-5.4×10^7
5	-2.5×10^8	-1.7×10^9	-1.4×10^9	-1.3×10^6	-2.5×10^8
6	4.3×10^6	-4.9×10^7	-4.6×10^7	7.5×10^6	-3.1×10^6
7	-2.6×10^6	-9.3×10^5	1.8×10^6	2.1×10^5	-2.8×10^6
8	-5.9×10^6	3.8×10^7	-1.4×10^6	-4.6×10^7	4.0×10^7
9	9.4×10^5	ND	ND	1.1×10^6	-2.0×10^5
10	-2.6×10^6	ND	ND	-1.1×10^6	-1.5×10^6
11	-1.5×10^6	-2.5×10^7	-2.5×10^7	-8.4×10^5	-6.6×10^5
12	-5.5×10^6	-3.7×10^8	-3.7×10^8	-7.8×10^6	2.3×10^6
13	-5.4×10^6	ND	ND	-3.1×10^6	-2.3×10^6
14	-3.4×10^6	ND	ND	-1.3×10^7	9.8×10^6
15.1	6.4×10^6	ND	ND	-1.4×10^7	2.1×10^7

Table 5- Change in potentially-toxic Microcystis *in sediments across years (i.e. April 2015 to April 2016 and November 2014 to November 2015), across overwintering periods (i.e. November 2014 to April 2015 and November 2015 to April 2016), and within years (i.e. April 2015 to November 2015).*

	Change (cell equivalents g^{-1})				
Site	April 2015 to April 2016	November 2014 to November 2015	November 2014 to April 2015	November 2015 to April 2016	April 2015 to November 2015
1.1	5.4×10^4	2.2×10^5	-4.3×10^4	-2.1×10^5	2.7×10^5
2	-1.2×10^5	2.0×10^5	-7.6×10^4	-3.9×10^5	2.7×10^5
3	-2.3×10^4	5.5×10^4	-1.0×10^5	-1.8×10^5	1.6×10^5
3.5	ND	-1.7×10^4	ND	-7.7×10^4	ND
4	2.1×10^5	3.5×10^6	-1.1×10^6	-4.4×10^6	4.6×10^6
5	-5.0×10^5	-1.7×10^6	-1.4×10^6	-2.5×10^5	-2.6×10^5
6	4.0×10^5	-6.4×10^4	1.6×10^3	4.7×10^5	-6.6×10^4
7	4.1×10^4	9.1×10^4	-1.8×10^5	-2.3×10^5	2.7×10^5
8	-9.6×10^4	3.7×10^6	3.7×10^4	-3.7×10^6	3.6×10^6
9	1.5×10^5	ND	ND	9.1×10^4	6.1×10^4
10	-9.5×10^3	ND	ND	-1.9×10^5	1.8×10^5
11	7.8×10^4	9.6×10^5	-4.5×10^5	-1.3×10^6	1.4×10^6
12	-1.0×10^4	-2.3×10^6	-2.7×10^6	-4.8×10^5	4.7×10^5
13	5.4×10^2	ND	ND	-6.1×10^5	6.2×10^5
14	2.5×10^3	ND	ND	-3.7×10^5	3.7×10^5
15.1	8.1×10^4	ND	ND	-4.3×10^5	5.1×10^5

Water column depth and distance offshore were plotted against total *Microcystis* (Figure 13). The relationship between the distance offshore and total *Microcystis* was not significant (R^2 = 9.8 x 10^{-3} and p=0.46). The relationship between the depth and total *Microcystis* was also not significant (R^2 = 2.0 x 10^{-3} and p=0.74). However, plotting depth against distance suggests that there is a bimodal distribution of data and that there tends to be an increase in cell abundance between 5 and 7 meters.

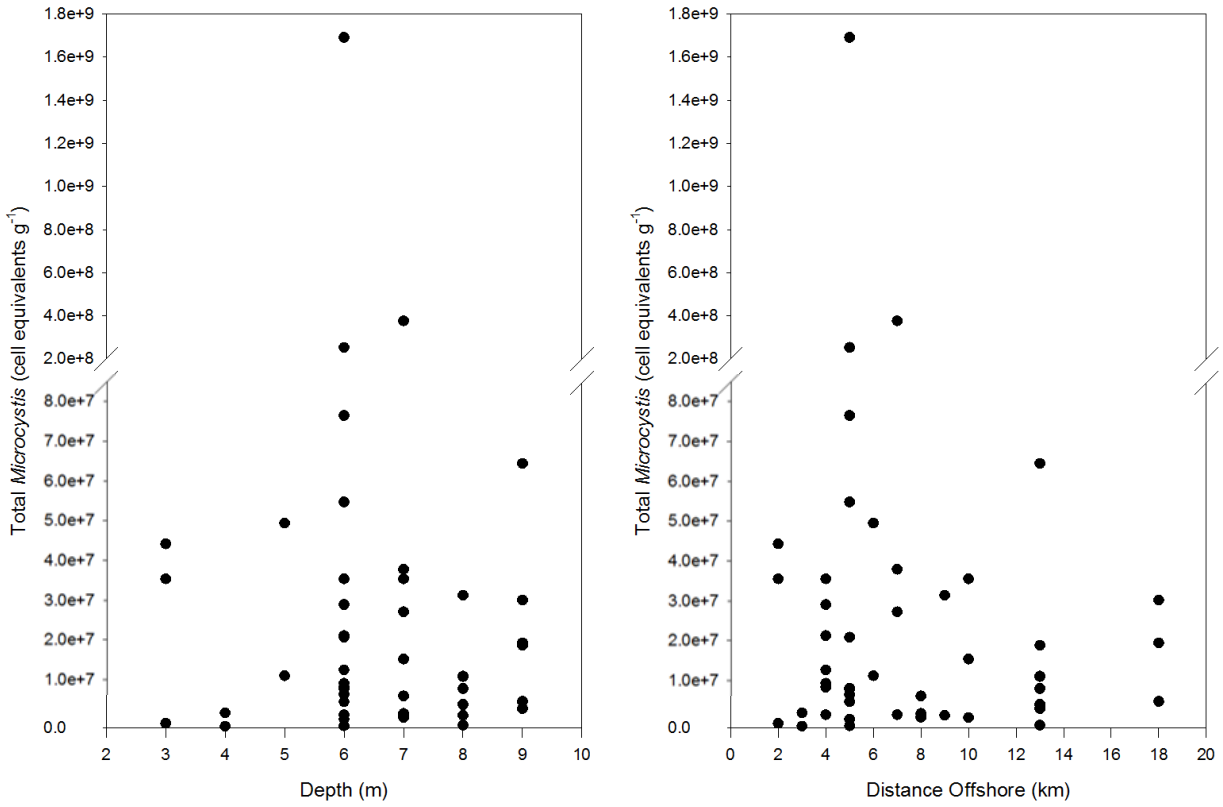

Figure 13- Total Microcystis *(cell equivalents g^{-1}) versus depth (m) and versus distance offshore (km).*

4.1.1 Sediment Pigment Analysis

Summary statistics for pigment analyses for all sampling time points are featured in Table 6. The concentration of phycocyanin and chlorophyll α exhibited large variations across seasons and between years (Table 6; Figure 14; Figure 15). Chlorophyll α declined by 56 and 22 %, respectively between two over-winter pairs. Phycocyanin slightly increased across the first winter-spring pair but then showed a similar 23% decline as chlorophyll α in the second year. The phycocyanin concentration in November 2015 was more than twice the level in November

2014, perhaps reflecting the large HABs bloom of that year even though it was not noted in the cell abundance or chlorophyll α values.

The Mann-Whitney Rank Sum test indicated a significant difference in chlorophyll α between April 2015 and November 2015 as well as April 2015 and April 2016. There were also significant differences in phycocyanin between November 2014 and November 2015, April 2015 and November 2015, April 2015 and April 2016, November 2015 and April 2016.

Table 6- Summary statistics for chlorophyll α and phycocyanin analyses. Note that units are per milligram wet weight.

	Chlorophyll α			Phycocyanin		
Time	Average (µg/g)	Min (µg/g)	Max (µg/g)	Average (µg/g)	Min (µg/g)	Max (µg/g)
Nov-14	6.96 ± 9.48	1.62	33.24	0.16 ± 0.07	0.08	0.31
Apr-15	3.94 ± 1.89	2.13	9.87	0.18 ± 0.19	0.00	0.67
Nov-15	6.35 ± 2.86	1.78	11.52	0.35 ± 0.11	0.17	0.65
Apr-16	5.00 ± 1.97	1.00	8.93	0.27 ± 0.07	0.18	0.40

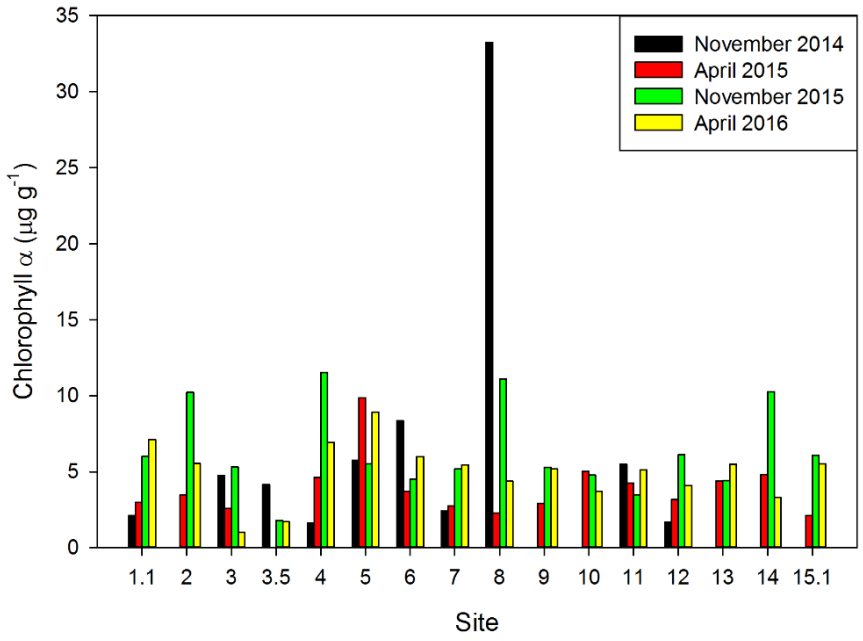

Figure 14- Chlorophyll α (µg/g wet weight) across the sampling extent and for all sampling periods.

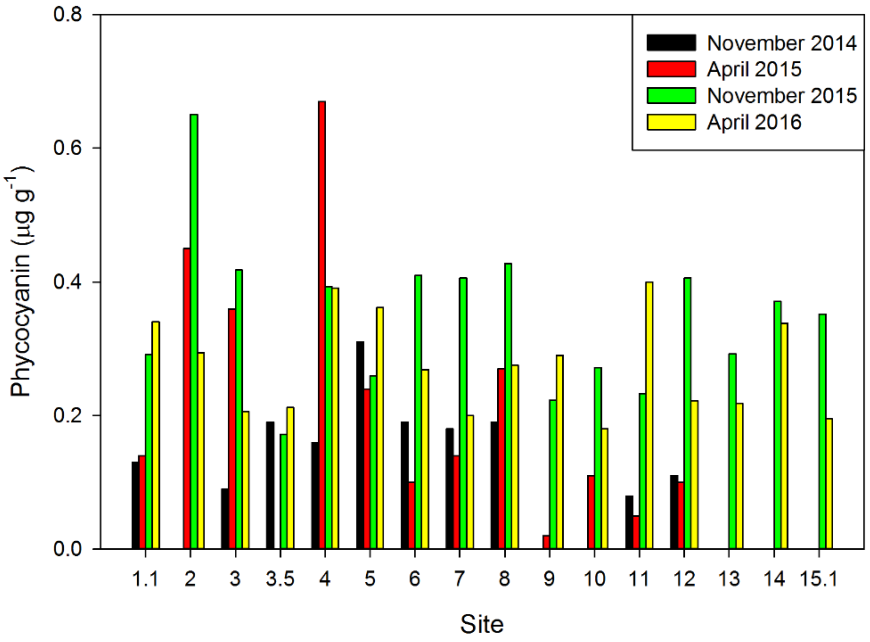

Figure 15- Phycocyanin (µg/g wet weight) across the sampling extent and for all sampling periods.

Pigment concentrations were plotted against total *Microcystis* (Figure 16). The relationship was not significant between either variable and total *Microcystis* abundance (for chlorophyll α, R^2= 1.3 x 10^{-4} and p=0.93; for phycocyanin, R^2= 1.6 x 10^{-3} and p=0.77).

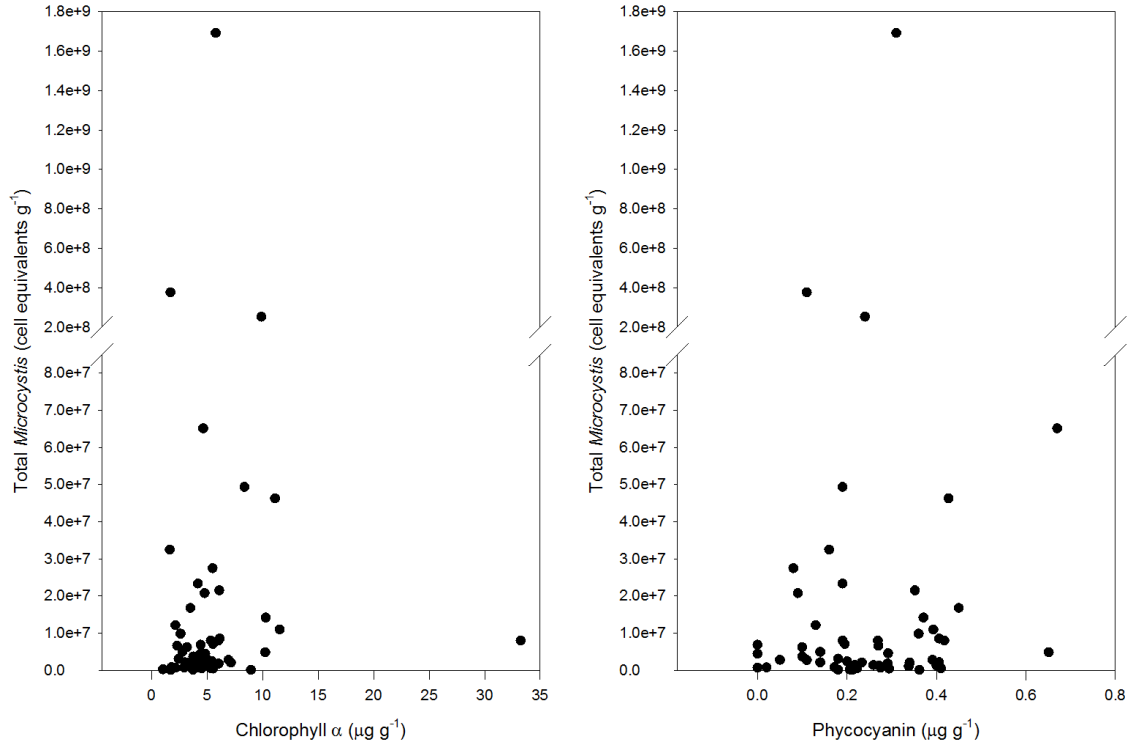

Figure 16- Total Microcystis (cell equivalents g^{-1}) versus chlorophyll α (µg g^{-1}) and total Microcystis (cell equivalents g^{-1}) versus phycocyanin (µg g^{-1})

4.1.2 Sediment Nutrient Analysis

Summary statistics for sediment nutrient analyses are shown in Table 7 and concentrations for all sampling time points are shown in Figures 17-19. Total phosphorus (TP) did not show a significant change between fall and winter, but concentrations during the second year were nearly 20% lower. Particulate organic carbon (POC) averaged about an 8% decline across the two winters and a similar decline for the second year, Particulate organic nitrogen (PON) showed the greatest decline between fall and spring, averaging 15%. PON in the second sampling year was about 5% lower than the first year. Ratios of C:N across all sampling events ranged from 11 to 57, with an average C:N ratio of 17 (Table 8).

The Mann-Whitney Rank Sum test indicated that, for all three measured nutrients, there was no statistical difference.

Table 7- Summary statistics for nutrient analysis. Note that units are per milligram dry weight.

	TP			PON			POC		
Time	Average (µg P/mg)	Min (µg P/mg)	Max (µg P/mg)	Average (µg N/mg)	Min (µg N/mg)	Max (µg N/mg)	Average (µg C/mg)	Min (µg C/mg)	Max (µg C/mg)
Nov-14	0.87 ± 0.17	0.61	1.11	2.57 ± 0.89	1.06	4.29	36.73 ± 5.28	27.28	46.62
Apr-15	0.83 ± 0.18	0.51	1.11	2.17 ± 0.71	0.87	3.56	32.99 ± 8.61	20.80	48.33
Nov-15	0.70 ± 0.18	0.31	0.95	2.44 ± 1.02	0.59	3.99	33.14 ± 10.99	15.82	56.10
Apr-16	0.71 ± 0.21	0.28	0.99	2.12 ± 0.96	0.41	3.26	31.56 ± 8.09	15.34	38.87

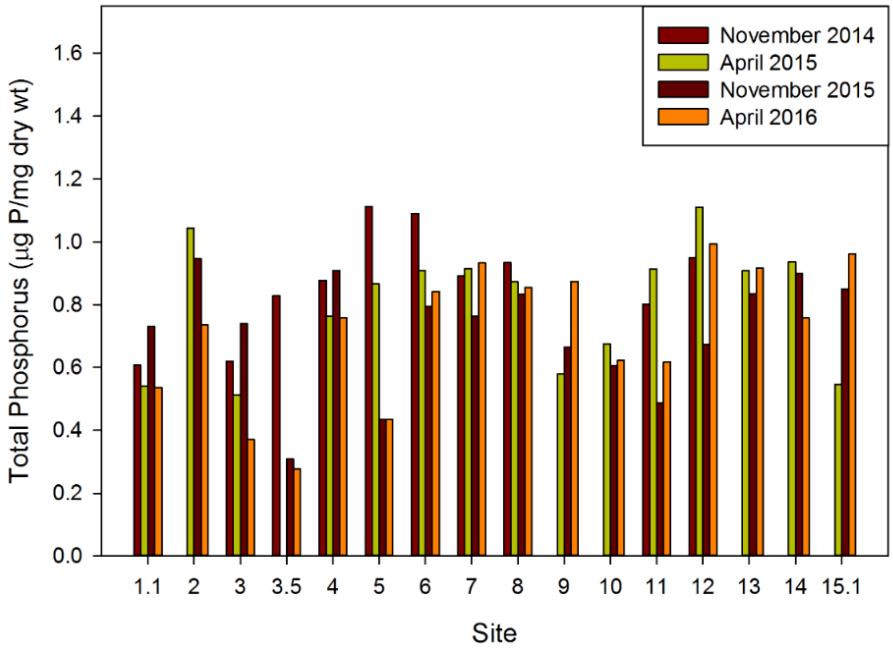

Figure 17- Total phosphorus content (µg P/mg dry weight) of sediment across space and time.

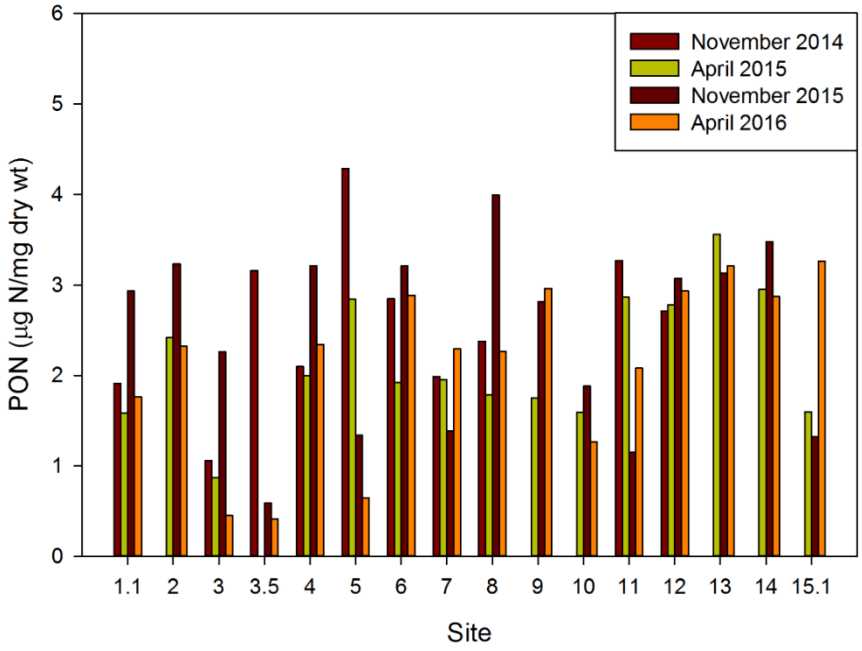

Figure 18- Particulate organic nitrogen content (µg N/mg dry weight) of sediment across space and time.

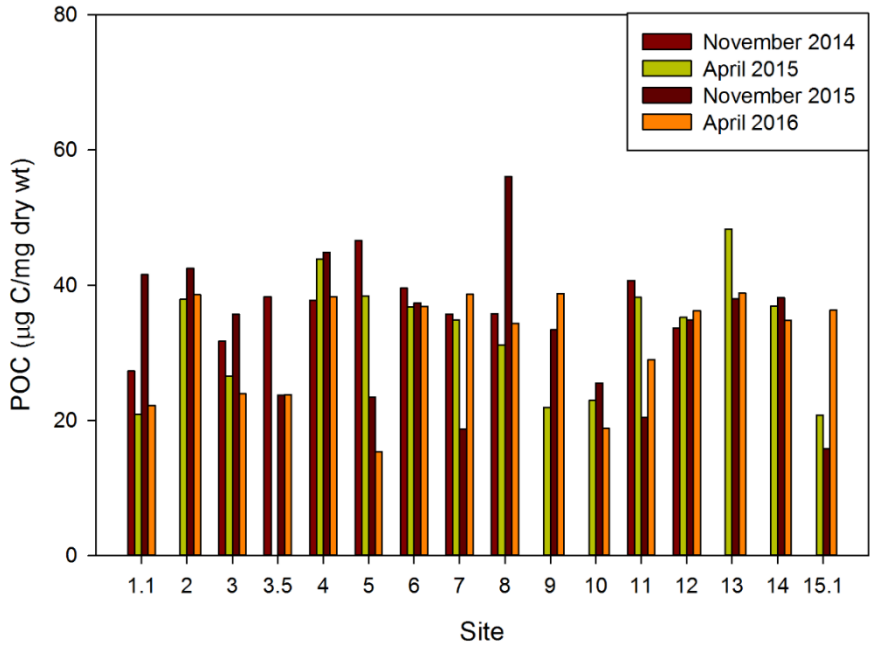

Figure 19- Particulate organic carbon content (µg C/mg dry weight) of sediment across space and time.

Table 8- C:N ratios of sediments across space and time. Ratios from 4-10 typically indicate autochthonous material (i.e. algae) and ratios >20 typically indicate allochthonous material (i.e. terrestrial organic matter). Samples that were not collected are indicated by "ND" (i.e. "No data").

	C:N Ratio			
Site	Nov-14	Apr-15	Nov-15	Apr-16
1.1	14	13	14	13
2	ND	16	13	17
3	30	31	15	53
3.5	12	ND	40	57
4	18	22	14	16
5	11	14	17	24
6	14	19	12	13
7	18	18	13	17
8	15	17	14	15
9	ND	13	12	13
10	ND	14	14	15
11	12	13	18	14
12	12	13	11	12
13	ND	14	12	12
14	ND	13	11	12
15.1	ND	13	12	11

The C:N ratios across space and time are within expected values. Ratios between 4 and 10 typically indicate autochthonous sources of organic matter (i.e. algae) and ratios >20 typically indicate allochthonous sources of organic matter (i.e. terrestrial organic matter) (Kaushal & Binford, 1999). Site 3 and Site 3.5 are both located near Maumee Bay and therefore are expected to have higher C:N ratios due the influence of the Maumee River and the allochthonous organic matter it delivers.

Nutrient concentrations were plotted against total *Microcystis* (Figure 20). The relationship between PON and total *Microcystis* was significant, but PON only explains 10% of the variance in total *Microcystis* abundance ($R^2 = 0.11$ and $p=0.01$). The relationship between POC and total *Microcystis* was not significant ($R^2 = 0.06$ and $p=0.07$).

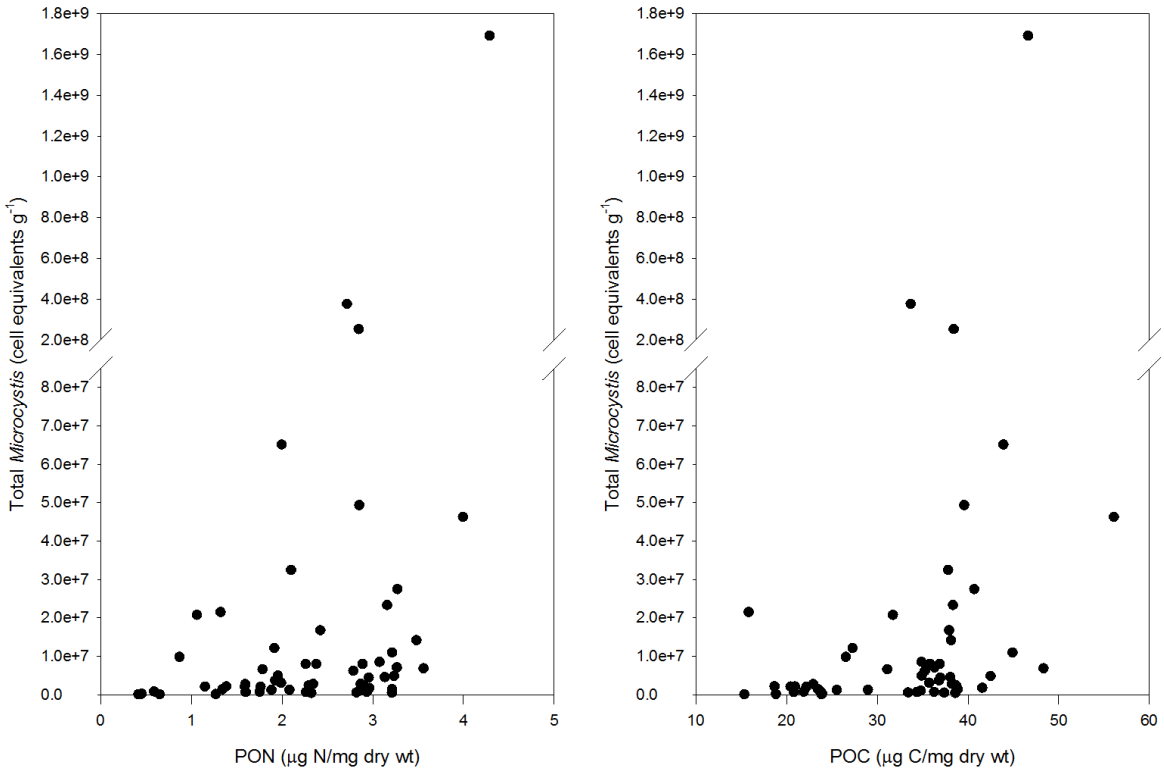

Figure 20- Total Microcystis (cell equivalents g^{-1}) versus particulate organic nitrogen (PON, µg N/mg dry weight) and total Microcystis (cell equivalents g^{-1}) versus particulate organic carbon (POC, µg C/mg dry weight).

4.2 Culture Experiments

Culture experiments were conducted for samples collected in April 2015, November 2015, and April 2016. As mentioned previously, culture experiments contained two components: the recruitment flasks, which were completed for all sampling events and in which changes in *Microcystis* over time were the result of both recruitment and growth processes, and the growth rate flasks, which were completed once in November 2015 and in which changes in *Microcystis* populations over time were the result of growth processes exclusively.

Culture data is separated into two sets of comparisons for ease of analysis: week 2 versus week 4 (t_2 vs t_4) and week 4 versus week 6 (t_4 vs t_6). In comparisons of t_2 versus t_4 (e.g. Figure 21), the t_2 values are corrected for dilution and the t_4 values are the original values. In comparisons of t_4 versus t_6 (i.e. Figure 22), the t_4 values are corrected for dilution and the t_6 values are the original values.

4.2.1 Recruitment Flasks

In the April 2015 culture experiments, 13 of the 16 recruitment flasks demonstrated accumulation in total *Microcystis* from t_2 to t_4 (Figure 21a); 15 of the 16 recruitment flasks

demonstrated accumulation in potentially-toxic *Microcystis* in the same time period (Figure 21b). From t_4 to t_6, 12 of the 16 recruitment flasks demonstrated further accumulation in total *Microcystis* (Figure 22a); 8 of the 16 recruitment flasks demonstrated accumulation in potentially-toxic *Microcystis* in the same period (Figure 22b).

At t_2, total *Microcystis* ranged from 4.91 x 10^3 to 1.65 x 10^5 cell equivalents ml^{-1} g^{-1} ($\bar{x}$ = 1.6 x 10^5 ± 1.6 x 10^5) and toxic *Microcystis* ranged from 10 to 1.40 x 10^4 cell equivalents ml^{-1} g^{-1} ($\bar{x}$ = 1.3 x 10^4 ± 1.6 x 10^4). At t_4, total *Microcystis* ranged from 4.35 x 10^3 to 1.89 x 10^5 cell equivalents ml^{-1} g^{-1} ($\bar{x}$ = 1.2 x 10^5 ± 1.2 x 10^5) and toxic *Microcystis* ranged from 8.08 x 10^2 to 2.41 x 10^4 cell equivalents ml^{-1} g^{-1} ($\bar{x}$ = 1.8 x 10^4 ± 1.8 x 10^4). At t_6, total *Microcystis* ranged from 1.66 x 10^3 to 3.56 x 10^5 cell equivalents ml^{-1} g^{-1} ($\bar{x}$ = 1.5 x 10^5 ± 2.5 x 10^5) and toxic *Microcystis* ranged from 59 to 2.08 x 10^4 cell equivalents ml^{-1} g^{-1} ($\bar{x}$ = 1.7 x 10^4 ± 2.1 x 10^4).

The instances of greatest and lowest abundances of total *Microcystis* in the April 2015 cultures both occurred at t_6 (Site 1.1 and Site 6, respectively). The instance of greatest abundance of toxic *Microcystis* was at week t_4 (Site 1.1) and the lowest at t_2 (Site 5).

In the November 2015 culture experiments, 8 of the 16 recruitment flasks demonstrated accumulation in total *Microcystis* from t_2 to t_4 (Figure 21c); 11 of the 16 recruitment flasks demonstrated accumulation in potentially-toxic *Microcystis* in the same time period (Figure 21d). From t_4 to t_6, 13 of the 16 recruitment flasks demonstrated accumulation in in total *Microcystis* (Figure 22c); 13 of the 16 recruitment flasks demonstrated accumulation in potentially-toxic *Microcystis* in the same period (Figure 22d).

At t_2, total *Microcystis* ranged from 502 to 1.32 x 10^5 cell equivalents ml^{-1} g^{-1} ($\bar{x}$ = 1.1 x 10^5 ± 1.5 x 10^5) and toxic *Microcystis* ranged from 31 to 5.09 x 10^3 cell equivalents ml^{-1} g^{-1} ($\bar{x}$ = 5.1 x 10^3 ± 6.8 x 10^3). At t_4, total *Microcystis* ranged from 365 (Site 10) to 3.54 x 10^4 cell equivalents ml^{-1} g^{-1} ($\bar{x}$ = 4.8 x 10^4 ± 4.6 x 10^4) and toxic *Microcystis* ranged from 17 to 5.07 x 10^3 cell equivalents ml^{-1} g^{-1} ($\bar{x}$ = 5.9 x 10^3 ± 7.0 x 10^3). At t_6, total *Microcystis* ranged from 0 to 1.53 x 10^5 cell equivalents ml^{-1} g^{-1} ($\bar{x}$ = 1.6 x 10^5 ± 2.5 x 10^5) and toxic *Microcystis* ranged from 72 to 1.97 x 10^4 cell equivalents ml^{-1} g^{-1} ($\bar{x}$ = 2.5 x 10^4 ± 3.6 x 10^4).

The instances of greatest and lowest abundances of total *Microcystis* in the November 2015 cultures both occurred at t_6 (Site 3 and Site 15.1, respectively). The instances of greatest and lowest abundances of toxic *Microcystis* both also occurred at week t_6 (Site 3 and Site 13, respectively).

In the April 2016 culture experiments, 13 of the 16 recruitment flasks demonstrated accumulation in total *Microcystis* from t_2 to t_4 (Figure 21e); 12 of the 16 recruitment flasks demonstrated accumulation in potentially-toxic *Microcystis* in the same time period (Figure 21f). From t_4 to t_6, 12 of the 16 recruitment flasks demonstrated accumulation in in total *Microcystis* (Figure 22e); 10 of the 16 recruitment flasks demonstrated accumulation in potentially-toxic *Microcystis* in the same period (Figure 22f).

At t_2, total *Microcystis* ranged from 33 to 2.36 x 10^4 cell equivalents ml^{-1} g^{-1} ($\bar{x}$ = 1.52 x 10^4 ± 2.1 x 10^4) and toxic *Microcystis* ranged from 1 to 9.23 x 10^3 cell equivalents ml^{-1} g^{-1} ($\bar{x}$ =

3.0 x 10^3 ± 7.9 x 10^3). At t_4, total *Microcystis* ranged from 3.88 x 10^2 (Site 14) to 3.04 x 10^4 cell equivalents ml^{-1} g^{-1} ($\bar{x}$ = 2.8 x 10^4 ± 3.0 x 10^4) and toxic *Microcystis* ranged from 35 to 5.79 x 10^3 cell equivalents ml^{-1} g^{-1} (3.6 x 10^3 ± 5.5 x 10^3). At t_6, total *Microcystis* ranged from 5.40 x 10^2 to 5.25 x 10^4 cell equivalents ml^{-1} g^{-1} ($\bar{x}$ = 4.9 x 10^4 ± 6.0 x 10^4) and toxic *Microcystis* ranged from 5 to 8.21 x 10^3 cell equivalents ml^{-1} g^{-1} ($\bar{x}$ = 4.5 x 10^3 ± 8.1 x 10^3).

The instance of greatest abundance of total *Microcystis* in the April 2016 cultures was at t_6 (Site 9) and lowest at t_2 (Site 12). The instance of greatest abundance of toxic *Microcystis* was at t_2 (Site 4) and the lowest at t_6 (Site 2).

Across all three sets of culture experiments, sediments from the following sites (in order) tended to experience the greatest growth in total *Microcystis* in the first two weeks: 11, 1.1, 4, 3, and 3.5. However, the sites that tended to experience the greatest growth of potentially-toxic *Microcystis* were the following (in order): 11, 1.1, 4, 7, and 8.

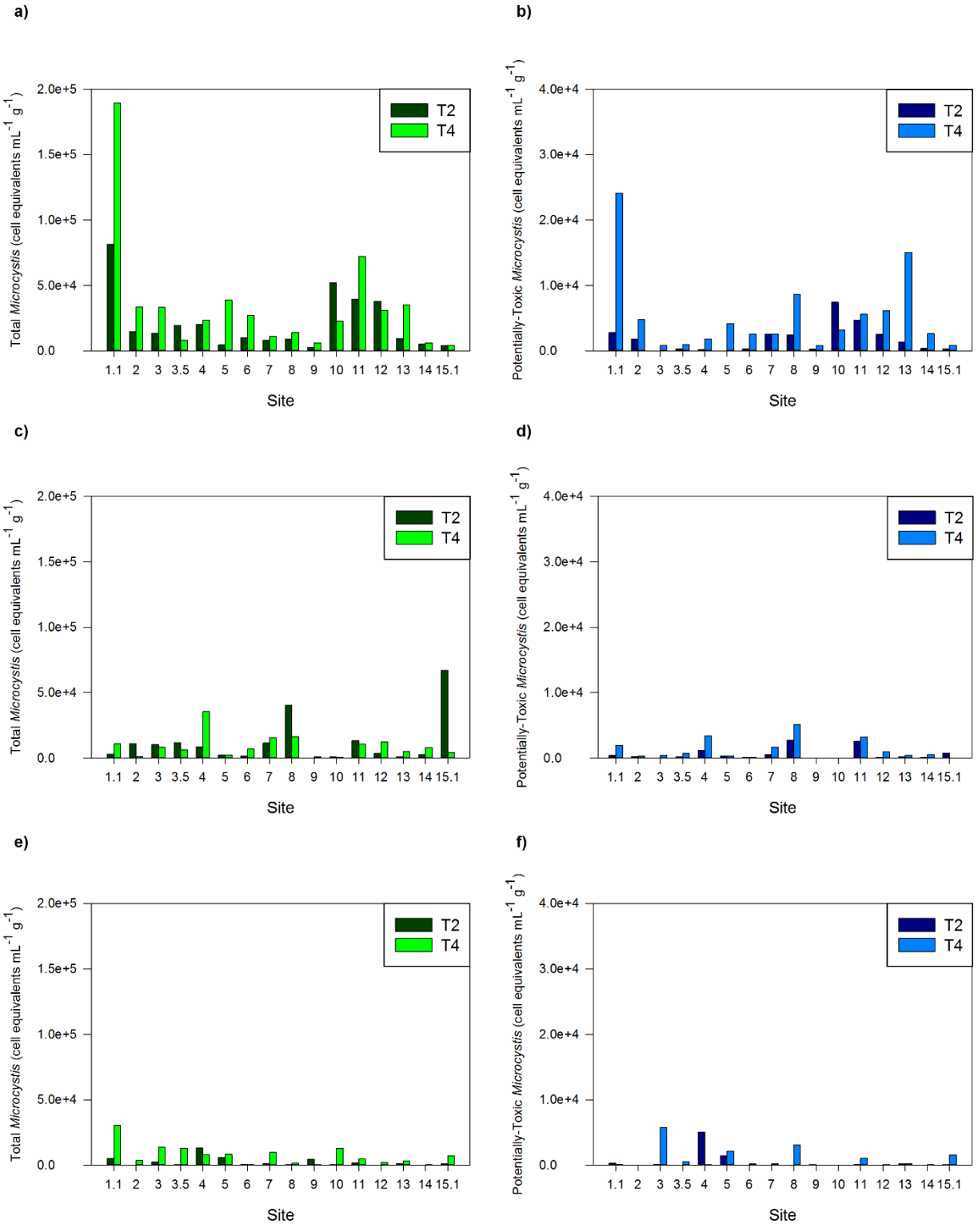

Figure 21- Results of culture experiments for April 2015 (a & b), November 2015 (c & d), and April 2016 (e & f) sampling events. Trends in both total and toxic Microcystis in each culture experiment varied across sites and seasons. Note that the axes for plots of toxic Microcystis are an order of magnitude less than those of total Microcystis.

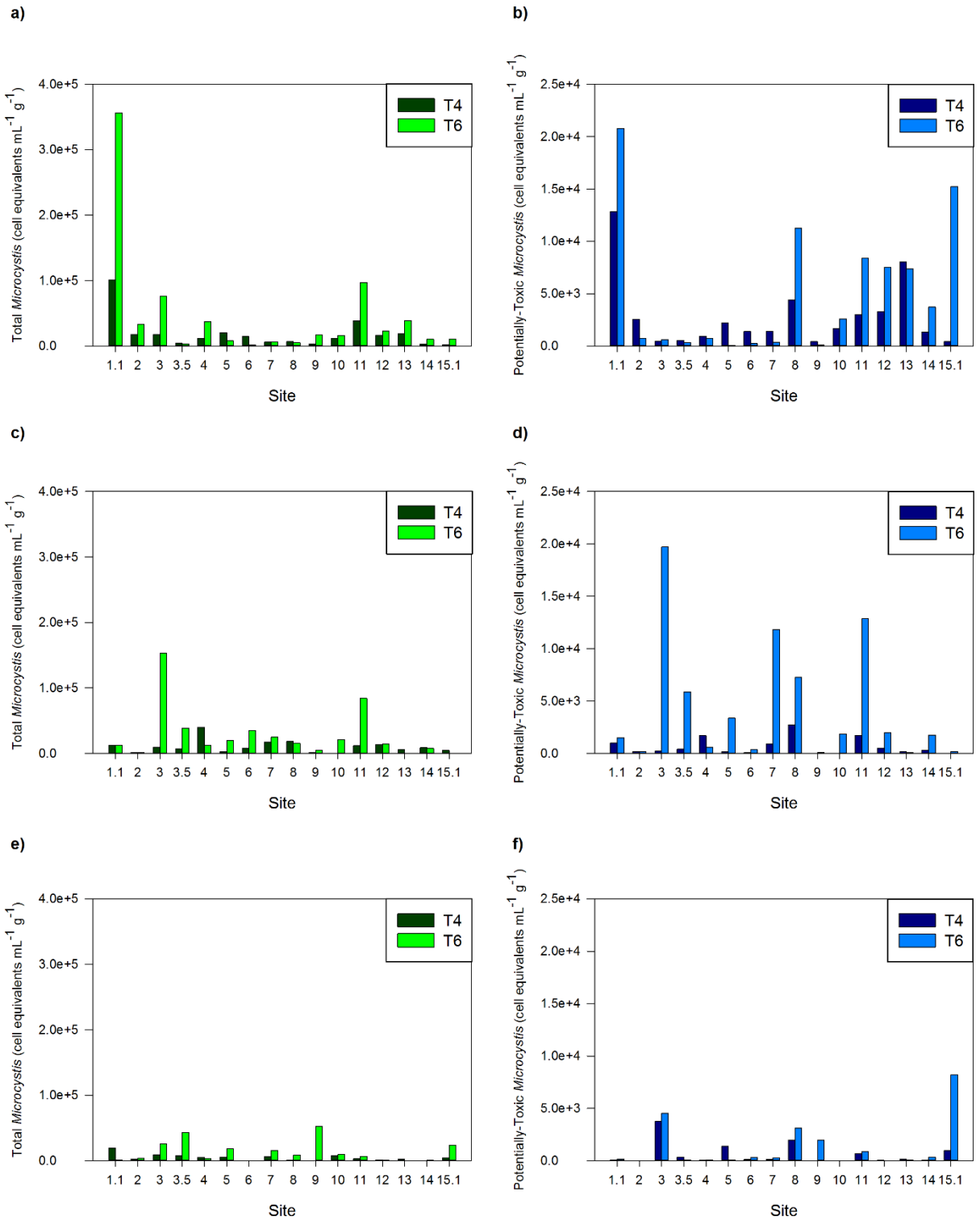

Figure 22- Results of culture experiments for April 2015 (a & b), November 2015 (c & d), and April 2016 (e & f) sampling events. Trends in both total and toxic Microcystis in each culture experiment varied across sites and seasons. Note that the axes for plots of toxic Microcystis are an order of magnitude less than those of total Microcystis

The percent of the total population that was potentially-toxic also varied across flasks and across time points (Figure 23). In April 2015 at t_6, the percent of potentially-toxic *Microcystis* exceeded 100% at Site 8 and Site 15.1 (220% and 143%, respectively). The percent of potentially-toxic *Microcystis* also exceeded 100% in April 2016 at t_4 at Site 8 (215%). Omitting cases in which the percent of potentially-toxic exceeded 100, the average fraction of potentially-toxic *Microcystis* for t_2, t_4, and t_6 was 9% ± 8%, 15% ± 13%, and 17% ± 24% respectively. The grand mean across all culture experiments was 14% ± 17%.

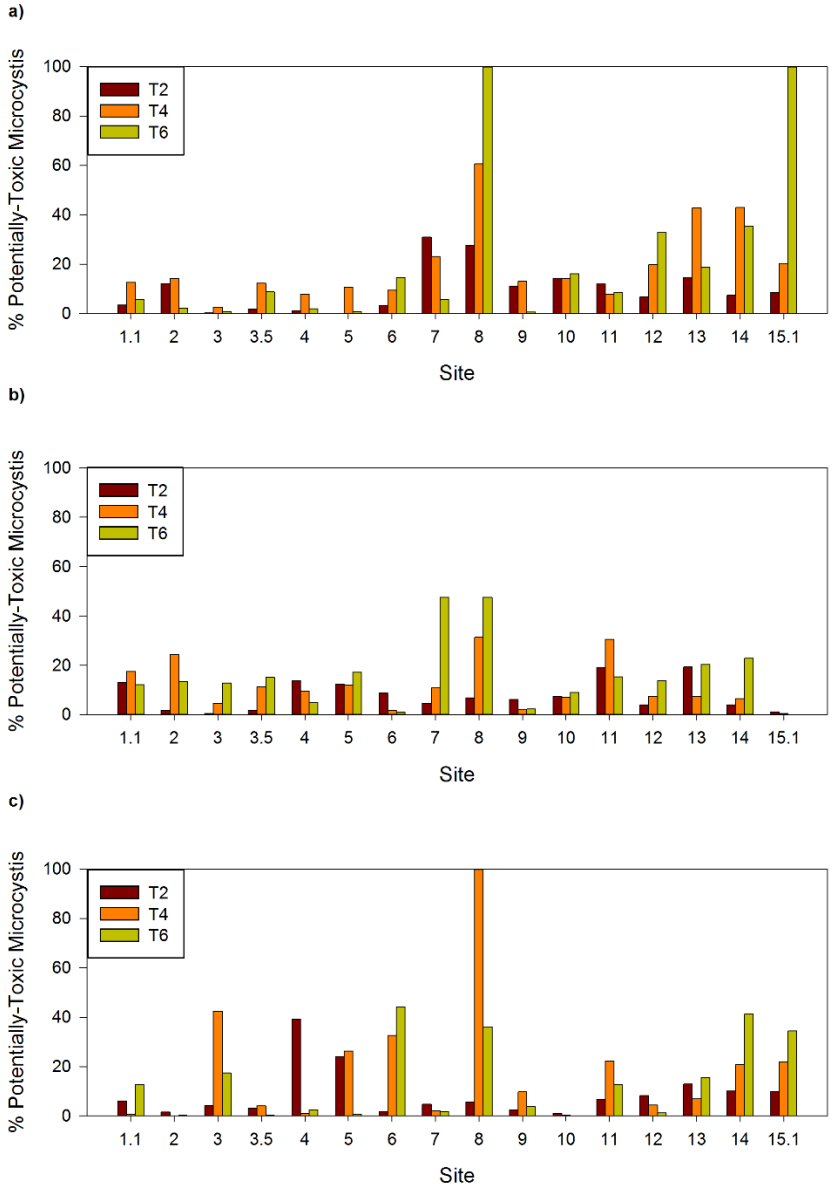

Figure 23- Percentage of potentially-toxic Microcystis *in recruitment flasks over the 6-week incubation period for a) April 2015 samples, b) November 2015 samples, and c) April 2016 samples. Note that some sites had values exceed 100%, suggesting that those samples have high percentages of potentially-toxic* Microcystis *such that measurement error caused them to exceed the total amount of* Microcystis.

Calculated accumulation rates are summarized in Table 9 and Table 10.

From t_0 to t_2, the average accumulation rate of total *Microcystis* was 6.7×10^3 cell equivalents mL^{-1} day^{-1} ($\pm 9.8 \times 10^3$). From t_2 to t_4, the average accumulation rate was 2.2×10^3 cell equivalents mL^{-1} day^{-1} ($\pm 3.8 \times 10^3$). From t_4 to t_6, the average accumulation rate was 6.4×10^3 cell equivalents mL^{-1} day^{-1} ($\pm 1.3 \times 10^4$).

From t_0 to t_2, the average accumulation rate of potentially-toxic *Microcystis* was 4.9×10^2 cell equivalents mL^{-1} day^{-1} ($\pm 8.3 \times 10^2$). From t_2 to t_4, the average accumulation rate was 4.5×10^2 cell equivalents mL^{-1} day^{-1} ($\pm 8.0 \times 10^2$). From t_4 to t_6, the average accumulation rate was 8.4×10^2 cell equivalents mL^{-1} day^{-1} ($\pm 1.7 \times 10^3$).

Table 9- Accumulation rates of total Microcystis *for all recruitment flasks.*

		Accumulation Rate (cell equivalents mL^{-1} day^{-1})		
Date	Site	t_0 to t_2	t_2 to t_4	t_4 to t_6
April 2015				
	1.1	3.3×10^4	2.2×10^4	5.1×10^4
	2	7.4×10^3	4.1×10^3	3.3×10^3
	3	9.0×10^3	6.7×10^3	2.0×10^4
	3.5	3.0×10^4	0	0
	4	9.2×10^3	7.5×10^2	6.2×10^3
	5	2.0×10^3	7.9×10^3	0
	6	4.1×10^3	3.7×10^3	0
	7	3.5×10^3	6.8×10^2	76
	8	6.4×10^3	1.9×10^3	0
	9	9.8×10^2	7.1×10^2	2.8×10^3
	10	3.2×10^4	0	1.4×10^3
	11	1.6×10^4	7.2×10^3	1.3×10^4
	12	1.6×10^4	0	1.4×10^3
	13	3.8×10^3	5.5×10^3	4.4×10^3
	14	2.0×10^3	1.9×10^2	1.6×10^3
	15.1	1.6×10^3	97	1.9×10^3
	Mean	$1.1 \times 10^4 \pm 1.1 \times 10^4$	$3.8 \times 10^3 \pm 5.5 \times 10^3$	$6.7 \times 10^3 \pm 1.3 \times 10^4$
November 2015				
	1.1	1.5×10^3	2.2×10^3	1.8×10^3
	2	7.7×10^3	0	1.9×10^2
	3	8.7×10^3	0	6.7×10^4
	3.5	2.3×10^4	0	3.5×10^4
	4	6.0×10^3	1.0×10^4	0
	5	1.9×10^3	0	8.2×10^3
	6	8.3×10^2	1.8×10^3	9.6×10^3
	7	7.3×10^3	1.5×10^3	6.3×10^3
	8	2.6×10^4	0	2.3×10^3
	9	1.6×10^2	1.9×10^2	1.3×10^3
	10	5.4×10^2	0	6.5×10^3
	11	5.9×10^3	0	1.7×10^4
	12	2.4×10^4	3.3×10^3	2.8×10^3
	13	5.8×10^2	1.5×10^3	0
	14	1.8×10^3	2.0×10^3	1.1×10^3
	15.1	3.6×10^4	0	0
	Mean	$8.2 \times 10^3 \pm 1.1 \times 10^4$	$1.4 \times 10^3 \pm 2.5 \times 10^3$	$9.9 \times 10^3 \pm 1.8 \times 10^4$
April 2016				
	1.1	2.2×10^3	7.2×10^3	0
	2	20	9.2×10^2	2.9×10^2
	3	1.1×10^3	2.6×10^3	4.0×10^3
	3.5	2.6×10^2	3.8×10^3	1.1×10^4
	4	5.7×10^3	0	0
	5	2.7×10^3	5.4×10^2	3.2×10^3
	6	3.1×10^2	0	1.0×10^2
	7	5.1×10^2	2.2×10^3	2.4×10^3
	8	1.9×10^2	2.9×10^2	2.1×10^3
	9	2.0×10^3	0	1.3×10^4
	10	1.9×10^2	3.1×10^3	2.9×10^2
	11	7.8×10^2	7.8×10^2	9.9×10^2
	12	12	7.1×10^2	0
	13	7.0×10^2	5.3×10^2	0
	14	1.5×10^2	14	1.4×10^2
	15.1	5.0×10^2	1.6×10^3	5.0×10^3
	Mean	$1.1 \times 10^3 \pm 1.5 \times 10^3$	$1.5 \times 10^3 \pm 1.9 \times 10^3$	$2.7 \times 10^3 \pm 4.0 \times 10^3$
	Grand Mean	$6.7 \times 10^3 \pm 9.8 \times 10^3$	$2.2 \times 10^3 \pm 3.8 \times 10^3$	$6.4 \times 10^3 \pm 1.3 \times 10^4$

Table 10- Accumulation rates of potentially-toxic Microcystis *for all recruitment flasks.*

		Accumulation Rate (cell equivalents mL^{-1} day^{-1})		
Date	Site	t_0 to t_2	t_2 to t_4	t_4 to t_6
April 2015				
	1.1	1.2×10^3	4.3×10^3	1.6×10^3
	2	9.1×10^2	6.4×10^2	0
	3	34	2.7×10^2	63
	3.5	5.6×10^2	5.4×10^2	0
	4	98	3.9×10^2	0
	5	2	9.5×10^2	0
	6	1.4×10^2	4.8×10^2	0
	7	1.1×10^3	13	0
	8	1.8×10^3	2.3×10^3	2.5×10^3
	9	1.1×10^2	1.0×10^2	0
	10	4.6×10^3	0	3.0×10^2
	11	1.9×10^3	1.9×10^2	1.2×10^3
	12	1.1×10^3	8.3×10^2	9.7×10^2
	13	5.5×10^2	2.9×10^3	0
	14	1.5×10^2	4.8×10^2	5.1×10^2
	15.1	1.3×10^2	1.2×10^2	3.3×10^3
	Mean	$8.9 \times 10^2 \pm 1.2 \times 10^3$	$9.0 \times 10^2 \pm 1.2 \times 10^3$	$6.5 \times 10^2 \pm 1.0 \times 10^3$
November 2015				
	1.1	2.0×10^2	4.2×10^2	1.4×10^2
	2	1.5×10^2	33	
	3	40	1.5×10^2	8.8×10^3
	3.5	3.6×10^2	5.1×10^2	5.4×10^3
	4	8.3×10^2	8.1×10^2	0
	5	2.3×10^2	0	1.4×10^3
	6	73	1	91
	7	3.4×10^2	4.4×10^2	4.1×10^3
	8	1.8×10^3	8.2×10^2	1.6×10^3
	9	10	0	29
	10	40	0	5.8×10^2
	11	1.1×10^3	1.5×10^2	2.5×10^3
	12	96	3.0×10^2	5.4×10^2
	13	1.1×10^2	80	0
	14	71	1.6×10^2	5.4×10^2
	15.1	4.1×10^2	0	48
	Mean	$3.7 \times 10^2 \pm 4.9 \times 10^2$	$2.4 \times 10^2 \pm 2.8 \times 10^2$	$1.7 \times 10^3 \pm 2.5 \times 10^3$
April 2016				
	1.1	1.3×10^2	0	18
	2	0	0	0
	3	46	1.3×10^3	1.8×10^2
	3.5	8	1.6×10^2	0
	4	2.2×10^3	0	4
	5	6.6×10^2	1.7×10^2	0
	6	5	44	57
	7	24	40	37
	8	11	8.4×10^2	3.1×10^2
	9	48	0	4.9×10^2
	10	2	9	0
	11	53	2.4×10^2	54
	12	1	31	0
	13	90	14	0
	14	15	12	69
	15.1	50	3.7×10^2	1.9×10^3
	Mean	$2.1 \times 10^2 \pm 5.6 \times 10^2$	$2.0 \times 10^2 \pm 3.7 \times 10^2$	$1.9 \times 10^2 \pm 4.7 \times 10^2$
	Grand Mean	$4.9 \times 10^2 \pm 8.3 \times 10^2$	$4.5 \times 10^2 \pm 8.0 \times 10^2$	$8.4 \times 10^2 \pm 1.7 \times 10^3$

4.2.2 Growth Rate Flasks

During the November 2015 culture experiments, additional subsamples were taken from 5 flasks (i.e. 2, 3, 6, 11, 15) during the regular biweekly subsampling at t_2 in effort to parse out the influence of growth versus recruitment accumulation of cells within the overlying water. The grand mean of the total growth rates was 0.17 days^{-1} and the grand mean of the potentially-toxic growth rate was 0.09 days^{-1}.

All 5 growth rate flasks experienced growth in total and potentially-toxic *Microcystis* from t_2 to t_4 (Figure 24; Figure 25; Figure 26). However, 4 of the corresponding recruitment flasks experienced a decrease in total *Microcystis* abundance and the remaining flask experienced negligible growth. While the corresponding recruitment flasks experienced reductions in total *Microcystis*, there was growth in the concentration of potentially-toxic *Microcystis* in 3 of the flasks.

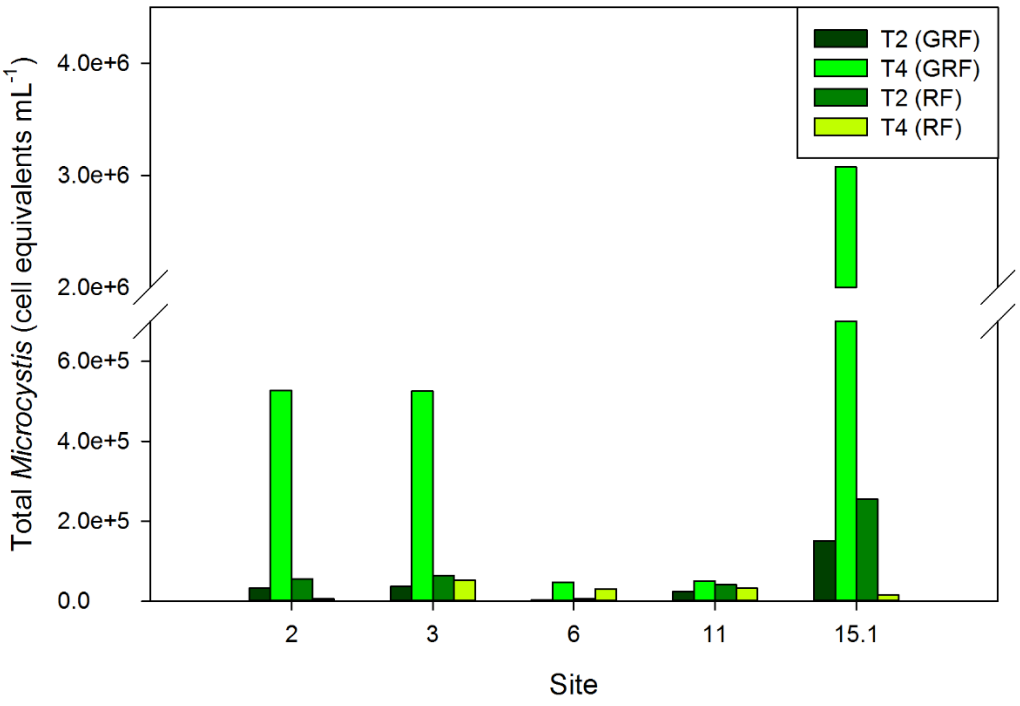

Figure 24- Change in total Microcystis *abundance in growth rate flasks (GRF) versus corresponding recruitment flasks (RF).*

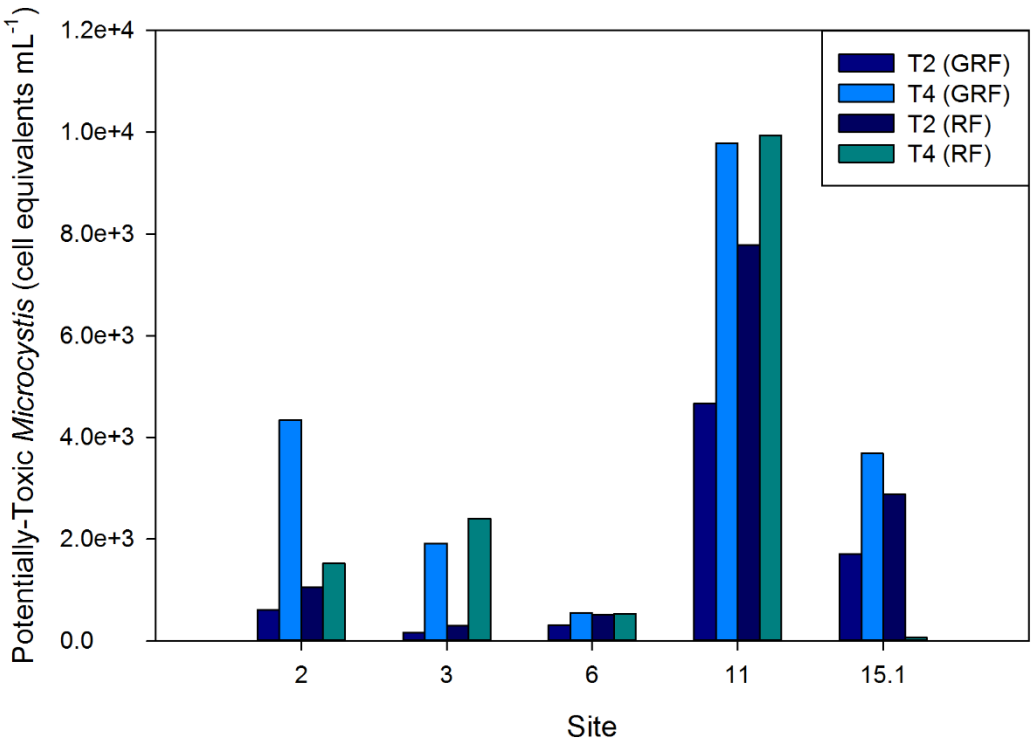

Figure 25- Change in potentially-toxic Microcystis *abundance in growth rate flasks (GRF) versus corresponding recruitment flasks (RF). Note that the scale of the axis is an order of magnitude less than that of the previous graph depicting total* Microcystis.

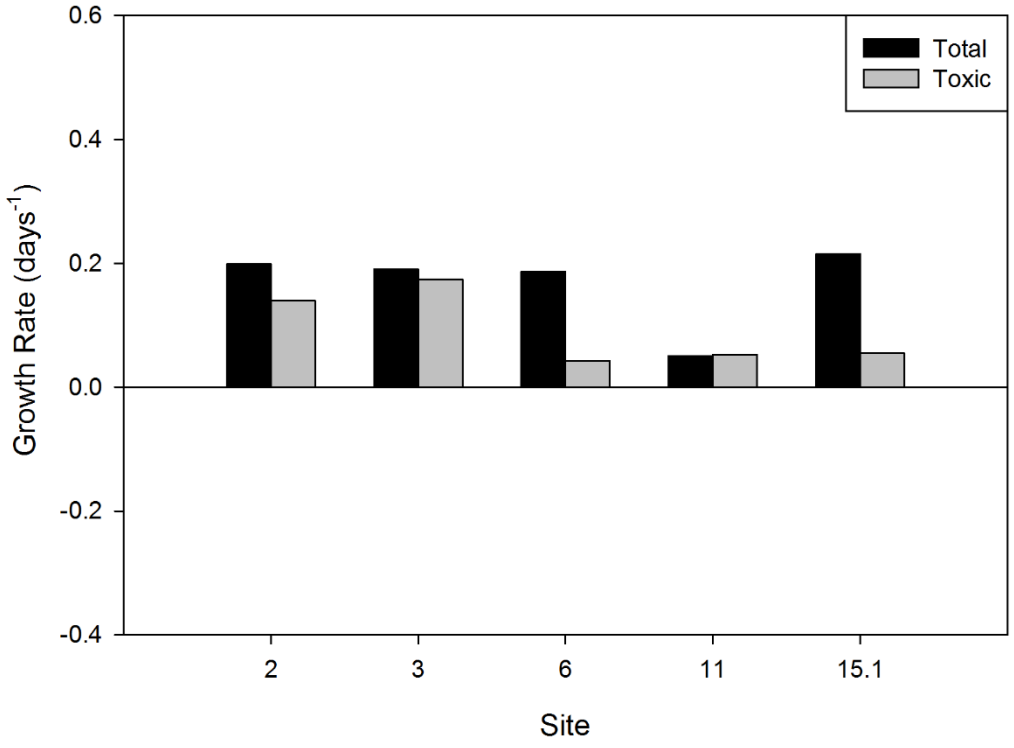

Figure 26- Calculated growth rates of total and potentially-toxic Microcystis *for growth rate flasks*

4.2.3 Apparent Accumulation Rates in Recruitment Flasks

To generate comparative growth rates based on the total observed increase in cell abundance from both recruitment and growth, results from the recruitment flasks were forced into the growth rate equation used to calculate rates for the growth rate flasks. The new accumulation rates (days^{-1}) across each 2-week interval for April 2015, November 2015, and April 2016 cultures are shown in Figure 27, Figure 28, Figure 29, respectively, and summarized in Table 11. Accumulation rates were not calculated from t_0 to t_2 due to uncertainty in what percentage of the sediment population initially inoculated the overlying water in the recruitment flasks.

The total *Microcystis* accumulation rates calculated using the growth rate formula varied from <0 to 0.38 day^{-1}. The potentially-toxic *Microcystis* accumulation rates calculated using the growth rate formula varied from <0 to 0.48 day^{-1}. The grand mean of the total accumulation rates was 0.10 day^{-1} and the grand mean of the toxic accumulation rates was 0.12 day^{-1}.

Table 11- Summary statistics of apparent accumulation rates (day^{-1}) of both total and potentially-toxic Microcystis.

		Apparent Total Accumulation Rate			Apparent Toxic Accumulation Rate		
Date	Interval	Average	Max	Min	Average	Max	Min
April 2015							
	t_2 to t_4	0.15	0.34	0.01	0.18	0.36	0.02
	t_4 to t_6	0.10	0.38	0.01	0.08	0.31	0.01
	t_2 to t_6	0.13	0.38	0.01	0.13	0.36	0.01
Nov 2015							
	t_2 to t_4	0.09	0.13	0.02	0.08	0.15	0.00
	t_4 to t_6	0.13	0.28	0.00	0.17	0.36	0.03
	t_2 to t_6	0.11	0.28	0.00	0.12	0.36	0.00
April 2016							
	t_2 to t_4	0.05	0.15	0.01	0.13	0.48	0.00
	t_4 to t_6	0.07	0.12	0.00	0.08	0.25	0.02
	t_2 to t_6	0.06	0.15	0.00	0.11	0.48	0.00
	Grand Mean	0.10			0.12		

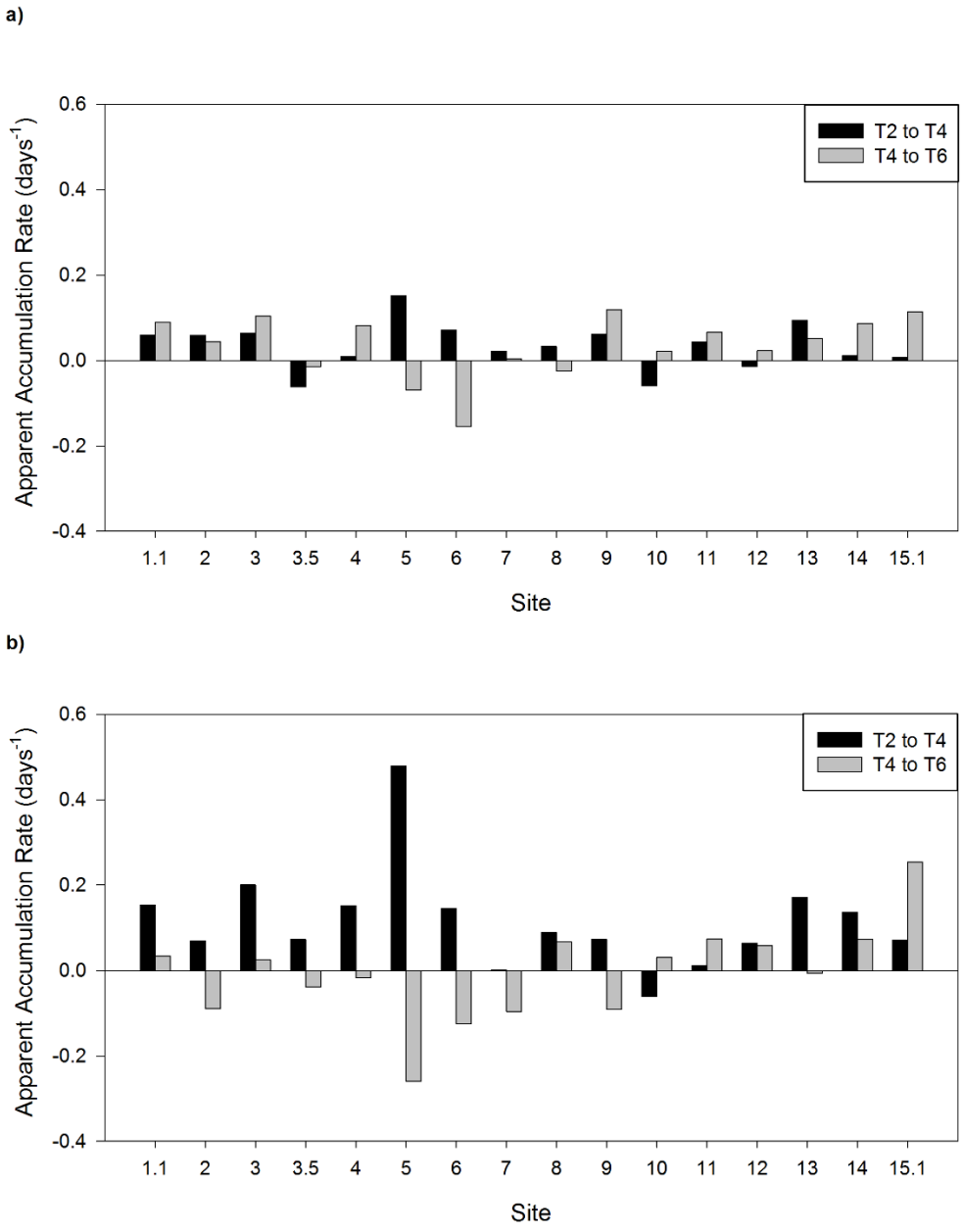

Figure 27- Apparent accumulation rates of a) total and b) potentially-toxic Microcystis *from April 2015 sampling.*

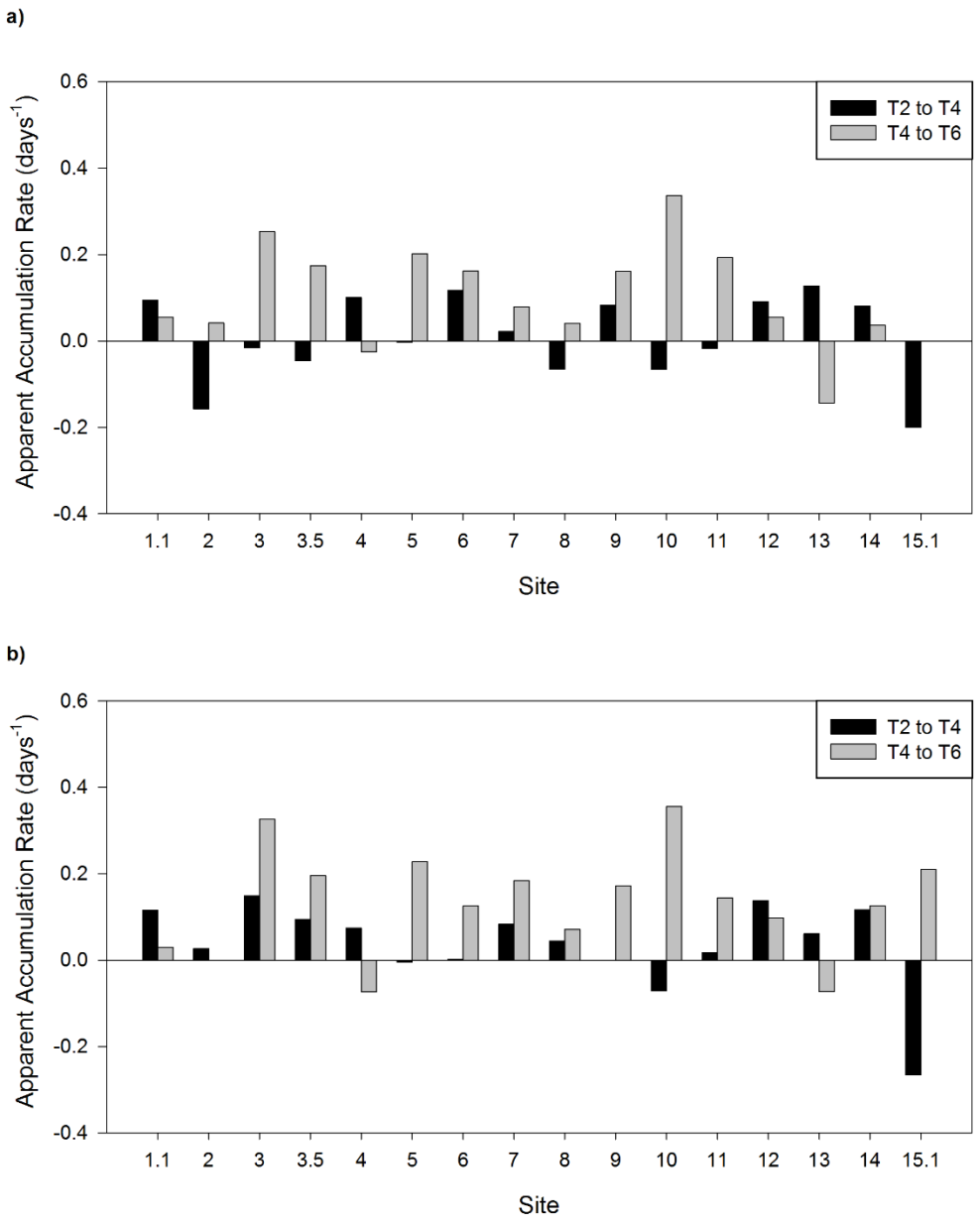

Figure 28- Apparent accumulation rates of a) total and b) potentially-toxic Microcystis *from November 2015 sampling event.*

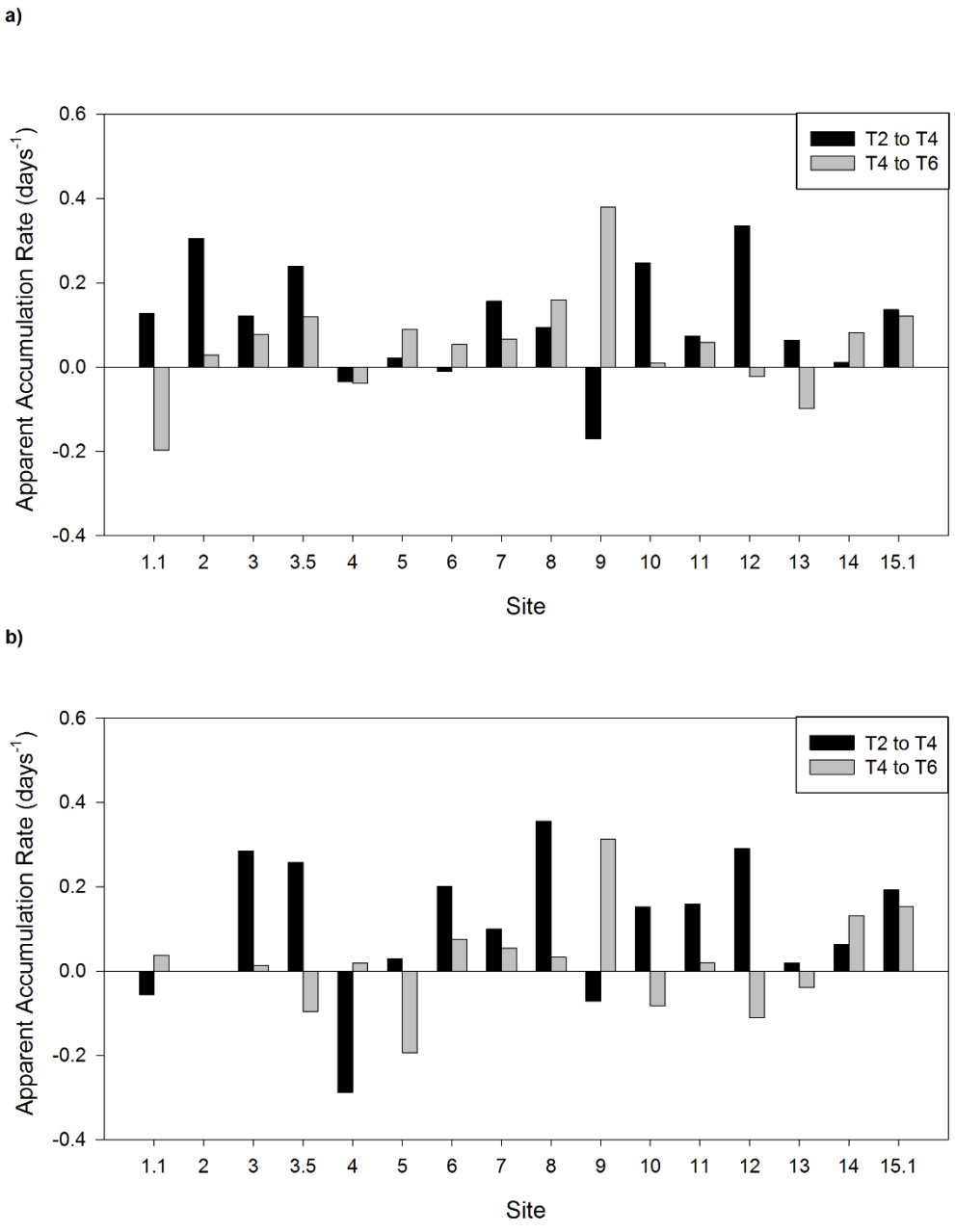

Figure 29- Apparent accumulation rates of a) total and b) potentially-toxic Microcystis *for April 2016 sampling event.*

5. Discussion

5.1 Spatial and Temporal Variation in Sediment Abundance

Across both sampling years, total *Microcystis* decreased from November to April by two or more orders of magnitude. The mortality of cells throughout the overwintering period reflects the results of pre-existing literature (Tsujimura et al., 2000; Brunberg and Blomqvist, 2002; Brunberg and Blomqvist, 2003; Verspagen et al., 2005; Rinta-Kanto et al., 2009; Latour et al., 2007). However, when considering all sampling periods relative to November 2014, the abundance of total *Microcystis* was considerably greater in November 2014 compared to subsequent sampling periods.

As with total *Microcystis*, the abundance of potentially-toxic *Microcystis* decreased from November to April in both sampling years. However, despite having lower total *Microcystis* abundance than the samples from November 2014, samples from November 2015 yielded a greater amount of potentially-toxic *Microcystis* across nearly the entire sampling extent. This is also reflected in the percent of potentially-toxic *Microcystis* numbers for the November 2015 sampling period. The elevated toxicity in November 2015 may have been the result of the Maumee River delivering larger loads of inorganic nitrogen to Western Lake Erie in 2015 and therefore promoting the dominance of toxic strains of *Microcystis* (Figure 30).

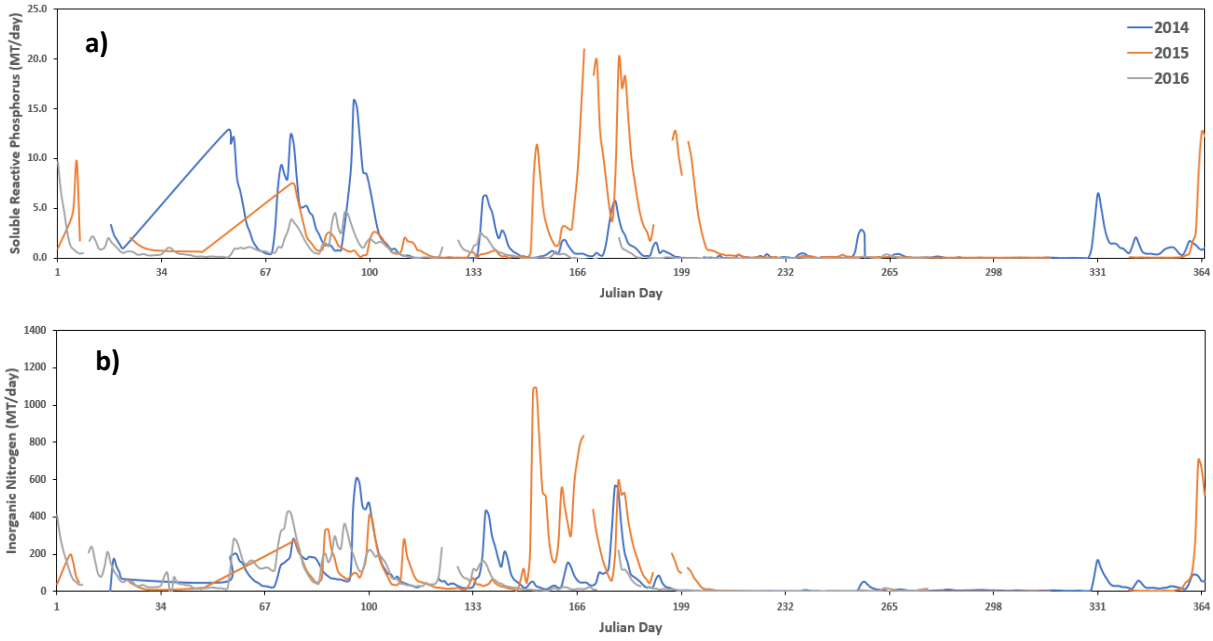

Figure 30- Daily loads for a) soluble reactive phosphorus (MT/day) and b) inorganic nitrogen (MT/day) were calculated based on daily discharge data taken by USGS at the Waterville, OH station and corresponding nutrient concentration data collected by Heidelberg University's National Center for Water Quality Research and calculation methodology as outlined by Obenour et al. (2014).

Surprisingly, the relative average abundance of total sediment *Microcystis* in the November following a bloom season did not seem to necessarily reflect the average annual bloom for that season. For example, the average annual bloom in 2015 had a CI value of 5 while

the average annual bloom in 2014 had a CI value of 1.5, where one CI equals 10^{20} cells (Stumpf et al., 2016). However, the average abundance of total *Microcystis* in the sediment was low in November 2015 relative to November 2014, even though 2015 was a substantially larger bloom year. In fact, the amount of total *Microcystis* in the sediment in November 2015 was not statistically different from the amount in the sediment preceding the bloom in April 2015. The October 1, 2015 Lake Erie HAB Bulletin disseminated by the Great Lakes Environmental Research Laboratory indicated that intense mixing and cold water led to the rapid weakening of the late season bloom [https://www.glerl.noaa.gov/res/HABs_and_Hypoxia/lakeErieHABArchive/bulletin_2015-024.pdf]; no such event was noted around the same time in 2014. This occurrence may have led to either reduced or diluted quantities of sediment *Microcystis* at the end of the 2015 bloom season despite the annual bloom being of greater magnitude.

In regard to spatial differences in *Microcystis* abundance, a high amount of variability existed between sites in all sampling events. A persistence map was generated by averaging the data for each site across all four sampling periods (Figure 31a). However, the sites that had the greatest and lowest average abundance across all four time points did not necessarily delineate where the previous or subsequent summer blooms persisted most. For example, even though Site 5 possessed the greatest abundance of total *Microcystis* by far in November 2015, the 2015 HAB Bloom persistence maps generated by the Michigan Tech Research Institute using remote sensed observations indicated that the bloom tended to persist less around Site 5 than many of the other site locations (Shuchman et al., 2016). This suggests that where summer blooms tend to persist most do not necessarily correspond to where the highest abundance of *Microcystis* cells end up in the sediment. A potential explanation for this could be that some site locations (e.g. 5) were more susceptible to resuspension and constant loss of freshly deposited cells, or that certain sites were exposed to higher amounts of tributary sediments coming from the Maumee River that would dilute the concentration of deposited cells. In both situations cells may have been deposited during the previous bloom period but there would be less immediately available on the surface to be recruit into the water column and contribute to the following summer blooms.

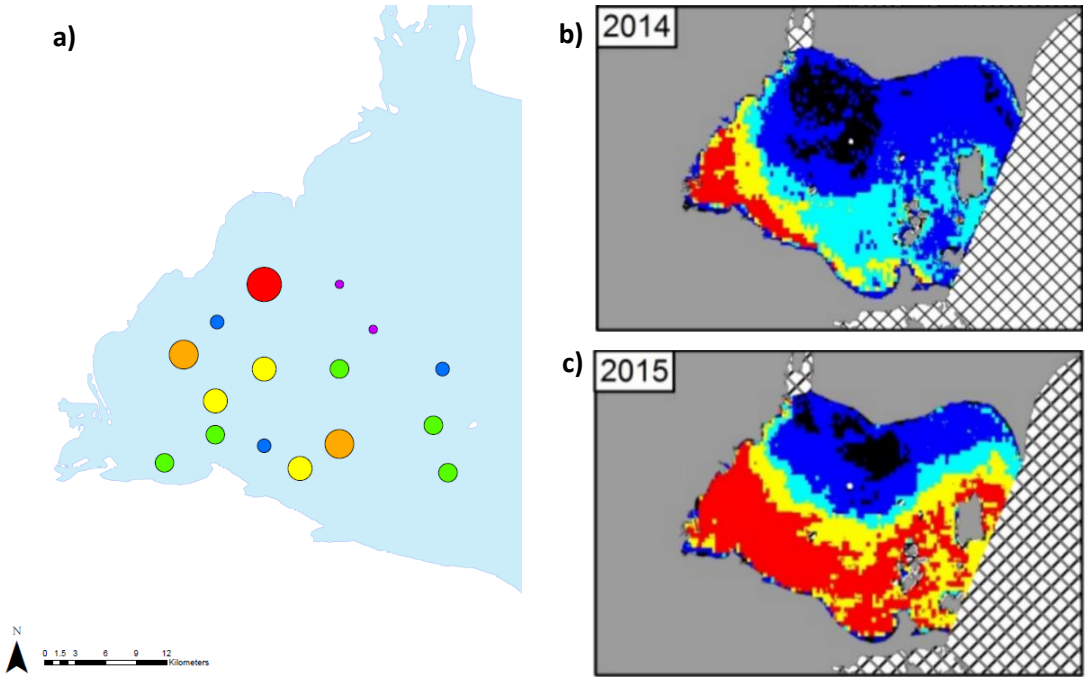

Figure 31- a) A persistence map of the relative abundance of total Microcystis *by site compared to HABs Time Series persistence map generated by the Michigan Tech Research Institute for b) 2014 and c) 2015.*

Also, despite the large differences in total and potentially-toxic *Microcystis* between sites, apart from PON, there was no relationship between site abundance and other measured parameters (i.e. chlorophyll α, phycocyanin, POC, distance offshore, and depth). It is particularly surprising that neither depth or distance offshore correlated with the amount of total *Microcystis* since previous literature suggested that both of those variables tend correspond to the accumulation of total *Microcystis* in the sediment (Verspagen et al., 2005; Brunberg & Blomqvist, 2002). This absence of correlation could be due to the influence of other overwintering phytoplankton or organic matter that has accumulated in the sediment. Nevertheless, the lack of correlation between *Microcystis* abundance and the other parameters suggests that commonly used proxies for estimating *Microcystis* cell abundance in the water column are not appropriate for estimating cell abundance in the sediments.

5.2 Cultures

Trends in total *Microcystis* growth over time varied between flasks. Some cultures experienced continuous accumulation in total *Microcystis* over the 6-week incubation period; other flasks had initial spikes in total *Microcystis* concentrations, only to have concentrations decrease or remain constant over the remainder of the incubation period. Possible explanations for the cultures that did not show constant increases over time may have been related to some settling or sticking to the sides of the flask. The over-lying media was not continuously stirred or stirred immediately before sampling to keep the sediment from being resuspended during sub-sampling. While samples were not analyzed for community composition, visual differences in

flasks suggested that different phytoplankton tended to dominate different flasks overtime (Figure 32). This latter observation could have also affected the accumulation rate of *Microcystis* if resource limitation had been created, which was unlikely given that nutrient-rich media was added every two weeks and cell densities were not unusually high.

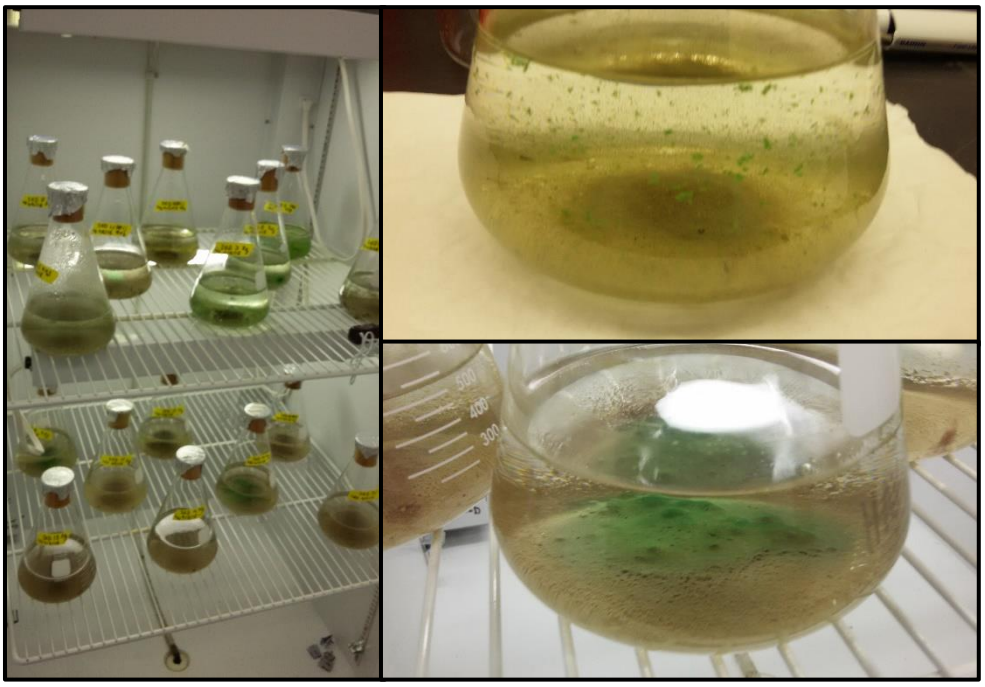

Figure 32- Throughout the six-week incubation period, visual differences indicated that different phytoplankton were proliferating in each flask, suggesting that competition may have been taking place.

Sampling methods may also potentially explain why the growth rate flasks experienced constant growth in both total and potentially-toxic *Microcystis* while most of the corresponding recruitment flasks experienced losses over the four and six week timepoints. The recruitment flasks contained sediment and were subject to the weekly turbulence that was part of the experimental design. During these turbulence events, the populations in the recruitment flasks may have been buried as the suspended sediments settled to the bottom of the flask, hindering growth of pelagic populations. The growth rate flasks did not contain sediments and therefore were not subject to the effects of turbulence and sedimentation processes, allowing for more advantageous growing conditions for the pelagic populations in those flasks. Alternatively, the difference in abundance could be because the entire contents of the growth rate flasks were filtered for analysis whereas only a portion of the recruitment flasks were filtered. Therefore, the growth rate flasks would have included any colonies that may have settled to the bottom whereas the recruitment flasks would not have included benthic populations.

Nevertheless, an accumulation of cells was seen in all cultures relative to t_0 (assuming the concentration of cell equivalents in the overlying media was equal to 0 at t_0). The fact that there was growth in all cultures confirms the general viability of the overwintering cells in the lake sediments. Not only was there a growth in total and potentially-toxic cell equivalents in the cultures, but, in many flasks, the percent of potentially-toxic *Microcystis* increased over the six-

week incubation period. While the seasonal average of percent potentially-toxic *Microcystis* was only slightly higher in the spring collections than the fall collection (i.e. 16% ± 23%, 11% ± 11%, 12% ± 13% for April 2015, November 2015, and April 2016, respectively), including the originally omitted values that exceeded 100% would have increased the averages for the spring events. This would have better reflected the pattern seen in nature of toxic strains of *Microcystis* dominating early in the bloom season, followed by the succession of non-toxic strains later in the bloom season as inorganic nitrogen is depleted. Ultimately, this suggests that potentially-toxic populations tend to become increasingly dominant over time when provided with sufficient nutrients.

5.3 Abundance versus Viability

When comparing total and potentially-toxic results for field sediments versus the recruitment flasks, which are assumed to represent abundance and viability of the sediment seed stocks, respectively, the sediment samples with the highest abundance were not always the ones with the greatest viability (Figure 33). For example, of the samples collected in April 2015, the sediments for Sites 5 and 15.1 had the greatest and lowest abundance, respectively. However, the corresponding culture for Site 5 yielded relatively low quantities of both total and toxic *Microcystis* over the 6-week period. The growth and quantity of total *Microcystis* in the corresponding culture for Site 15.1 was like that of Site 5. Further, by t_6, a far greater quantity of potentially-toxic *Microcystis* was measured in the Site 15.1 recruitment flask compared to Site 5 recruitment flask. The recruitment flask that yielded the greatest quantity of both total and potentially-toxic *Microcystis* overtime was that grown from the Site 1.1 sediments, which had a relatively low abundance compared to many of the sites. This suggests that other factors impact the vitality of vegetative seed stocks besides the abundance of *Microcystis* at a given location.

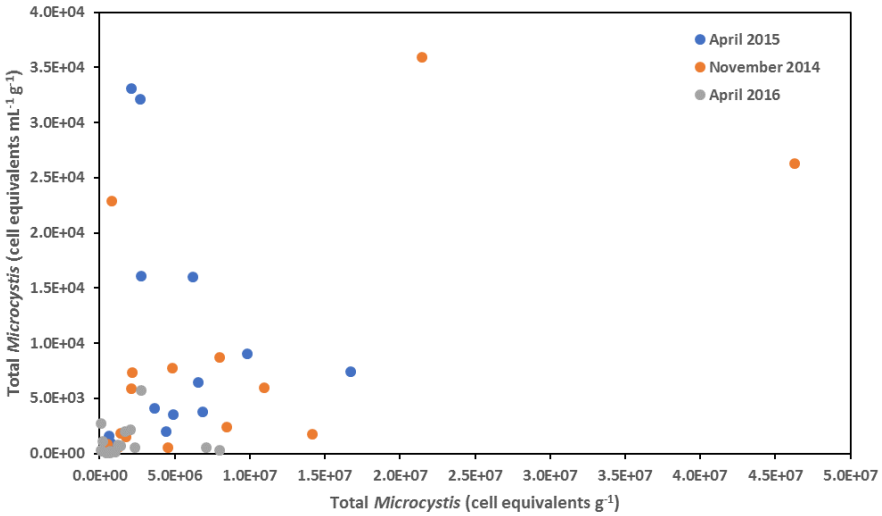

Figure 33- Microcystis *vitality (i.e. amount of* Microcystis *in overlying water at t_2, cell equivalents mL^{-1} g^{-1}) plotted against* Microcystis *abundance (i.e. sediment abundance, cell equivalents g^{-1}). Not shown in the extent of this graph is an outlier point for Site 5 in April 2015 at location (2.5E08, 2.0E03).*

Further, when comparing the estimated abundance in the sediment used to inoculate the recruitment flasks versus the concentration of total and potentially-toxic *Microcystis* in the overlying water at t_2, results suggest substantial growth occurred once cells recruited into the overlying water. For example, in the April 2015 culture experiments, the 5 grams of wet sediment from Site 8 used to inoculate a recruitment flask contained an estimated 1.6×10^7 *Microcystis* cell equivalents; at t_2, the overlying water in the flask contained an estimated 5.41×10^7 *Microcystis* cell equivalents, which is over twice the amount initially estimated to be in the raw sediments. Applying the same analysis to the other recruitment flasks yields similar results of cell equivalent concentrations (both total and potentially-toxic) ranging from being twice to ten times the estimated amount used to inoculate the flask (See Supplemental Material). it is important to note that these calculations are made assuming a homogenous distribution of cells in both the initial quantity of raw sediment used to inoculate the flask and in the overlying water at t_2.

There are several possible explanations for why cell densities at t_2 were higher than expected. First, calculations were made assuming a homogenous distribution of cells in both the initial quantity of raw sediment used to inoculate the flask and in the overlying water at t_2. In fact, sediment samples may not have been sufficiently homogenized before inoculating the flasks and therefore the amount of *Microcystis* in the sediment may have been greater than expected based on calculations alone. Second, growth may have been a more important contributing factor to pelagic populations than recruitment rates in those initial 2 weeks. Nevertheless, the analysis supports the theory that sediment seed stocks of *Microcystis* are readily recruited to the water column when provided with sufficient nutrients, temperature, and light conditions.

5.4 Potential Contribution of Sediment Recruitment to Annual Algal Blooms

The analysis of both field sediment and recruitment flask results together provides some insight regarding whether sediment recruitment is relevant to bloom initiation, growth, and spatial extent in Western Lake Erie. Comparison based simply on over-wintering cell abundance cannot fully explain the initiation of subsequent blooms, however, utilizing results from the grow-out studies and fairly conservative growth rate estimates indicate how important this source of inocula may be for maintaining persistent blooms.

For example, based on 2015 NOAA GLERL weekly monitoring data covering the same study area, an average increase of 30 µg/L chlorophyll α was observed over a 1-week period in August signaling the rise of a cyanobacteria bloom. Assuming an average depth of 7 m and an area of 375 km^2 (i.e. the size of an area that encapsulates all the site locations in this study), an increase in 30 µg/L chlorophyll α corresponds to ~79 MT of chlorophyll α. Based on the average chlorophyll α content of *Microcystis* cells measured in Western Lake Erie (0.006125 g/g cell dry wt.; Chaffin et. al 2012), 79 MT of chlorophyll α equates to 2.7×10^{20} cells. Based on the total abundance of *Microcystis* cells in the sediments in April 2015, the top 2 cm of sediment in the 375 km^2 area could contribute an average of 4.8×10^{20} cells, which is 178% of the total cell accumulation observed within the water column (see Supplemental Materials for additional

details of calculation). Granted, this calculation assumes 1) that all the *Microcystis* cells in the top 2 cm of the area migrated into the water column in the span of a week and 2) that no growth/decay in the *Microcystis* populations have occurred since the discrete sampling event in April 2015, which are both unrealistic assumptions. Based on total suspended solids monitoring data by the Great Lakes Environmental Research Laboratory, <2 mm of sediment is resuspended during resuspension events (See Supplemental Material). Therefore, it is more realistic to only consider that a fraction of the sediment is resuspended or regularly exposed to the water column. If only the cells in the top 2 mm of the sediment are resuspended, then recruitment could account for 17.8% of the total cell accumulation in the water column.

Given the importance of growth immediately following recruitment observed in the culture experiments, a more meaningful way to assess the potential contribution of sediment recruitment can be done using the average growth rate determined through the growth rate flask experiments. Given the same assumptions as previously noted, if all the *Microcystis* cells in the top 2 cm of our area migrated into the water column, it would result in an initial average cell concentration of 1.83×10^5 cells mL^{-1}. Using an average growth rate of 0.17 $days^{-1}$, the concentration would be 6.01×10^5 after 7 days. However, the average growth rate of *Microcystis* determined in this study (0.17 $days^{-1}$) is lower than the growth rates reported in literature (~0.27 day^{-1}, Wilson et al., 2006; Robarts & Zohary, 1987; Hesse & Kohl, 2001). Further, as previously noted, it is more likely that only a fraction of the populations in the top 2 cm of sediment will be recruited in each year. Therefore, Table 12 shows the outcomes if only a fraction (*f*) of the populations in the top 2 cm are recruited into the water column and under different possible growth rate conditions (see Supplemental Materials for additional details of calculation).

Table 12- Concentration of total Microcystis *in the water column (cell equivalents mL^{-1}) given the number of days elapsed (t, days) and the fraction of the sediment populations recruited to the water (f).*

		Total *Microcystis* (cell equivalents mL^{-1})			
μ ($days^{-1}$)	t (days)	*f*=1	*f*=0.5	***f*=0.1**	***f*=0.01**
0.17					
	0	1.83E+05	9.15E+04	**1.83E+04**	**1.83E+03**
	7	6.01E+05	3.01E+05	**6.01E+04**	**6.01E+03**
0.27†					
	0	1.83E+05	9.15E+04	**1.83E+04**	**1.83E+03**
	7	1.21E+06	6.06E+05	**1.21E+05**	**1.21E+04**
0.35‡					
	0	1.83E+05	9.15E+04	**1.83E+04**	**1.83E+03**
	7	2.12E+06	1.06E+06	**2.12E+05**	**2.12E+04**

† Wilson et al., 2006
‡ Robarts & Zohary, 1987

The fraction of the 30 μg/L of chlorophyll α increase that can potentially be explained by sediment recruitment ranges from 1.83×10^3 to 2.12×10^6 cell equivalents per mL, depending on the fraction of sediment populations that are recruited from the top 2 cm of the sediment and the

time elapsed. Based on internal data at the Great Lakes Environmental Research Laboratory, <2 mm of sediment is resuspended during a mixing event (See Supplemental Material), so the more realistic outcomes are those where $f \leq 0.1$. Assuming $f = 0.1$, recruitment and subsequent growth can explain 59%, 118%, or 209% of the spatially corresponding increase in 30 µg/L of chlorophyll α after 7 days (assuming µ= 0.1, 0.27, or 0.35 $days^{-1}$, respectively). Using a more conservative sediment exposure percentage of $f = 0.01$, which may represent a more averaged condition, recruitment and subsequent growth can explain 6%, 12%, or 21% of the same increase in chlorophyll α (assuming µ= 0.1, 0.27, or 0.35 $days^{-1}$, respectively).

The magnitude of this potential contribution of over-wintering cells to bloom initiation, and the large spatial extent over which blooms rapidly develop provide strong evidence for the importance of this sediment recruitment process for subsequent bloom development. It is unlikely that seeding from riverine input or growth from extremely rare concentrations in the water column can fully explain the spatial and temporal scales over which blooms develop. Of course, these calculations do not take into consideration the many processes that disrupt or enhance growth rates in Western Lake Erie. It also assumes that all the sediment *Microcystis* that can be recruited is done so simultaneously and that growth initiates immediately. Therefore, these calculations should only be used to discuss the *potential* contribution of sediment recruitment to bloom initiation and not the absolute contribution.

6. Conclusion

This study has demonstrated that *Microcystis* seed stock viability and abundance vary both in space and time. While sediment populations experience a high amount of loss during the overwintering period, the seed stocks that do survive are viable and capable of inoculating the water column. However, as culture experiments demonstrated, the abundance of *Microcystis* in the sediments does not necessarily correlate to how viable those seed stocks are. Further, except for particulate organic nitrogen, there was no correlation between the abundance of total *Microcystis* and sediment characteristics, depth, or distance offshore. Additional research will need to be done to understand what other factors control the distribution and viability of sediment seed stocks throughout Western Lake Erie.

Subsequent comparisons of both sediment abundance to culture results and to subsequent bloom development suggest that sediment recruitment alone cannot fully explain the extent of the subsequent annual bloom or the inter-annual variability in bloom size. However, when recruitment is paired with subsequent continual growth, then it is possible to explain a large portion of the average annual bloom. What portion of the annual bloom can be explained by sediment recruitment and subsequent growth is dependent on the number of cells that migrate into the water column and remain there. While culture experiments suggested a large portion of sediment populations migrate into the water column, there is considerable uncertainty as to whether sediment populations behave the same way in Western Lake Erie.

Several complications arose throughout this study. First, time and resource constraints hindered our ability to collect duplicate cores and to conduct replicate culture experiments, limiting our ability to utilize statistics to analyze differences among site locations. Second, experimental design for the culture experiments was not ideal. There existed limited guidance in literature for a uniform way of performing these experiments, so a significant amount of trial and error occurred in initial experiments. Further, we were unable to meaningfully separate contributions of growth versus recruitment regarding changes in *Microcystis* concentrations in the overlying water of flasks. Our understanding of the importance of this recruitment process could be improved by designing future recruitment experiments that would be able to parse out recruitment rates versus growth rates.

Despite the difficulties that arose throughout this study, the results have offered greater insight into the spatial and temporal variation in overwintering *Microcystis* sediment seed stocks and how they relate to subsequent blooms. Whereas previous studies primarily assessed Lake Erie sediment populations during the summer months, this study assessed populations prior and post bloom season. Future studies should seek to analyze sediments throughout the entire bloom (i.e. spring recruitment, summer blooms, fall settling) to better comprehend the role of sediment populations throughout the entire cycle of bloom development.

References

Andersen, J. M. (1976). “An ignition method for determination of total phosphorus in lake sediments. *Water Research*, 10(4), 329-331.

Bertram, P.E.. (1993). Total phosphorus and dissolved oxygen trends in the central basin of Lake Erie, 1970-1991.” *J. Great Lakes Res.*, 19, 224-236. Web.

Boström, B., A. K. Pettersson, I. Ahlgren. (1988). “Seasonal dynamics of a cyanobacteria-dominated microbial community in surface sediments of a shallow eutrophic lake.” *Aquat. Sci.*, 51, 53-78. Print.

Bridgeman, T. B., J. D. Chaffin, J. E. Filbrun (2013). "A Novel Method for Tracking Western Lake Erie Microcystis Blooms, 2002-2011." *Journal of Great Lakes Research,* 39 (1), 83-89. Print.

Bridgeman, T. B., J. D. Chaffin, D. D. Kane, J. D. Conroy, S. E. Panek, and P. M. Armenio (2011). "From River to Lake: Phosphorus partitioning and algal community compositional changes in Western Lake Erie." *Journal of Great Lakes Research,* 38, 90-97. Print.

Brunberg, A. K. (2002). "Benthic Overwintering of Microcystis Colonies under Different Environmental Conditions." *Journal of Plankton Research,* 24(11), 1247-252. Print.

Brunberg, A. K., and P. Blomqvist. (2003). "Recruitment of Microcystis (Cyanophyceae) From Lake Sediments: The Importance of Littoral Inocula." *Journal of Phycology,* 39, 58-63. Print.

Carr, N. G. and B.A. Whitton. (1982). “The Biology of Cyanobacteria.” Blackwell Scientific Publications: Oxford.

Chaffin, J. D., T. B. Bridgeman, S. A. Heckathorn, S. Mishra. (2011). “Assessment of *Microcystis* growth rate potential and nutrient status across a trophic gradient in Western Lake Erie.” *J. Gt. Lakes Res.*, 37, 92-100.

Chaffin, J. D., TB Bridgeman, SA Heckathorn, AE Krause. (2012). “Role of Suspended Sediments and Mixing in Reducing Photoinhibition in the Bloom-Forming Cyanobacterium Microcystis.” *Journal of Water Resource and Protection*, 4, 1029-1041. Web.

Chaffin, J. D., T. B. Bridgeman, D. L. Bade. (2013). “Nitrogen constrains the growth of late summer cyanobacterial blooms in Lake Erie.” *Adv. Microbiol.*, 3, 16-26.

Chaffin, J. D., V. Sigler, T. B. Bridgeman. (2014a). "Connecting the blooms: tracking and establishing the origin of the record-breaking Lake Erie Microcystis bloom of 2011 using DGGE." *Aquatic Microbial Ecology,* 73, 29-39. Print.

Chaffin, J.D., T. B. Bridgman, D. L. Bade, C. N. Mobilian. (2014b). “Summer phytoplankton nutrient limitation in Maumee Bay of Lake Erie during high-flow and low-flow years.” *J. Gt. Lakes Re.*, 40, 524-531. Print.

Conroy, J. D. (2007). “Testing the algal loading hypothesis: The importance of Sandusky River phytoplankton inputs to offshore Lake Erie processes.” Ohio State University, Columbus: Ohio.

Conroy, J. D., D. D. Kane, and D. A. Culver. (2008). “Declining Lake Erie ecosystem health – Evidence from a multi-year, lake-wide, plankton study.” in *Checking the Pulse of Lake Erie* (pp. 369-408). New Delhi, India: Ecovision World Monograph Series.

Conroy, J. D., D. D. Kane, R. D. Briland, and D. A. Culver. (2014). "Systemic, early-season Microcystis blooms in western Lake Erie and two of its major agricultural tributaries (Maumee and Sandusky rivers)." *Journal of Great Lakes Research,* 40, 518-23. Print.

Davis, T.W., D.L. Berry, G.L Boyer, C.J. Gobler. (2009). “The effects of temperature and nutrients on the growth and dynamics of toxic and non-toxic strains of Microcystis during cyanobacteria blooms.” *Harmful Algae*, 8, 715-725.

Davis, T.W., M.J. Harke, M.A Marcoval, J. Goleski, C. Orano-Dawson, D. L. Berry, C. J. Gobler. (2010). “Effects of nitrogenous compounds and phosphorus on the growth of toxic and non-toxic strains of Microcystis during cyanobacterial blooms.” *Aquatic Microbial Ecology*, 61, 149-162.

Davis, T.W., S.B. Watson, M.J. Rozmarynowycz, J.J.H. Ciborowski, R.M. McKay, G.S. Bullerjahn.

(2014). “Phylogenies of Microcystin-Producing Cyanabacteria in the Lower Laurentian Great Lakes Suggest Extensive Genetic Connectivity.” *PLoS One*, 9(9), e106093. doi:10.1371/journal.pone.0106093

DePinto, J.V., T.C. Young, S.C. Martin. (1986). “Impact of phosphorus control measures on water quality of the Great Lakes.” Environ. Sci. Technol., 20, 225-243. Web.

Fahnenstiel, G. L., D. F. Millie, J. Dyble, R. W. Litaker, P. A. Tester, M. J. Mccormick, R. Rediske, and D. Klarer. (2008). "Microcystin Concentrations and Cell Quotas in Saginaw Bay, Lake Huron." *Aquatic Ecosystem Health & Management*, 11(2), 190-95. Web.

Gobler, C. J., J. M. Burkholder, T. W. Davis, M. J. Harke, T. Johengen, C. A. Stow, D. B. Van de Waal. (2016). “The dual role of nitrogen supply in controlling the growth and toxicity of cyanobacterial blooms.” *Harmful Algae*, 54, 87-97.

Harke, M. J., M. M. Steffen, C. J. Gobler, T. G. Otten, S. W. Wilhelm, S. A. Wood, H. W. Paerl. (2016). “A review of the global ecology, genomics, and biogeography of the toxic cyanobacterium.” *Harmful Algae*, 54, 4-20. Web.

Hesse, K. and J. G. Kohl. (2001). Cyanotoxins: occurences, causes, and consequences (pp. 104-115). Berlin, Germany: Springer-Verlag. Print.

Kaushal, Sujay and Michael W. Binford. (1990). "Relationship between C:N ratios of lake sediments, organic matter sources, and historical deforestation in Lake Pleasant, Massachusetts, USA.” *Journal of Paleolimnology*, (22), 439-442. Web.

Kaebernick, M., Neilan, B.A., Borner, T., Dittmann, E. (2000). “Light and the transcriptional response of the microcystin biosynthesis gene cluster.” *Appl. Environ. Microbiol*, 66, 3387-3392. Print.

Kutovaya, Olga A., R. M. L. Mckay, B. F. Beall, S. W. Wilhelm, D. D. Kane, J. D. Chaffin, T. B. Bridgeman, and G. S. Bullerjahn. (2012) "Evidence against Fluvial Seeding of Recurrent Toxic Blooms of Microcystis Spp. in Lake Erie's Western Basin." *Harmful Algae*, 15, 71-77. Print.

Latour, D., M. J. Salencon, J.L. Reyss, and H. Giraudet. (2007). “Sedimentary Imprint of Microcystis Aeruginosa (Cyanbacteria) Blooms in Grangent Reservoir (Loire, France).” *Journal of Phycology*, 43, 417-425. Print.

Makarewicz, J.C. and P. Bertram. (1989). “Evidence for the restoration of the Lake Erie ecosystem.” *Bioscience*, 41, 216-223. Web.

Michalak, A. M., E. J. Anderson, D. Beletsky, et al. (2013) "Record-setting Algal Bloom in Lake Erie Caused by Agricultural and Meteorological Trends Consistent with Expected Future Conditions." *Proceedings of the National Academy of Sciences*, 110(16), 6448-6452.

Neilan, B.A., Jacobs, D., DelDot, T., Blackall, L.L., Hawkins, P.R., Cox, P.T., Goodman, A.E. (1997). “rRNA sequences and evolutionary relationships among toxic and nontoxic cyanobacteria of the genus Microcystis.” *Int. J. Sys. Bacteriol.* 47, 693-697. Print.

Obenour, D. R., A. D. Gronewold, C. A. Stow, D. Scavia. (2014). “Using Bayesian hierarchical model to improve Lake Erie cyanobacteria bloom forecasts.” *Water Resour. Res.*, 50, 7847-7860.

Oliver, R. L. and G. G. Gant. (2000). “Freshwater Blooms” in B. A. Whitton and M. Potts (eds.). *The Ecology of Cyanobacteria* (pp. 149-194). London, United Kingdom: Kluwer Academic.

Otten, Timothy G. and Hans W. Paerl. (2011). "Phylogenetic Inference of Colony Isolates Comprising Seasonal Microcystis Blooms in Lake Taihu, China." *Microb Ecol Microbial Ecology*, 62(4), 907-18. Web.

Potts, M. and B. Whitton. (2000). “The Ecology of Cyanobacteria.” Blackwell Scientific Publications: Oxford.

Reynolds, C. S., J. H. M. Jaworski, H. A. Cmiech, and G. F. Leedale. (1981). “On the annual cycle of the blue-green-alga Microcystis aeruginosa Kutz Emend Elenkin.” *Philosophical Transactions of the Royal Society of London Series B: Biological Sciences*, 293, 419-77. Print.

Rinta-Kanto, J.M, A.J.A. Ouellette, G.L. Boyer, M.R. Twiss, T. B. Bridgeman, S. W. Wilhelm. (2005). “Quantification of toxic Microcystis spp. during the 2003 and 2004 blooms in western Lake Erie using quantitative real-time PCR.” *Environmental Science and Technology*, 39, 4198-4205. Print.

Rinta-Kanto, J. M., M. A. Saxton, J. M. Debruyn, J. L. Smith, C. H. Marvin, K. A. Krieger, G. S. Sayler, G. L. Boyer, and S. W. Wilhelm. (2009). "The Diversity and Distribution of Toxigenic Microcystis Spp. in Present Day and Archived Pelagic and Sediment Samples from Lake Erie." *Harmful Algae,* 8(3), 385-94. Print.

Robarts, R. D. and T. Zohary. (1987). "Temperature effects on photosynthetic capacity, respiration, and growth rates of bloom-forming cyanobacteria." *New Zealand Journal of Marine and Freshwater Research*, 21(3), 391-399. Web.

Rosa, F. & N. M. Burns. (1987). "Lake Erie central basin oxygen depeletion changes from 1929-1980." *J. Great Lakes Res.*, 13, 684-696.

Scavia, Donald, J. David Allan, Kristin K. Arend, et al. (2014) "Assessing and Addressing the Re-eutrophication of Lake Erie: Central Basin Hypoxia." *Journal of Great Lakes Research,* 40(2), 226-246.

Schertzer, W. M., P. F. Hamblin, D. C. L. Lam. (2008). "Lake Erie Thermal Structure: Variability, Trends, and Potential Changes" in M. Munawar and R. Heath (eds.). *Checking the Pulse of Lake Erie* (pp. 3-34). New Delhi, India: Aquatic Ecosystem Health and Management.

Schindler, D.W.. (2006). "Recent advances in the understanding and management of eutrophication." *Proc. R. Spc. B*, 279, 4322-4333. Web

Schindler, D.W.. (2012). "The dilemma of controlling cultural eutrophication of lakes." *Limnol. Oceanogr*., 51, 356-363. Web

Sejnohova, L. and B. Marsalek. (2012). "Microcystis" in *Ecology of Cyanobacteria II: Their Diversity in Space and Time* (pp. 195-221). London, United Kingdom: Springer.

Shuchman, Robert, Mike Sayers, Amanda Grimm, and Glenn Sullivan. (2016). "Multi-Satellite Harmful Algal Bloom Observation Summary 1997-2015". February 2016. Presentation.

Smith, V.H. and D.W. Schindler. (2009). "Eutrophication science: where do we go from here?" *Trends Ecolo. Evol.*, 24, 201-207. Web.

Speziale, B. J., S. P. Schreiner, P.A. Giammatteo, and J.E. Schindler. (1984). "Comparison of N, N-Dimethylformamide, Dimethyl Sulfoxide, and Acetone for Extraction of Phytoplankton Chlorophyll." *Canadian Journal of Fisheries and Aquatic Sciences,* 41(10), 1519-1522. Web.

Stumpf, Richard P., Laura T. Johnson, Timothy T. Wynne, and David B. Baker. (2016). "Forecasting annual cyanobacterial bloom biomass to inform management decisions in Lake Erie." *Journal of Great Lakes Research*, 42, 1174-1183. Web.

Stumpf, Richard P., T. T. Wynne, D. B. Baker, G. L. Fahnenstiel. (2012). "Interannual Variability of Cyanobacterial Blooms in Lake Erie." *PLoS ONE*, 7(8), e42444. Web.

Tillet, D., Dittman, E., Erhard, M., von Dohren, H., Borner, T., Neilan, B.A. (2000). "Structural organization of microcystin biosynthesis in Microcystis aeruginosa PCC7806: an integrated peptide-polyketide synthetase system." *Chem. Biol.*, 7, 753-764. Print.

Tsujimura, S., H. Tsukada, H. Nakahara, T. Nakajima, and M. Nishino. (2000). "Seasonal variations of Microcystis populations in sediments of Lake Biwa, Japan." *Hydrobiologia*, 434, 183-92. Print.

Qin, Boqiang, Guangwei Zhu, Guang Gao, Yunlin Zhang, Wei Li, Hans W. Paerl, and Wayne W. Carmichael. (2009). "A Drinking Water Crisis in Lake Taihu, China: Linkage to Climatic Variability and Lake Management." *Environmental Management,* 45(1), 105-12. Web.

United States EPA. (2016, May 4). Lake Erie. Retrieved from the Environmental Protection Agency website: https://www.epa.gov/greatlakes/lake-erie

Vanderploeg, Henry A., James R. Liebig, Wayne W. Carmichael, Megan A. Agy, Thomas H. Johengen, Gary L. Fahnenstiel, and Thomas F. Nalepa. (2001). "Zebra Mussel (*Dreissena Polymorpha*) Selective Filtration Promoted Toxic *Microcystis* Blooms in Saginaw Bay (Lake Huron) and Lake Erie." *Canadian Journal of Fisheries and Aquatic Sciences,* 58(6), 1208-221. Web.

Verspagen, Jolanda M. H., E. M. Snelder, P. M. Visser, K. D. Johnk, B. W. Ibelings, L. R. Mur, and J. Huisman. (2005). "Benthic-pelagic Coupling in the Population Dynamics of the Harmful Cyanobacterium Microcystis." *Freshwater Biology,* 50, 854-67. Print.

Wetzel, R.G.. (2001). *Limnology: Lake and River Ecosystems, 3rd edition*. Academic Press: San Diego, CA.

Wilson, Alan E., Whitney A. Wilson, and Mark E. Hay. (2006). “Intraspecific Variation in Growth and Morphology of the Bloom-Forming Cyanobacterium *Microcystis aeruginosa*.” *Applied and Environmental Microbiology*, 72(11), 7386-7389. Web.

Zohary, Tamar, and Richard D. Robarts. (1990). "Hyperscums and the Population Dynamics of Microcystis Aeruginosa." *J Plankton Res Journal of Plankton Research*, 12(2), 423-32. Web.

Supplemental Material

Date	Site	Total Microcystis (16S copies * g dry wt^{-1})	SD	Toxic Microcystis (mcyD copies * g dry wt^{-1})	SD	Percent Toxic
Nov-14						
	1.1	12,097,498	4,695,108	102,437	63,337	1%
	2	589,418,700	62,243,517	199,605	96,555	0%
	3	20,733,312	751,744	130,360	81,368	1%
	3.5	23,318,708	9,766,716	95,538	85,546	0%
	4	32,477,233	11,034,444	1,173,962	735,636	4%
	5	1,691,605,417	74,061,550	1,929,965	931,784	0%
	6	49,361,544	27,369,459	133,503	74,311	0%
	7	3,088,592	1,419,404	196,883	69,628	6%
	8	7,970,051	6,331,554	75,458	53,028	1%
	9	-	-	-	-	-
	10	-	-	-	-	-
	11	27,438,214	9,572,100	467,136	264,043	2%
	12	376,437,050	131,114,522	2,744,418	1,132,131	1%
	13	-	-	-	-	-
	14	-	-	-	-	-
	15.1	-	-	-	-	-
Apr-15						
	1.1	2,100,448	366,867	59,206	49,102	3%
	2	16,736,934	3,270,052	124,063	58,357	1%
	3	9,844,619	7,680,340	26,774	13,445	0%
	3.5	-	-	-	-	-
	4	65,111,010	23,023,250	49,116	57,539	0%
	5	253,419,291	47,337,195	506,504	263,041	0%
	6	3,673,406	97,116	135,091	250,638	4%
	7	4,927,452	2,643,332	18,743	27,234	0%
	8	6,591,354	3,804,362	112,502	41,903	2%
	9	748,492	68,768	11,339	13,792	2%
	10	2,725,542	32,324	27,755	28,023	1%
	11	2,751,565	1,205,573	17,523	13,407	1%
	12	6,206,340	1,859,673	19,172	15,533	0%
	13	6,834,652	6,993,457	30,574	30,368	0%
	14	4,405,595	945,424	18,094	15,569	0%
	15.1	644,424	271,496	9,515	12,095	1%
Nov-15						
	1.1	1,768,328	90,842	324,006	208,773	18%
	2	4,841,868	2,866,262	395,572	166,200	8%
	3	7,969,337	5,297,038	185,696	97,901	2%
	3.5	784,380	470,651	78,182	43,614	10%
	4	10,960,858	4,061,891	4,692,819	1,617,817	43%
	5	1,373,062	1,436,855	251,680	224,368	18%
	6	531,435	422,385	69,418	28,760	13%
	7	2,157,782	1,375,074	287,935	203,695	13%
	8	46,286,311	11,728,158	3,722,725	2,499,609	8%
	9	549,385	136,450	72,196	13,930	13%
	10	1,223,455	1,095,705	208,830	124,979	17%
	11	2,087,884	2,068,791	1,424,700	323,079	68%
	12	8,486,322	411,620	485,919	184,938	6%
	13	4,537,038	4,499,613	645,376	324,474	14%
	14	14,163,248	2,450,838	386,093	318,766	3%
	15.1	21,494,430	2,361,532	517,832	274,164	2%
Apr-16						
	1.1	2,060,816	557,481	113,345	20,089	5%
	2	443,452	194,615	9,047	3,490	2%
	3	221,201	81,622	4,279	3,549	2%
	3.5	65,652	19,076	1,401	849	2%
	4	2,771,867	1,084,988	261,427	133,628	9%
	5	83,096	62,674	5,432	3,810	7%
	6	7,979,282	3,789,346	535,461	46,003	7%
	7	2,367,014	612,381	60,101	14,227	3%
	8	679,505	544,172	16,377	11,353	2%
	9	1,691,739	1,105,966	162,775	31,507	10%
	10	126,616	203,825	18,287	350	14%
	11	1,249,496	156,662	95,119	47,759	8%
	12	688,538	585	8,900	2,873	1%
	13	1,401,014	28,834	31,116	3,917	2%
	14	1,017,453	415,889	20,560	1,448	2%
	15.1	7,088,754	220,657	90,940	95,612	1%

Table S 1- Total and toxic Microcystis of raw sediments across all sampling seasons, including standard deviations and percent potentially-toxic Microcystis.

			T2				T4				T6			
Date	Site	Sed in Flask (g)	Total Microcystis (16S copies * mL^{-1})	Toxic Microcystis (mcyD copies * mL^{-1})	Total Microcystis (16S copies * mL^{-1} * g^{-1})	Toxic Microcystis (mcyD copies * mL-1 * g-1)	Total Microcystis (16S copies * mL^{-1})	Toxic Microcystis (mcyD copies * mL^{-1})	Total Microcystis (16S copies * mL^{-1} * g^{-1})	Toxic Microcystis (mcyD copies * mL-1 * g-1)	Total Microcystis (16S copies * mL^{-1})	Toxic Microcystis (mcyD copies * mL^{-1})	Total Microcystis (16S copies * mL^{-1} * g^{-1})	Toxic Microcystis (mcyD copies * mL-1 * g-1)
Apr-15														
	1.1	2.8	463,371	16,049	165,489	5,732	530,164	67,457	189,344	24,092	997,607	58,209	356,288	20,789
	2	3	103,857	12,708	34,619	4,236	100,984	14,319	33,661	4,773	99,780	2,174	33,260	725
	3	4.7	126,172	480	26,845	102	157,437	4,016	33,497	854	359,982	3,022	76,592	643
	3.5	11.6	413,761	7,847	35,669	676	95,650	11,836	8,246	1,020	41,870	3,664	3,609	316
	4	3.4	128,361	1,376	37,753	405	79,806	6,244	23,472	1,837	126,575	2,456	37,228	722
	5	3.2	27,615	31	8,630	10	124,770	13,326	38,991	4,164	25,392	188	7,935	59
	6	3	56,961	1,925	18,987	642	81,547	7,756	27,182	2,585	4,986	718	1,662	239
	7	3.1	48,964	15,173	15,795	4,895	35,194	8,140	11,353	2,626	19,840	1,133	6,400	365
	8	5.1	90,191	24,923	17,684	4,887	72,772	44,155	14,269	8,658	26,044	57,494	5,107	11,273
	9	2.8	13,739	1,538	4,907	549	17,308	2,261	6,181	808	48,615	340	17,362	121
	10	4.6	449,410	64,205	97,698	13,958	104,150	14,773	22,641	3,212	72,794	11,816	15,825	2,569
	11	3.1	225,089	26,996	72,609	8,708	223,743	17,392	72,175	5,610	301,007	26,056	97,099	8,405
	12	3.2	224,343	15,098	70,107	4,718	99,753	19,787	31,173	6,184	73,409	24,083	22,940	7,526
	13	3	52,526	7,737	17,509	2,579	105,581	45,221	35,194	15,074	117,322	22,142	39,107	7,381
	14	3	28,069	2,090	9,356	697	18,394	7,897	6,131	2,632	31,490	11,185	10,497	3,728
	15.1	3.1	22,338	1,881	7,206	607	13,492	2,743	4,352	885	32,840	47,162	10,594	15,214
Nov-15														
	1.1	3.8	21,059	2,756	5,542	725	41,718	7,334	10,978	1,930	45,940	5,626	12,089	1,481
	2	5.1	108,401	2,045	21,255	401	6,248	1,524	1,225	299	5,954	802	1,167	157
	3	6.3	121,693	560	19,316	89	52,212	2,410	8,288	383	963,678	124,165	152,965	19,709
	3.5	13.8	320,497	5,072	23,224	368	86,933	9,823	6,300	712	532,962	80,809	38,620	5,856
	4	5.2	83,972	11,596	16,148	2,230	184,311	17,456	35,444	3,357	64,739	3,084	12,450	593
	5	6.2	26,214	3,249	4,228	524	13,569	1,626	2,189	262	122,298	20,914	19,725	3,373
	6	4.3	11,616	1,021	2,701	237	30,547	532	7,104	124	149,673	1,549	34,808	360
	7	5.3	102,799	4,753	19,396	897	81,746	8,909	15,424	1,681	131,653	62,564	24,840	11,805
	8	4.9	368,398	24,962	75,183	5,094	79,299	24,855	16,184	5,073	74,671	35,536	15,239	7,252
	9	4.5	2,258	140	502	31	3,840	75	853	17	19,472	444	4,327	99
	10	4.4	7,604	563	1,728	128	1,607	111	365	25	91,125	8,164	20,710	1,855
	11	3.1	82,162	15,564	26,504	5,021	32,522	9,939	10,491	3,206	260,272	39,881	83,959	12,865
	12	5.2	33,308	1,338	6,405	257	64,024	4,860	12,312	935	73,409	10,203	14,117	1,962
	13	5.2	8,056	1,556	1,549	299	25,829	1,945	4,967	374	1,846	376	355	72
	14	5.2	25,017	997	4,811	192	41,669	2,733	8,013	526	39,789	9,094	7,652	1,749
	15.1	3.8	503,161	5,692	132,411	1,498	15,596	70	4,104	18	-	704	-	185
Apr-16														
	1.1	4	30,302	1,856	7,575	464	121,532	575	30,383	144	4,808	614	1,202	153
	2	3.6	278	4	77	1	13,083		3,634		12,260	19	3,406	5
	3	3.3	14,967	641	4,535	194	45,043	19,095	13,649	5,786	85,586	14,890	25,935	4,512
	3.5	4.3	3,588	112	834	26	54,667	2,244	12,713	522	185,656	370	43,176	86
	4	3.4	80,400	31,388	23,647	9,232	27,024	308	7,948	90	10,171	253	2,991	75
	5	3.4	38,055	9,181	11,193	2,700	27,819	7,308	8,182	2,149	62,433	309	18,363	91
	6	4	4,270	73	1,068	18	2,016	658	504	164	2,739	1,207	685	302
	7	3.6	7,188	335	1,997	93	35,155	744	9,765	207	55,965	989	15,546	275
	8	3.8	2,605	147	686	39	5,493	11,817	1,446	3,110	32,941	11,906	8,669	3,133
	9	3.5	28,195	677	8,056	193	1,405	136	401	39	183,691	6,953	52,483	1,987
	10	3.5	2,633	27	752	8	45,373	124	12,964	35	32,615	24	9,319	7
	11	3.6	10,979	740	3,050	206	17,054	3,790	4,737	1,053	24,595	3,137	6,832	871
	12	5.1	169	14	33	3	10,055	441	1,971	86	4,558	59	894	12
	13	3.7	9,815	1,257	2,653	340	12,662	862	3,422	233	1,999	311	540	84
	14	3.5	2,159	216	617	62	1,358	282	388	80	2,778	1,143	794	327
	15.1	3.6	7,050	700	1,958	194	25,531	5,607	7,092	1,558	85,988	29,548	23,885	8,208

Table S 2- Total and toxic cell equivalents per mL in recruitment flasks at t1, t2, and t3. Numbers do NOT account for dilution effects.

Calculations for 5.3 Abundance versus Vitality

To understand what percentage of the sediment seed stocks might contribute to populations in the overlying water, the qPCR results for the populations in the overlying water were compared to what the expected total populations in the raw sediments would be. To make this comparison, total expected raw sediment populations were calculated as follows:

$$x_a^* = x_a * w_a$$

where x_a is the expected cell concentration based on the results of the qPCR analysis of the raw sediment (cell equivalents per gram wet weight of sediment), w_a is the amount of sediment used to inoculate flask *a* (grams), and x_a^* is the expected amount of *Microcystis* in the starting amount of sediment (cell equivalents).

Total pelagic populations were calculated as follows:

$$x_a^* = x_a * v_a$$

where N_a is the expected cell concentration based on the results of the qPCR analysis of the overlying water (cell equivalents per mL), v_a is the volume of media in flask *a* (mL), and N_a^* is the expected amount of *Microcystis* in the entire flask (cell equivalents) at t_2. Results are shown in Table S 3.

Date	Site	Sed in Flask (g)	Total Microcystis in Sediment (16S copies)	Toxic Microcystis in Sediment (mcyD copies)	Total Microcystis in Recruitment Flask at t_2 (16S copies)	Toxic Microcystis in Recuitment Flask in t_2 (mcyD copies)	Total Ratio	Toxic Ratio
Apr-15								
	1.1	2.8	2.73E+06	7.70E+04	2.78E+08	9.63E+06	10182%	12512%
	2	3	1.62E+07	1.20E+05	6.23E+07	7.62E+06	384%	6334%
	3	4.7	2.98E+07	8.10E+04	7.57E+07	2.88E+05	254%	355%
	3.5	11.6	-	-	2.48E+08	4.71E+06		
	4	3.4	9.60E+07	7.24E+04	7.70E+07	8.25E+05	80%	1140%
	5	3.2	3.01E+08	6.02E+05	1.66E+07	1.83E+04	5%	3%
	6	3	3.94E+06	1.45E+05	3.42E+07	1.16E+06	866%	796%
	7	3.1	5.85E+06	2.23E+04	2.94E+07	9.10E+06	502%	40910%
	8	5.1	1.60E+07	2.73E+05	5.41E+07	1.50E+07	338%	5469%
	9	2.8	1.00E+06	1.52E+04	8.24E+06	9.23E+05	820%	6064%
	10	4.6	5.58E+06	5.68E+04	2.70E+08	3.85E+07	4832%	67787%
	11	3.1	2.34E+06	1.49E+04	1.35E+08	1.62E+07	5781%	108870%
	12	3.2	5.53E+06	1.71E+04	1.35E+08	9.06E+06	2433%	53009%
	13	3	4.80E+06	2.15E+04	3.15E+07	4.64E+06	657%	21631%
	14	3	2.84E+06	1.17E+04	1.68E+07	1.25E+06	592%	10737%
	15.1	3.1	9.79E+05	1.45E+04	1.34E+07	1.13E+06	1369%	7811%
Nov-15								
	1.1	3.8	3.37E+06	6.17E+05	1.26E+07	1.65E+06	375%	268%
	2	5.1	1.22E+07	9.98E+05	6.50E+07	1.23E+06	532%	123%
	3	6.3	3.47E+07	8.08E+05	7.30E+07	3.36E+05	210%	42%
	3.5	13.8	1.10E+07	1.10E+06	1.92E+08	3.04E+06	1741%	276%
	4	5.2	2.67E+07	1.14E+07	5.04E+07	6.96E+06	189%	61%
	5	6.2	6.62E+06	1.21E+06	1.57E+07	1.95E+06	237%	161%
	6	4.3	1.14E+06	1.48E+05	6.97E+06	6.12E+05	614%	413%
	7	5.3	6.51E+06	8.69E+05	6.17E+07	2.85E+06	948%	328%
	8	4.9	1.06E+08	8.53E+06	2.21E+08	1.50E+07	208%	176%
	9	4.5	1.47E+06	1.93E+05	1.35E+06	8.41E+04	92%	44%
	10	4.4	3.00E+06	5.12E+05	4.56E+06	3.38E+05	152%	66%
	11	3.1	4.82E+06	3.29E+06	4.93E+07	9.34E+06	1022%	284%
	12	5.2	2.25E+07	1.29E+06	2.00E+07	8.03E+05	89%	62%
	13	5.2	1.09E+07	1.55E+06	4.83E+06	9.33E+05	44%	60%
	14	5.2	3.07E+07	8.36E+05	1.50E+07	5.98E+05	49%	72%
	15.1	3.8	3.43E+07	8.27E+05	3.02E+08	3.42E+06	879%	413%
Apr-16								
	1.1	4	3.62E+06	1.99E+05	1.82E+07	1.11E+06	502%	559%
	2	3.6	4.84E+05	9.87E+03	1.67E+05	2.62E+03	35%	27%
	3	3.3	5.65E+05	1.09E+04	8.98E+06	3.84E+05	1590%	3520%
	3.5	4.3	2.10E+05	4.47E+03	2.15E+06	6.75E+04	1027%	1509%
	4	3.4	3.35E+06	3.16E+05	4.82E+07	1.88E+07	1439%	5955%
	5	3.4	1.84E+05	1.21E+04	2.28E+07	5.51E+06	12382%	45693%
	6	4	1.05E+07	7.05E+05	2.56E+06	4.39E+04	24%	6%
	7	3.6	2.89E+06	7.35E+04	4.31E+06	2.01E+05	149%	274%
	8	3.8	6.37E+05	1.54E+04	1.56E+06	8.80E+04	245%	573%
	9	3.5	2.04E+06	1.96E+05	1.69E+07	4.06E+05	829%	207%
	10	3.5	1.97E+05	2.84E+04	1.58E+06	1.64E+04	803%	58%
	11	3.6	1.54E+06	1.17E+05	6.59E+06	4.44E+05	428%	379%
	12	5.1	1.00E+06	1.30E+04	1.01E+05	8.30E+03	10%	64%
	13	3.7	1.25E+06	2.77E+04	5.89E+06	7.54E+05	473%	2727%
	14	3.5	9.63E+05	1.95E+04	1.30E+06	1.30E+05	134%	666%
	15.1	3.6	5.93E+06	7.61E+04	4.23E+06	4.20E+05	71%	551%

Table S 3- Calculated results for amount of total and toxic Microcystis in raw sediment used to inoculate recruitment flasks versus the number of total/toxic cells that were in the overlying water.

Based on these calculations, most recruitment flasks, regardless of season or location, had quantities in the overlying water that well exceeded the calculated amount of total and potentially-toxic *Microcystis* in the sediment used to inoculate the flasks.

Calculations for Discussion 5.4 Potential Contribution of Sediment Recruitment

To estimate the potential contribution of *Microcystis* sediment recruitment to the average annual bloom, a theoretical area was established to enable quantitative comparisons between benthic and pelagic populations of *Microcystis*. Since values for variables and constants are developed based on the 16 sites analyzed in this study, an area encapsulating those sites was used for this analysis (Figure S 1). The area is ~375 km^2 and, assuming an average depth of 7 m, contains a water volume of 2.625 x 10^{12} L.

To determine the mass of sediment in the top 2 cm of that same area, an approximate bulk density of sediment (~900 kg m^{-3}) was generated based on measured characteristics of collected sediment samples.

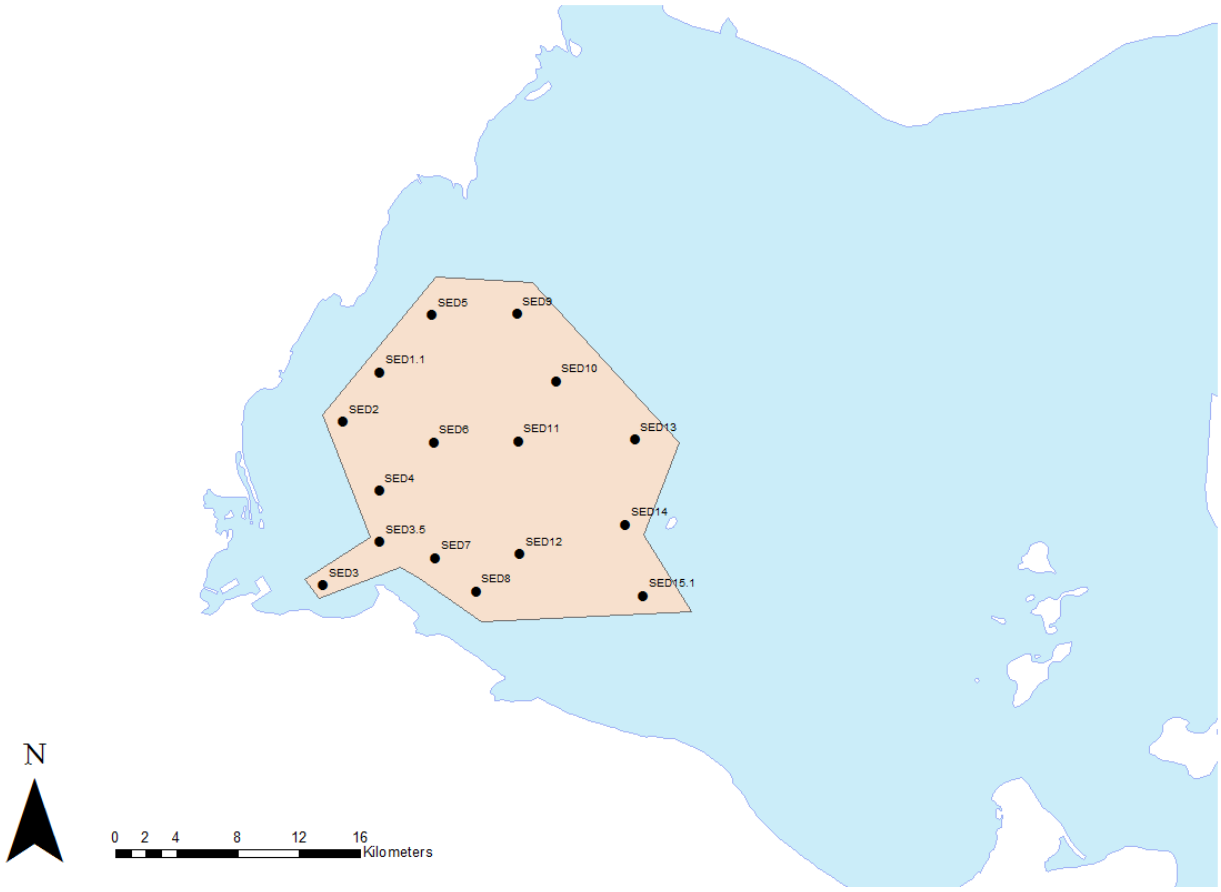

Figure S 1- Working area for discussion analysis

Using the conversion factor between 1 CI (cyanobacteria index), cell quantity, and MT of cyanobacteria dry weight (Stumpf et al. 2012; Obenour et al. 2014), we can determine the expected concentration of *Microcystis* cells in our area.

$$79\ MT\ Chla * \frac{10^6 g\ Chla}{1\ MT\ Chla} * \frac{1\ g\ cell\ dry\ wt}{0.006125\ g\ Chla} * \frac{MT\ cell\ dry\ wt}{10^6 g\ cell\ dry\ wt} * \frac{1\ CI}{4800\ MT\ cell\ dry\ wt} * \frac{10^{20}}{1\ CI} * \frac{1}{2.625\ x\ 10^{12}\ L} * \frac{1\ L}{10^3 mL} = \frac{1.02 * 10^5\ cells}{mL}$$

If all the *Microcystis* cells in the top 2 cm of our area migrated into the water column, it would result in an initial average cell concentration of 1.83 x 10^5 cells mL^{-1}.

Calculated growth rates were used to predict changes in *Microcystis* concentrations given an elapsed number of days using the following formula:

$$x_t = x_0 e^{\mu t}$$

Where x_0 is the initial concentration of cells in the water column, x_t is the concentration of cell equivalents at time *t* (days), and μ is the growth rate of cells ($days^{-1}$). The growth rate used in this calculation (0.17 $days^{-1}$) was developed based on the average of all non-negative apparent accumulation rates across all recruitment flasks.

The average amount of sediment resuspension during a storm event in Western Lake Erie (≤ 2 mm of surface sediment) was estimated by using the calculated sediment density, known changes in lake turbidity attributed to sediment resuspension during storm events, and the relationship between turbidity and total suspended matter (TSM). Assuming that the top 2 mm of sediment is resuspended during a storm event, the average water column depth is 7 m, and the average density of the sediment is 0.9 g/cm^3, the corresponding change in TSM in the water column would be approximately 260 mg/L. According to internal data at the Great Lakes Environmental Research Laboratory, sediment resuspension during a typical storm event in Western Lake Erie causes an average increase of 100 mg/L, so even assuming the top 2 mm of sediment gets resuspended is generous, but still makes more relative sense that assuming that even the top centimeter of sediment gets resuspended.